INFORMATION TO USERS

This manuscript has been reproduced from the microfilm master. UMI films the text directly from the original or copy submitted. Thus, some thesis and dissertation copies are in typewriter face, while others may be from any type of computer printer.

The quality of this reproduction is dependent upon the quality of the copy submitted. Broken or indistinct print, colored or poor quality illustrations and photographs, print bleedthrough, substandard margins, and improper alignment can adversely affect reproduction.

In the unlikely event that the author did not send UMI a complete manuscript and there are missing pages, these will be noted. Also, if unauthorized copyright material had to be removed, a note will indicate the deletion.

Oversize materials (e.g., maps, drawings, charts) are reproduced by sectioning the original, beginning at the upper left-hand corner and continuing from left to right in equal sections with small overlaps. Each original is also photographed in one exposure and is included in reduced form at the back of the book.

Photographs included in the original manuscript have been reproduced xerographically in this copy. Higher quality 6" x 9" black and white photographic prints are available for any photographs or illustrations appearing in this copy for an additional charge. Contact UMI directly to order.

UMI

A Bell & Howell Information Company
300 North Zeeb Road, Ann Arbor MI 48106-1346 USA
313/761-4700 800/521-0600

Characterization of Mutant

N^2, N^2-Dimethylguanosine-Specific tRNA Methyltransferases

from *Saccharomyces cerevisiae*

Melanie Reuben

A Thesis in the Department of Chemistry

Presented in partial fulfilment of the requirements for

the Degree of Master of Science

at Concordia University

Montréal, Québec, Canada

April 15, 1997

ABSTRACT

Characterization of Mutant

N^2,N^2-Dimethylguanosine-Specific tRNA Methyltransferases

from *Saccharomyces cerevisiae*

Melanie Reuben

N^2,N^2-dimethylguanosine-specific tRNA methyltransferase (m_2^2Gtase) is an enzyme which uses S-adenosylmethionine as a substrate to catalyze the transfer of two methyl groups to the 2-amino group of guanosine at position 26 in tRNA. Neither the tertiary structure nor the location of the active sites are known for m_2^2Gtase. In an attempt to characterize this enzyme, the *trm*1 gene from the *Saccharomyces cerevisiae* strain SN1015-2a, which lacks functional m_2^2Gtase, was clone and sequenced. Based on the wild-type *TRM*1 sequence, oligonucleotides were designed and the mutant *trm*1 gene was isolated from SN1015-2a genomic DNA by polymerase chain reaction (PCR). Sequence comparison to the wildtype *TRM*1 gene revealed 14 silent point mutations and 4 amino acid substitutions that are common to two PCR products: Gly^{3}→Ser, Thr^{203}→Ser, Ser^{467}→Leu, and Gly^{517}→Arg. Sub-cloning and site-directed mutagenesis were employed and the single amino acid substitution, Ser^{467}→Leu, was identified as the mutation responsible for inactivating m_2^2Gtase. To elucidate the function of Ser^{467}, new mutant enzymes with Thr, Ala and Cys at this position were created. Kinetic studies yielded apparent K_M and V_{max} values that were similar to those of the wild-type m_2^2Gtase demonstrating that Ser at position 467 is not required for enzyme activity.

ACKNOWLEDGEMENTS

I am indebted to several people to whom over the past few years, I have had the good fortune to work with and talk to concerning issues considered in this thesis. I do not suppose that I can thank all of them, but I want to offer special expressions of gratitude to the following: To my supervisor, Dr. Paul Joyce, for his invaluable advice and guidance which kept me on track, yet allowed me the freedom to work and make decisions on my own. Dr. Joyce read this manuscript with the utmost care and wrote me pages and pages of comments. I feel fortunate to have such an excellent and tireless critic as a supervisor. To Dr. Pam Hanic-Joyce, for without her good leads and sage advice, I would probably still be doing experiments. To my committee members, Dr. Joanne Turnbull and Dr. Storms, who provided excellent and helpful suggestions. I would also like to offer my sincere gratitude to Dr. Paul Clarke of McGill University, who was very understanding and supportive throughout my stage as a full-time employee and a part-time graduate student.

This thesis would not have been possible without the unwavering love and support of my family. A special thanks to my parents, Anne and Richard for encouraging me to to pursue my M.Sc., to my Aunt Clarissa and to my sisters and brothers: Chantal, Richard, Melissa, and Nicholas. This thesis is a small token of love and appreciation for all they mean to me, both collectively and individually.

I would also like to extend my thanks to the Beffert family, especially Gisela and Manfred, whose regular dose of love and encouragement kept me going.

Most of all, I thank my husband, Uwe Beffert, for his constant help and advice. As always, he has been my greatest intellectual influence and my strongest source of encouragement and inspiration. Uwe had to listen, advise and humour me over the past 4½ years, and it is his enthusiastic love and support which kept me sane. It is to him that this thesis is dedicated to.

TABLE OF CONTENTS

LIST OF FIGURES

LIST OF TABLES

ABBREVIATIONS

bp - Base pair

BSA - Bovine serum albumin

C - Celsius

CPM - Counts per minute

DTT - Dithiothreitol

dH_2O - Distilled water

EDTA - Ethylenediaminetetraacetic acid

EtOH - Ethanol

g - Gram

IPTG - Isopropyl-β-D-thio-galactopyranoside

kDa - Kilo Dalton

LB - Luria Broth

m - Methyl

min - Minute

NET-NP - NaCl / EDTA / Tris / NP-40

OD - Optical density

PEG - Polyetheleneglycol

RT - Room temperature

SAM - S-adenosylymethionine

SC - Synthetic complete

SDS - Sodium dodecyl sulfate

SE - Standard Error

TE - Tris / EDTA

TBE - Tris-Borate / EDTA

TBS-T - Tris·HCl / NaCl / Tween-20

TEA - Tris-acetate / EDTA

TSE - Tris / EDTA / NaCl

WT - Wild-type

Xg - Times gravity

X-Gal - 5-bromo-4-chloro-3-indolyl-β-galactoside

YPD - Yeast extract / peptone / dextrose

YT - Yeast extract / tryptone

Introduction

I. INTRODUCTION

Transfer ribonucleic acids (tRNAs) are low molecular weight RNA molecules that are required for the growth and maintenance of all cells. They are known for their vital role as amino acid carriers in protein synthesis, but they also have been shown to participate in cell wall biosynthesis (Stewart *et al.*, 1971) and the regulation of the activity and synthesis of enzymes (Littauer and Inouye, 1973). In order to take part in these cellular processes, tRNAs must undergo numerous post-transcriptional processes prior to becoming fully functional. Such maturation events include 5' and 3' processing, splicing of introns (if present), the addition of a 3' cytidine, cytidine, adenosine sequence, and specific base or nucleoside modifications (Bjork *et al.*, 1987). To date, more than 80 modified nucleosides have been characterized in tRNAs with methylated nucleosides being the most abundant. Transfer RNA methyltransferases are the enzymes which are responsible for the transfer of methyl groups to specific positions in tRNAs during their biosynthesis. In yeast, N^2,N^2-dimethylguanosine-specific tRNA methyltransferase (m_2^2Gtase) has been shown to dimethylate a guanosine residue at position 26 (G_{26}) in cytoplasmic and mitochondrial tRNAs (Phillips and Kjellin-Straby, 1967; Smolar and Svensson, 1974). The DNA encoding m_2^2Gtase (*TRM1*) has been cloned and sequenced (Ellis *et al.*, 1987), and a yeast strain producing an inactive enzyme has been isolated (Phillips and Kjellin-Straby, 1967). Identification of the mutation(s) at the *TRM1* locus in this strain should provide important insights into the molecular mechanism of the enzyme.

1. The Structure of tRNA.

Transfer RNAs are relatively small and well characterized RNAs of known three-dimensional structure. The first nucleotide sequence of a tRNA was determined by Holley *et al.* (1965) for yeast $tRNA^{Ala}$. By predicting potential intramolecular base-pairing patterns, the cloverleaf secondary structure was derived (Holley *et al.*, 1965). The more than 2000 different tRNAs or tRNA genes that have been sequenced from a wide range of organisms have revealed that the cloverleaf pattern, which allows for a maximum of base pairing (~60%), remains the paradigm of tRNA structure. This cloverleaf secondary structure is shown in Figure 1. In general, all tRNAs share the following features: a) they are single chains containing between 65 and 93 ribonucleotides each, b) they contain many modified bases, typically between 7 and 23 per molecule, c) the 5' end of tRNAs is phosphorylated and the 5' terminal residue is guanosine, d) the base sequence at the 3' end of tRNAs is 3' cytidine, cytidine, adenosine (CCA), and e) about half of the nucleotides in tRNAs are base paired to form double helices. The five groups of bases that are not base paired form the 3' CCA terminal region, the ribothymine-pseudouracil-cytosine (TΨC) loop, the "extra arm" which contains a variable number of residues, the DHU loop which contains several dihydrouracil residues, and the anticodon loop (Figure 1).

The three-dimensional structure of yeast $tRNA^{Phe}$ was first solved in 1974 from X-ray crystallographic studies conducted by Klug and Rich (Robertus *et al.*, 1974; Chen *et al.*, 1975). The tertiary structure is L-shaped, compact, and highly ordered (Figure 2). This model confirmed that the base pairing in the cloverleaf pattern postulated on the basis of sequence studies was correct. X-ray analyses of other prokaryotic and eukaryotic tRNAs have shown that their molecular architecture follows this same plan.

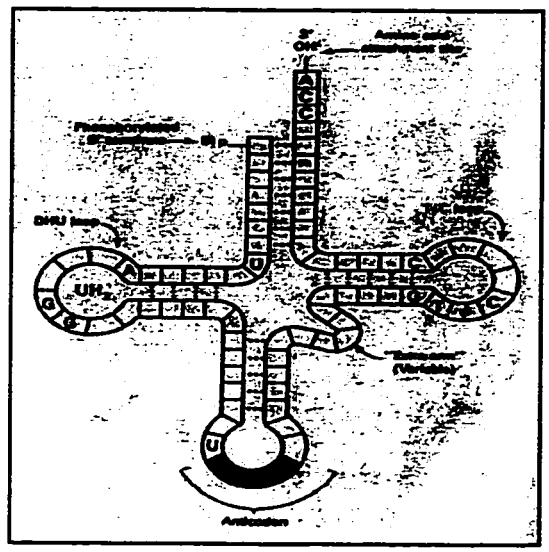

Figure 1. Structure of tRNA Molecule. The structure (Stryer, 1988) is based on the cloverleaf model proposed by Holley *et al.* (1965).

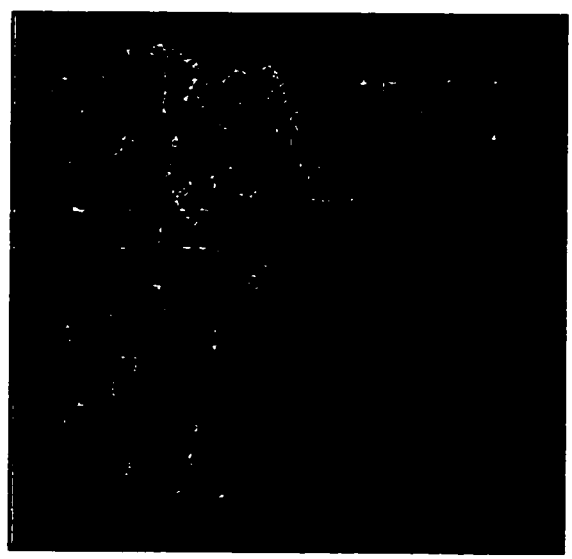

Figure 2. Three Dimensional L-Shaped Structure of Yeast Phenylalanine tRNA (Robertus *et al.*, 1974; Chen *et al.*, 1975). The structure (Stryer, 1988) is based on an electron-density map at 3-Å resolution.

2. The Biosynthesis of tRNA.

In all prokaryotic and eukaryotic systems examined to date, tRNAs are not synthesized directly as mature functional molecules, but arise from processing and modification of precursor tRNA molecules transcribed from tRNA genes. In eukaryotic systems, tRNA precursors are synthesized by RNA polymerase III from single tRNA genes as monocistronic transcripts (Hopper, 1978), although some dimeric precursors have been found (Schmidt *et al.*, 1980). These primary transcripts undergo a series of enzymatic reactions which cleave, trim, and splice the precursors, as well as reactions which add terminal nucleotides and which modify specific nucleoside residues. More specifically, maturing of eukaryotic precursor tRNAs involves; a) endonucleolytic processing of the 5'-leader sequence yielding a tRNA with a 5'-phosphate, b) removal of the 3'- trailer sequence by endonucleolytic cleavage or exonuclease action, c) 3' end-addition of CCA by ATP(CTP):tRNA nucleotidyltransferase, d) the splicing of introns if present, and e) modification of specific nucleoside residues (Bjork *et al.*, 1987). Maturation events involving nucleoside modifications will be further examined here.

3. Modified Nucleosides in tRNA.

The tRNA molecule is unique among other cellular RNA species because its primary structure contains a large number of modified nucleosides. The chain lengths of tRNAs vary between 65 and 93 nucleotides, and the content of modified bases can reach 25 percent (Grosjean *et al.*, 1995). Modified nucleosides in tRNAs were first identified in the late 1940's (Hotchkiss, 1948) and to date, more than 80 different modified

nucleosides have been identified in tRNA (Bjork, 1995). Among the majority of modifications are methylation (m), pseudo- (Ψ) and dihydrouridylation (D), and thiolation (s) (Bjork *et al.*, 1987). Other naturally occurring nucleosides contain hyper-modifications, which result from the attachment of a more complex side chain to the major nucleoside. Most modified nucleosides are introduced by modification at specific positions of a specific precursor tRNA by specific enzymes. The modified nucleosides D, Ψ, Um (2'-*O*-methyluridine), ac^4C (*N*^{4}-acetylcytidine), Cm (2'-O-methylcytidine), m^1G (1-methylguanosine), m^7G (7-methylguanosine), Gm (2'-O-methylguanosine), m^1A (1-methyladenosine), t^6A (*N*-[*N*-(9-β-D-ribofuranosylpurin-6-yl)carbamoyl]threonine), mt^6A (*N*-[(9-ß-D-ribofuranosylpurin-6-yl)*N*-methylcarbamoyl]threonine), and I (inosine) are present in tRNAs from the three phylogenetic kingdoms Archaebacteria, Eubacteria, and Eukaryotes (Figure 3) (Bjork *et al.*, 1987). Some modified nucleosides are, however, specific to a particular kingdom, suggesting that these nucleoside modifications have been introduced after the three phylogenetic kingdoms split (Bjork *et al.*, 1987). The range of nucleoside modification varies from organism to organism with eukaryotic tRNAs containing the largest variety and abundance of modified nucleosides (Bjork *et al.*, 1987).

The structural complexities of many modified nucleosides, their locations at specific sites in the tRNA molecule, and their presence in a wide variety of organisms enforce the fact that they play an important role in tRNA function. However, most of the modifications are not likely to be essential for viability, but instead play important roles in modulating tRNA properties. Persson (1993) summarizes the possible roles for some modifications that have been elucidated. For instance, the presence of a modified

nucleoside may be involved in; a) improving the efficiency of the tRNA in the decoding event, b) influencing the fidelity of protein synthesis, c) maintaining the correct reading frame during protein synthesis, and d) playing some role in intermediary metabolism, development, or the cell cycle. Despite the fact that the role of the majority of modified nucleosides still remains obscure, the above examples suggest that tRNA modification may act as a regulatory device (Persson, 1993).

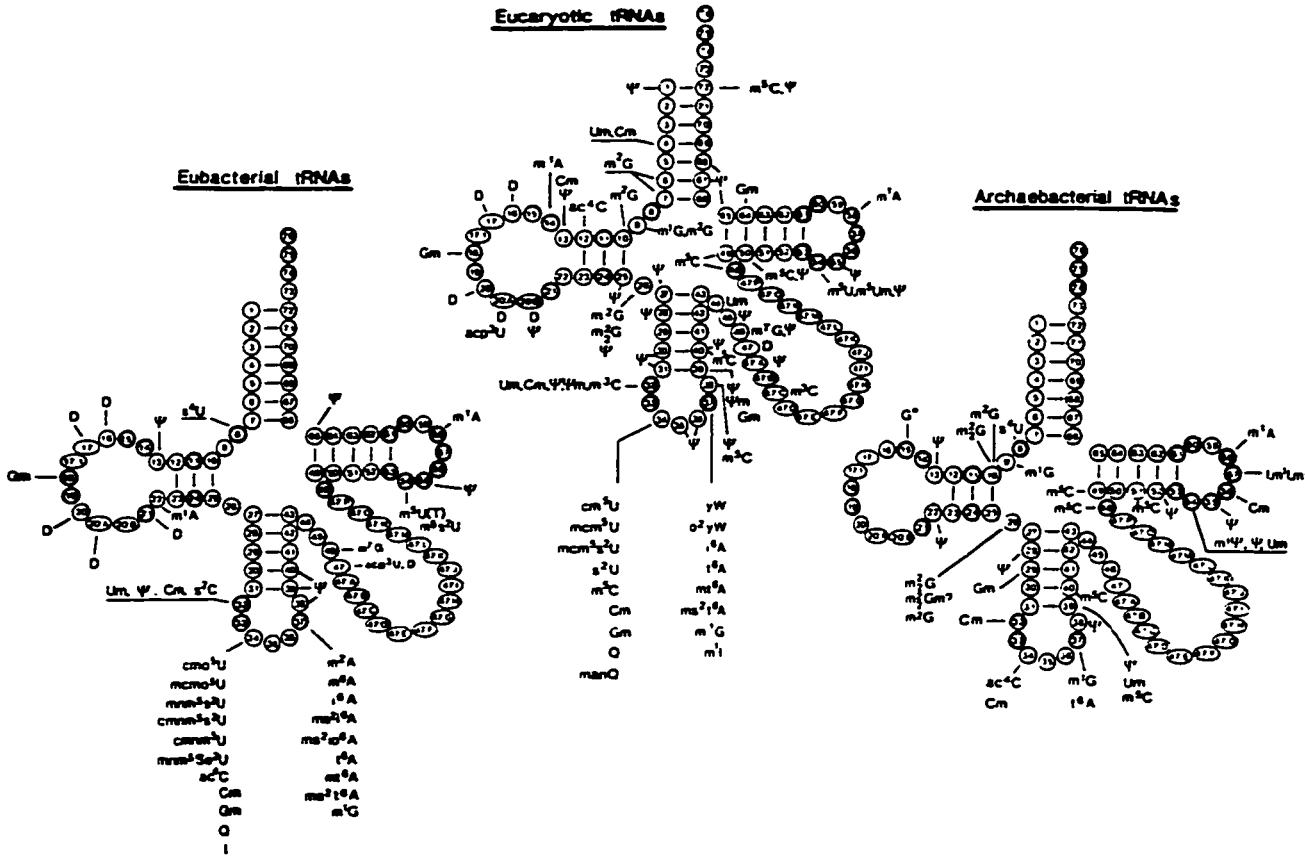

Figure 3. Modified Nucleosides Present in tRNA from Eubacteria, Eukaryotes and Archaebacteria (Bjork *et al.*, 1987).

4. tRNA Methylations.

The methylation of nucleosides represents a major modification step in tRNA maturation. Although the biological roles of these methylations are not clearly defined, the methylated nucleosides account for 30-70% of the modified nucleosides in tRNA (Nau, 1976). This methylation process is catalyzed by a number of specific enzymes which belong to the tRNA methylase class. The existence of these enzymes capable of methylating certain bases in tRNA was first shown by Fleissner and Borek (1962). The methylases are base specific and site specific, and transfer methyl groups from S-adenosylmethionine (SAM) to specific nucleosides. There may be single or multiple modifications of either purine or pyrimidine bases, or the 2' hydroxyl group of ribose. Methyl groups are also present in the structure of hyper-modified nucleosides. More than 20 methylated nucleosides have been identified in tRNA (Hall and Dunn, 1975), and Table 1 lists several of these methylated nucleosides and compares their relative amounts in different cell types (Salvatore, 1977).

The exact biological role of methylated nucleosides is not entirely understood. Several attempts have been made to elucidate the function of methylated nucleosides with very little progress. These experiments were conducted *in vitro* with undermethylated tRNA (not a homogeneous unmethylated population) obtained from *E. coli* methionine auxotrophs during methionine starvation (Borek *et al.*, 1955). In spite of some useful results in uncovering the biosynthetic pathway of methylated nucleosides, the methods were not selective or specific enough to unravel the specific roles of these modified nucleosides. The most interesting results have come from the isolation of mutants with

altered tRNA methylase activity. This is a difficult task, since there is no known effect of tRNA methylation which might be used as a selection method. Mutant strains of *E. coli* lacking ribothymidine (Bjork and Isaksson, 1970) and 7-methylguanosine (Marinus *et al.*, 1975), and of *S. cerevisiae* lacking N^2,N^2-dimethylguanosine in their tRNAs (Phillips and Kjellin-Straby, 1967), have been isolated by a batch screening technique. The tRNAs extracted from these organisms are very different from those obtained after methionine starvation in that they specifically lack one methylated nucleoside, and are otherwise perfectly normal. Such mutants are useful tools for studying the effects of loss of methylation at specific sites in tRNAs.

	Relative Amounts		
Methylated Nucleosides	**HeLa**	**Yeast**	***E. coli***
1-methylguanosine and 7-methylguanosine	21.1	22.9	43.6
1-methyladenosine	19.9	12.5	-
N^2-methylguanosine	11.9	16.7	-
N^2,N^2-dimethylguanosine	17.5	24.9	-
1-methylinosine	3.1	1.1	-
5-methylcytidine	16.5	7.8	-
5-methyluridine	10.0	14.1	36.5
2-methyladenosine	-	-	19.8
3-methyluridine	+	-	-
2'-*O*-methyluridine	+	+	-
2'-*O*-methylcytidine	+	+	-
3-methylcytidine	+	-	-
N^6-methyladenosine	-	-	-

Table 1. Methylated Nucleosides in tRNA of Eukaryotic and Prokaryotic Cells. The figures indicate the percentage of each methylated nucleoside relative to the total amount (data compiled from Salvatore, 1977). The symbol + refers to suggested trace presence.

5. The Occurrence of $m_2^2G_{26}$ in tRNA.

The occurrence of methylated guanines from several sources was first reported by Smith and Dunn (1959). The modified base N^2,N^2-dimethylguanosine (m_2^2G) is almost always present in tRNA from higher organisms but has not been found in tRNAs from eubacteria such as *E. coli* (Table 1). However, in archaebacterial tRNAs, m_2^2G is present at position 10 and 26 (Bjork *et al.*, 1987). In eukaryotes, m_2^2G is found in almost all tRNAs (cytoplasmic, mitochondrial and chloroplastic) having a guanosine at position 26 (G_{26}) at the junction between the D-stem and the anticodon stem (Figure 4) (Edqvist *et al.*, 1995). Out of 129 eukaryotic nucleus encoded tRNAs with guanosine-26, 103 (80%) have $m_2^2G_{26}$, 17 (13%) have m^2G_{26} and only 9 tRNAs (7%) have an unmodified G_{26} (Edqvist *et al.*, 1995).

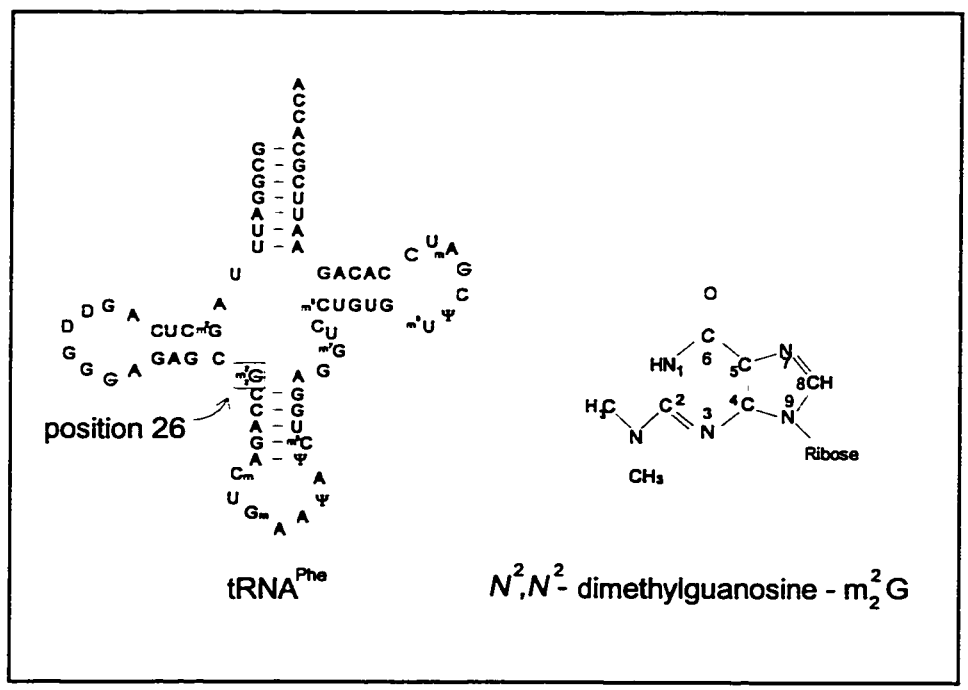

Figure 4. Location and Structure of N^2,N^2-dimethylguanosine (m_2^2G) in Yeast $tRNA^{Phe}$.

6. The Possible Role of $m_2^2G_{26}$

In yeast, a mutation in the structural gene for the enzyme responsible for the $m_2^2G_{26}$ modification, results in no phenotype other than the lack of $m_2^2G_{26}$ in mitochondrial and cytoplasmic tRNAs (Phillips and Kjellin-Straby, 1967; Smolar and Svensson, 1974). Therefore, this modified nucleoside is not essential for the yeast when growing under standard laboratory conditions. The role of $m_2^2G_{26}$ in relation to structure-function relationships of tRNA was investigated in the extremely thermophilic Archaean *Pyrococcus furiosus* (Kowalak *et al.*, 1994). The levels of modified nucleosides in hydrolysates of unfractionated tRNAs from *P. furiosus* grown at 70, 85, and 100°C were determined by directly combined liquid chromatography-mass spectrometry. In this study, the level of certain modified nucleosides, including m^2G_{26}, $m_2^2G_{26}$ and $m_2^2Gm_{26}$ (N^2,N^2,2'-*O*-trimethylguanosine) was shown to be correlated with the enforced greater thermostability of selected tRNA molecules. Earlier work involving three-dimensional models of yeast $tRNA^{Phe}$ derived from X-ray crystallographic data also suggested that $m_2^2G_{26}$ functions as a molecular hinge (Holbrook *et al.*, 1978; Sussman *et al.*, 1978). This hinge adjusts the angular position of the D-stem and the anticodon stem during protein synthesis, thus maintaining a certain rigidity/flexibility that may facilitate the interactions of the tRNAs with various macromolecules within the cell. Nuclear magnetic resonance studies on the resonance of the methyl proton in yeast $tRNA^{Phe}$ also provided evidence to support the notion that $m_2^2G_{26}$ has an important role in regulating the stacking and the conformational dynamics of this region of the tRNA molecule (Boyle *et al.*, 1980). However, it should be noted that $m_2^2G_{26}$ may not be essential for the hinge since the yeast $tRNA^{Asp}$ does not contain this modified nucleoside and displays practically the same hinge conformation as yeast $tRNA^{Phe}$ (Moras *et al.*, 1980). A more recent study has

proposed that the presence of $m^2_2G_{26}$ in cytosolic tRNAs may prevent the molecule from adopting an unusual mitochondrial tRNA pattern folding and instead, allow it to fold into the canonical cloverleaf model (Steinberg and Cedergren, 1995). Through screening the tRNA and tRNA gene database, it was demonstrated that some cytosolic tRNAs have the potential to fold into alternate structures. It was further noted that when a tRNA had the potential for this alternate folding, m^2_2G was found at positions 10 and 26 presumably to block the formation of this non-standard folding pattern.

7. *N*^{2},*N*^{2}-Dimethylguanosine-Specific Methyltransferase (m^2_2Gtase).

The enzyme, *N*^{2},*N*^{2}-dimethylguanosine-specific tRNA methyltransferase (m^2_2Gtase), is responsible for the formation of $m^2_2G_{26}$ in tRNA. It catalyzes the transfer of methyl groups from two molecules of S-adenosylmethionine to the nitrogen at position 2 of guanosine-26 in tRNAs (Figure 5). The formation of $m^2_2G_{26}$ may be catalyzed in a one-step or two-step process. In a heterologous system, incubating purified m^2_2Gtase from *Tetrahymena pyriformis* with *E. coli* tRNA devoid of $m^2_2G_{26}$, resulted in the accumulation first of the monomethylated form of G_{26} (m^2G_{26}) and subsequently the dimethyl derivative (Reinhart *et al.*, 1986). It was concluded that the enzymatic formation of $m^2_2G_{26}$ is a two-step process which requires dissociation of the enzyme from the monomethylated tRNA intermediate. However, evidence for a one-step reaction was provided when a homologous system using partially purified yeast m^2_2Gtase and yeast tRNA was employed. Enqvist *et al.*(1994) showed that the dimethylation reaction was so efficient that no m^2G_{26}

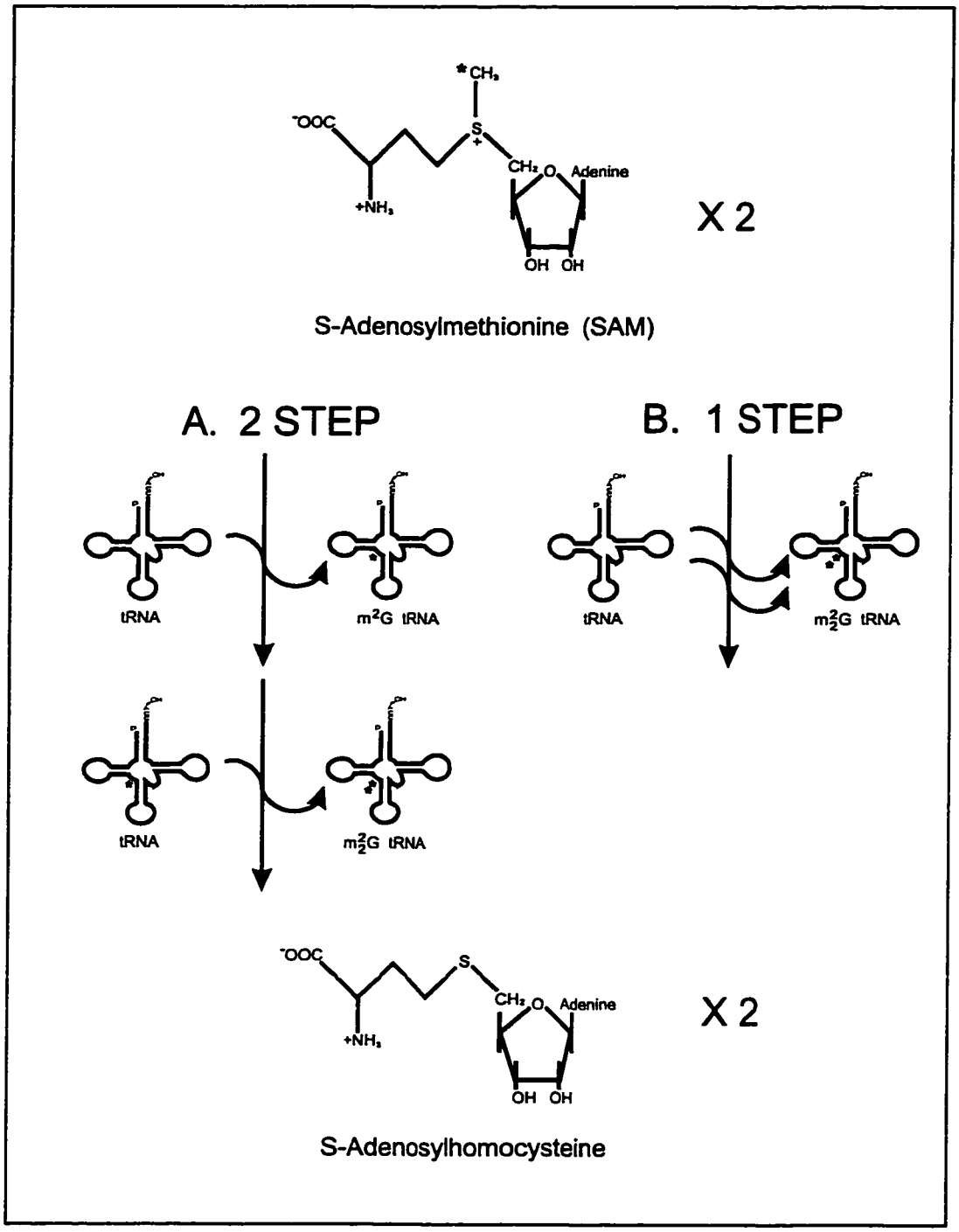

Figure 5. The Reaction Catalyzed by N^2,N^2-Dimethylguanosine-Specific tRNA Methyltransferase (m^2_2Gtase). Each of the methyl groups on the N_2 atom of guanosine-26 arises from S-adenosylymethionine (SAM). The asterisk denotes the tritium labelled methyl group transferred from SAM to tRNA.

intermediate was detectable. Based on this, it was proposed that the enzymatic formation of $m_2^2G_{26}$ involved a single tRNA-enzyme association event without the release of the intermediate monomethylated product. Each of the two methylation reactions might be catalyzed either by a distinct subunit or by one of the subunits of a multi-enzyme complex. Edqvist *et al.* (1995) suggest that the presence of monomethylated G_{26} may result when the tRNA dissociates from the enzyme after the first methylation if the molecule does not bind tightly enough to the enzyme. This may explain the accumulation of the monomethylated form as seen by Reinhardt *et al.* (1986) in a heterologous system utilizing *E. coli* tRNA and the *Tetrahymena* enzyme.

Recently, emphasis has been placed on investigating what characteristics of a tRNA molecule the yeast m_2^2Gtase recognizes in order for the N^2,N^2-dimethylation of G_{26} to occur. Although G_{26} is a prerequisite for the biosynthesis of $m_2^2G_{26}$, it is in itself not sufficient for the formation of m_2^2G since in some cases eukaryotic tRNAs have an unmodified G_{26}. Despite the fact that *S. cerevisiae* contains an m_2^2Gtase able to catalyze the formation of $m_2^2G_{26}$, yeast $tRNA^{Asp}$ does not contain such a base modification. The structural elements in tRNA required for modification by yeast m_2^2Gtase were investigated by using yeast $tRNA^{Asp}$ transcripts in a homologous *in vitro* system (Edqvist *et al.*, 1992). When mutations were introduced into a synthetic yeast $tRNA^{Asp}$ gene such that the nucleotides in positions 11, 24, and 25 of the D-stem were changed to those found in yeast $tRNA^{Phe}$ (Figure 6), methylation at G_{26} occurred. Furthermore, when $tRNA^{Phe}$ which normally contains G_{26} was altered such that two G-C base pairs in the D-stem were

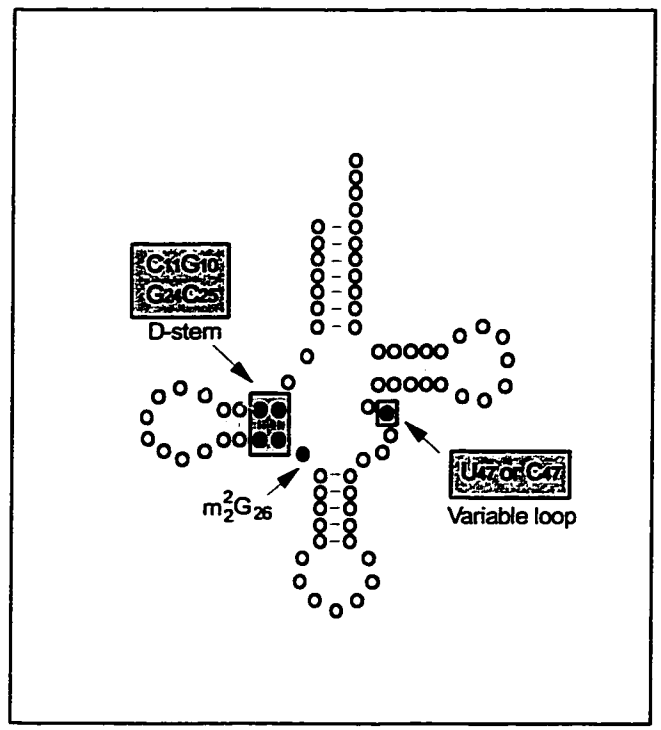

Figure 6. The tRNA Identity Elements for $m_2^2G_{26}$ Modification by N^2,N^2-Dimethylguanosine-Specific tRNA Methyltransferase. The consensus nucleotides of m_2^2G containing eukaryotic tRNAs are in boxes and the black dots correspond to the positions discussed in the text.

exchanged for the two corresponding ones in $tRNA^{Asp}$ and the variable loop was decreased to four bases, the dimethylation of G_{26} no longer occurred. Based on these results, the recognition signals for the N^2,N^2-dimethylation of G_{26} were determined to be: (i) a consensus G_{24}-C_{25} base paired with G_{10}-C_{11} in the D-stem, and (ii) a variable loop consisting of at least five nucleotides (Figure 6). Crystallographic data of both yeast $tRNA^{Phe}$ (Holbrook *et al.*, 1978; Sussman *et al.*, 1978) and $tRNA^{Asp}$ (Moras *et al.*, 1980) reveal that the amino group at position 2 of G_{26} is more buried in $tRNA^{Asp}$ than in $tRNA^{Phe}$. Thus, the introduction of the above elements may influence the G_{26} dimethylation by introducing local structural changes in the tRNA to make the amino group more accessible to the enzyme, rather than being directly involved in base-specific interactions with the methyltransferase (Edqvist *et al.*, 1995).

Detailed studies on the m^2_2Gtase mechanism have proven difficult as the enzyme appears to be relatively unstable (Saridakis, 1995) and is present in low levels in the yeast cell (Rose *et al.*, 1992). The only native m^2_2Gtase that has been purified to homogeneity is from the protozoan *Tetrahymena pyriformis* (Reinhart *et al.*, 1986). The molecular mass of this enzyme was estimated to be 200 kDa by gel filtration, and 240-250 kDa by nondenaturing electrophoresis on polyacrylamide gel. In yeast, m^2_2Gtase is responsible for the modification of both nucleus and mitochondria encoded tRNAs (Smolar and Svensson, 1974; Hopper *et al.*, 1982; Ellis *et al.*, 1986). Immunolocalization studies suggest that the enzyme is localized to the periphery of the nuclear inner membrane as well as to mitochondria, but is below the level of detection by this method in the cytoplasm (Rose *et al.*, 1992).

8. The *TRM*1 Gene.

Although m_2^2Gtase has yet to be purified from yeast, the gene encoding this enzyme (*TRM*1) has been cloned and sequenced. The nucleotide sequence of the *TRM*1 gene reveals an open reading frame of 570 amino acids capable of coding for a protein with a predicted molecular mass of 63 kDa. Heterologous expression of the *TRM*1 gene in *E. coli* leads to the formation of $m_2^2G_{26}$ in several *E. coli* tRNAs (Ellis *et al.*, 1986). Since *E. coli* lacks this enzyme and the $m_2^2G_{26}$ modification is not present in *E. coli* tRNAs, these results demonstrate that the *TRM*1 gene product has the ability to catalyze the transfer of both methyl groups to G_{26} in tRNA.

The yeast *TRM*1 gene is also of interest because it produces functionally similar enzymes that are targeted to different cellular compartments. *TRM*1 is responsible for the modification of G_{26} to $m_2^2G_{26}$ in both nuclear and mitochondrial tRNAs (Hopper *et al.*, 1982), and the methyltransferase protein is known to be transported into the yeast nucleus as well as into yeast mitochondria (Rose *et al.*, 1992). The enzyme, therefore, must contain the information necessary for its dual localization within the cell. The role of the m_2^2Gtase amino-terminal sequences in mitochondrial protein import is well established. The gene contains two in-frame ATGs and can produce two forms of the enzyme which differ in the presence or absence of 16 amino-terminal amino acids depending on which ATG is used as the start site for translation (Ellis *et al.*, 1987). Data derived from mutagenesis and *in vitro* and *in vivo* import studies showed that both forms of the enzyme contain functional mitochondrial targeting information although the enzyme containing the 16 additional amino terminal residues is more efficiently imported into the

mitochondrion (Ellis *et al.*, 1989). Furthermore, amino acids 95 to 102 (KKSKKKRC) were demonstrated to be necessary and sufficient for the nuclear localization of the enzyme (Rose *et al.*, 1992).

9. The Mutant *trm*1 Gene.

In yeast, the *trm*1 mutation results in the lack of $m_2^2G_{26}$ in tRNAs in the cytosol and mitochondria (Phillips and Kjellin-Straby, 1967; Smolar and Svensson, 1974). Strains carrying this *trm*1 mutation do not show any detectable physiological phenotype for any criteria tested other than the loss of methyltransferase activity. It has been demonstrated that the lack of m_2^2G at position 26 seems to have no effect on the growth rate of mutant cells (Hopper *et al.*, 1982). The yeast strain bearing the *trm1* mutation was generated by UV and X-ray treatment of a wild-type *S. cerevisiae* strain. The resulting D38 strain containing the *trm*1 lesion (Phillips and Kjellin-Straby, 1967) was mated to a commonly used strain J15-13C (Hopper *et al.*, 1980) yielding the meiotic segregant, SN1015-2a. The SN1015-2a strain is a uracil auxotroph and carries the *trm*1 allele. Although this strain lacks m_2^2G at position 26 in its tRNAs, it does produce protein that cross reacts with an antibody raised to the 16 C-terminal amino acids of yeast m_2^2Gtase (Li *et al.*, 1989). The presence of a protein of the expected size suggests that a missense mutation or a small in-frame deletion is responsible for the lack of enzyme activity. To date, neither the *trm*1 gene nor the mutant m_2^2Gtase have been characterized further.

10. tRNA and S-Adenosyl-Methionine Substrates and Enzyme Mechanisms.

In spite of what is known about the *TRM1* gene product in terms of its localization patterns and its tRNA identity elements, little is known about how m_2^2Gtase interacts with its two substrates, tRNA and SAM. Furthermore, no tRNA methylase has been crystallized or co-crystallized with its RNA or SAM substrate. Studies have suggested that there are different modes of RNA recognition by the modifying enzymes (Gu and Santi, 1991; Holmes *et al.*, 1992). Some enzymes require an intact three-dimensional structure of their substrates, as in the case of *E. coli* tRNA (m^1G) methyltransferase (Holmes *et al.*, 1992), while others, such as *E. coli* tRNA (m^5U54) methyltransferase (Gu and Santi, 1991), are only dependent on fragments of RNA molecules. There is a wealth of information regarding SAM in terms of its binding motifs in methyltransferases (Wu *et al.*, 1992; Kagan and Clarke, 1994; Hamahata *et al.*, 1996). There also has been a recent focus on the interaction of DNA methyltransferases with SAM. For example, the crystal structures of the *Hha*I DNA methyltransferase (Kumar *et al.*, 1992; Cheng *et al.*, 1993) and adenine-specific methyltransferase M.*Taq* I (Labahn *et al.*, 1994) complexed with SAM were recently obtained. The mechanisms of only a few RNA modification enzymes are known (Gu and Santi, 1992; Takata *et al.*, 1994). The best known mechanism is from tRNA (m^5U54)methyltransferase which catalyzes the methylation of uridine-54 of tRNA through a covalent enzyme-uracil intermediate by SAM (Gu and Santi, 1992). The enzymatic mechanism, including the stereochemical course of the methylation reaction and the enzyme-tRNA interaction are reviewed by Kealey *et al.* (1994).

11. Objectives.

Although the tRNA methyltransferases were discovered over 30 years ago, purification of the enzymes has been slow, thus inhibiting their study. To date, most studies have investigated the structural features of yeast tRNAs that are required for specific methylation, but have yet to examine the methylases themselves with respect to their molecular mechanisms of action. The availability of the mutant *S. cerevisiae* strain SN1015-2a, which was shown to produce a non-functional tRNA m_2^2Gtase, may enable a study of the methylase enzyme itself to be initiated. SN1015-2a mutant m_2^2Gtase is a prime candidate for this study because it is believed that point mutation(s) in the gene are responsible for the lack of enzyme activity. It would be of interest to define these mutations to determine whether or not they suggest a role for specific amino acids in the structure or function of the enzyme. The purpose of this work was to characterize m_2^2Gtase by: 1) isolating the mutant *trm*1 gene, 2) attempting to identify the amino acid residue(s) of the mutant m_2^2Gtase responsible for loss of enzyme activity, and 3) defining the roles of these residues.

Materials and Methods

II. MATERIALS AND METHODS

1. Yeast Strains.

The yeast strains employed were SN1015-2a (*MAT*α-*sup*4 *trm*1 *trm*2 *gal*1 *gal*7 *ade*2-1 *leu*1 *ura*3 *met lys*2-1 *tyr ura*3-1), W303-1b (*MAT*a *ade*2-1 *his*3-11,15 *leu*2-3,112 *ura*3-1 *trp*1-1 *can*1-100), DBY745 (*MAT*α *leu*2-3 *ura*3-52 *ade*1-101), and DBY745ΔTRM (*trm*1:: *Leu*2 *MAT*α *leu*2-3 *ura*3-52 *ade*1-101). Other strains assayed for m_2^2Gtase activity were *Kluyveromyces lactis* CBS2360/7, *Candida glabrata* CBS138, *Saccharomyces exiguus* CBS379, *Schizosaccharomyces pombe* CBS972 and *Sarcomycopses fibuligera*. Yeast strains were maintained on YPD or selective medium minus the appropriate nutritional ingredient for selection of plasmid expression. These strains were kindly provided by Dr. N.C. Martin (University of Louisville) with the exception of *S. pombe* which was obtained from Dr. G.C. Johnston (Dalhousie University).

2. *E. coli* Strains.

E. coli strains used to propagate plasmids and for site-directed mutagenesis were:

JM83 - *ara* Δ*(lac-pro) rpsL thi* ϕ80 d*lacZ*ΔM15)

JM101 - *supE thi* Δ(l*ac-proAB*)

F'[*traD*36 *proAB*$^+$ *lacI*^{q} *lacZ*ΔM15]

JM105 - *sup*E *end*A *sbcB*15 *hsdR*4 r*psL thi* Δ(*lac-proAB*)

F'[*traD*36 *proAB*$^+$ *lacI*^{q} *lacZ*ΔM15]

CJ236 - *dut*1 *ung*1 *thi*-1 *relA*1/pCJ105(cam^{r}F')

3. Plasmids.

(i) YCp50TRMXba2-3: YCpTRMXba2-3 was provided by Dr. N. C. Martin (University of Louisville). A fragment containing 532 bp upstream and 1890 bp downstream of the first ATG of the wild-type *TRM1* allele was inserted into the *Eco*RI and *Hin*dIII sites of the yeast shuttle vector YCp50 and an *Xba*I site was introduced immediately upstream of the first in-frame start codon (Ellis *et al.*, 1987).

(ii) YCpPJMR4: The *TRM1* allele from YCp50TRM*Xba*2-3 was inserted into the *Eco*RI and *Sal*I sites of a modified YCp50 vector (Figure 7a). YCp50 was modified by the removal of a 1559 bp *Hpa*I/*Sma*I fragment and by filling in the *Xho*I site at position 4705.

(iii) YCpPJMR9: YCpPJMR4 was modified such that a 1114 bp *Bam*HI fragment (bases 636 to 1751 of the original *TRM1* sequence) and an *Ava*I/*Sal*I fragment from the 3' noncoding region of the *TRM1* gene were removed (Figure 7a).

(iv) pTRMPCR1-3' and pTRMPCR2-3': The 1114 bp *Sau*3AI fragment containing the three mutations found at the 3' end of the PCR1 or PCR2 product (bases 636 to 1751 of the original *TRM1* sequence) was inserted into the *Bam*HI site of YCpPJMR9. Plasmids containing either of the hybrid *TRM1*/PCR products were digested with *Eco*RI and *Eco*RV and the corresponding fragments were inserted into the yeast shuttle vector YCp50 resulting in pTRMPCR1-3' and pTRMPCR2-3' (Figure 7b).

(v) pTRMPCR1-Arg: An *Eco*RI/*Hin*dIII fragment containing the *TRM1* allele from YCp50TRM*Xba*2-3 was moved into the pBluescriptII KS+ (BSKS) vector that had its *Apa*I site removed. The 242 bp *Apa*I/*Nco*I fragment of the WT *TRM1* gene containing Gly^{517} was replaced with the 242 bp *Apa*I/*Nco*I fragment from the *trm1* PCR1 product which contains Arg^{517}. The *TRM1* gene now harboring the Arg mutation was subsequently moved into YCp50 as an *Eco*RI/*Hin*dIII fragment resulting in the generation of pTRMPCR1-Arg (Figure 7c).

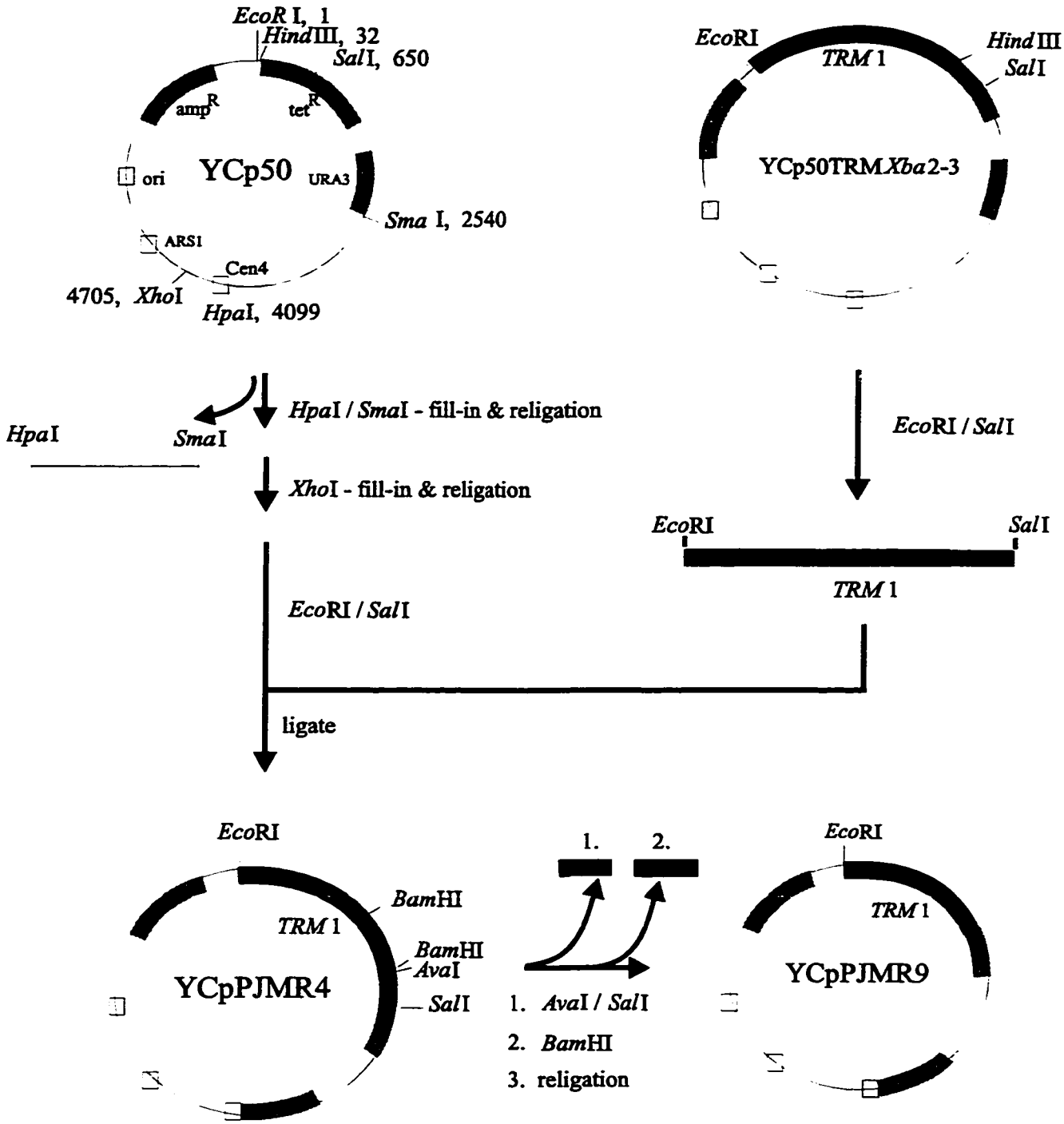

Figure 7a. Construction of Plasmids YCpPJMR4 and YCpPJMR9.

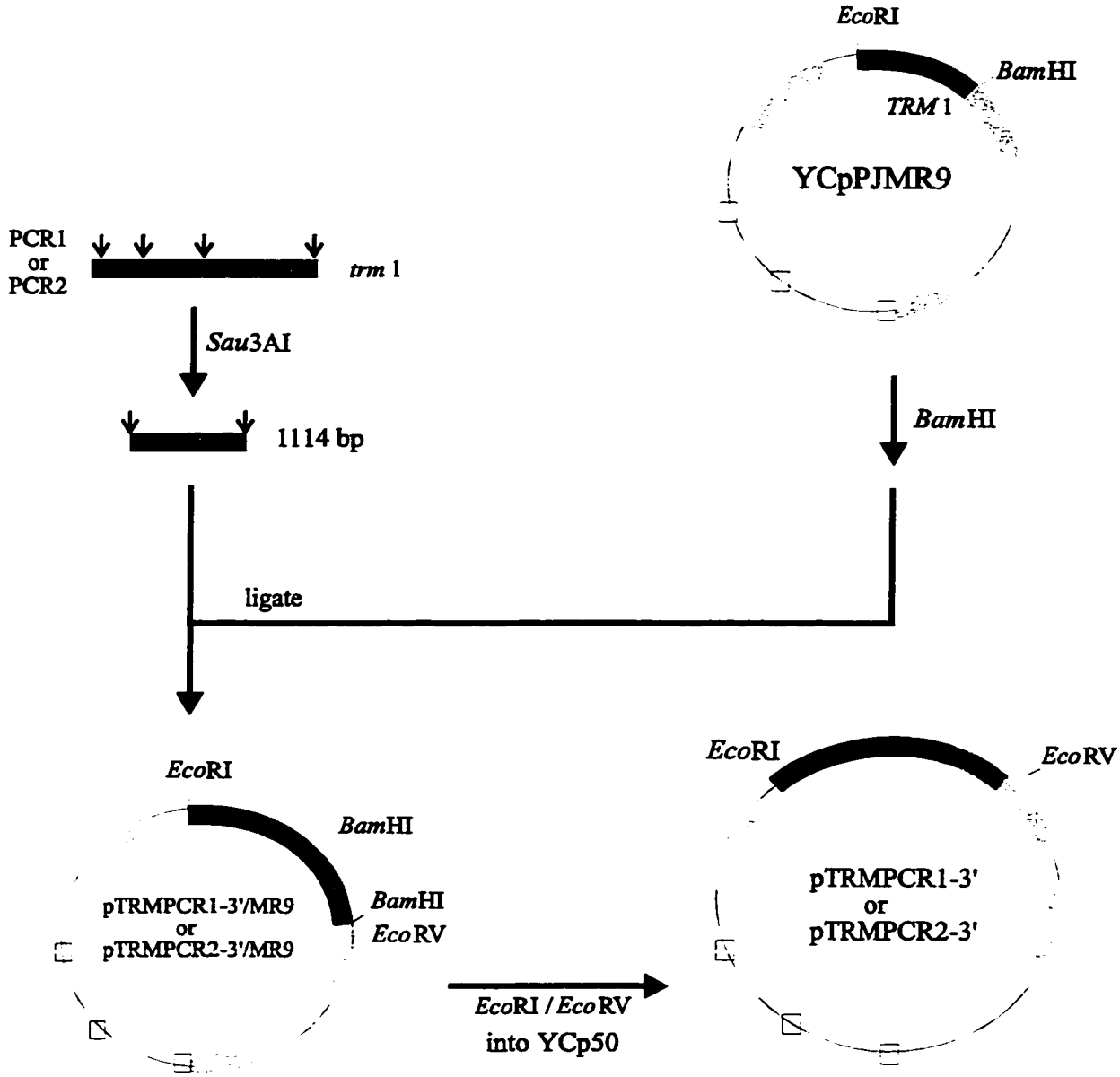

Figure 7b. Construction of Plasmids pTRMPCR1-3' and pTRMPCR2-3'.

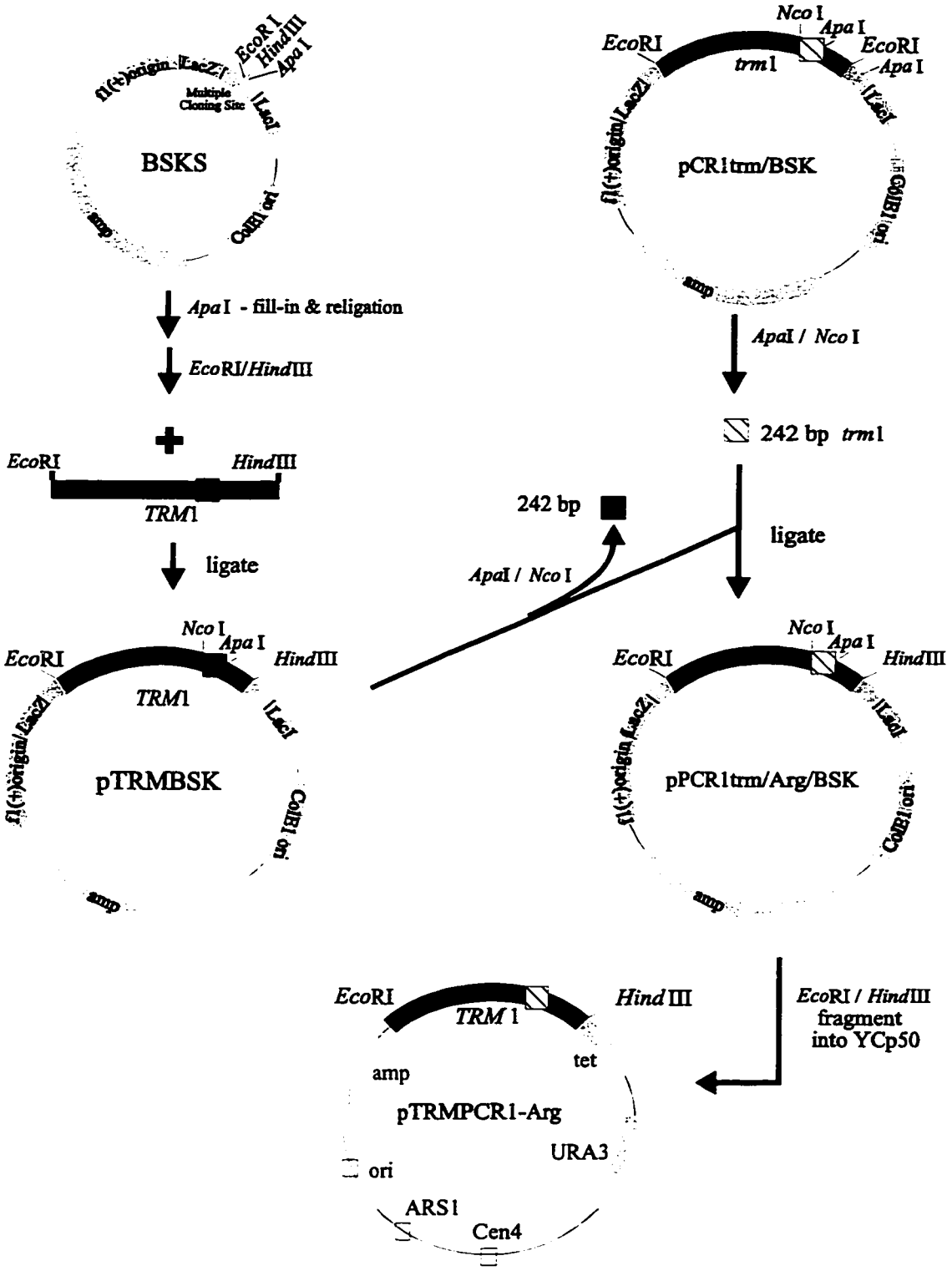

Figure 7c. Construction of Plasmid pTRMPCR1-Arg.

(vi) pTRMPCR1-Asn, pTRMPCR1-Ser and pTRMPCR1-Gly: The oligonucleotides employed to change Thr^{427} to Asn, Leu^{467} to Ser and Arg^{517} to Gly are listed in Table 2. The mutations in each case were carried out on a 1114 bp *Bam*HI fragment of *trm*1 DNA cloned into the *Bam*HI site of M13mp19. Screening was accomplished initially through enzyme restriction analysis and then sequencing was performed to confirm the presence of the desired mutations. After the screening process, the *Bam*HI fragment was isolated from phage replicative form DNA and re-inserted into the *Bam*HI site of YCpPJMR9. The resulting plasmids are: pTRMPCR1-Asn in which Thr^{427} was converted to the wild-type residue Asn, pTRMPCR1-Ser where Leu^{467} is changed to Ser, and pTRMPCR1-Gly where Arg^{517} is changed to Gly.

(vii) pTRMSer-Leu, pTRMSer-Ala, pTRMSer-Thr and pTRMSer-Cys: The oligonucleotides employed to change Ser^{467} to Leu, Ala, Thr, and Cys are listed in Table 2. The DNA modified in each case was a 1114 bp *Bam*HI fragment of *TRM*1 DNA cloned into the *Bam*HI site of M13mp19. Screening was accomplished by restriction enzyme pattern analysis and by sequencing. After the screening process, the *Bam*HI fragment was isolated from phage replicative form DNA and re-inserted into the *Bam*HI site of YCpPJMR9. Resulting plasmids are: pTRMSer-Leu, pTRMSer-Ala, pTRMSer-Thr and pTRMSer-Cys.

#	5' Oligonucleotide 3'	Mutation	Restriction site introduced
1	CCACTCAACCA**CCCGGG**CATTGCCG	Arg^{517} → Gly	*Sma*I
2	TTGG**GCATGC**GTCAA**TGA**ACATTCAAA	Leu^{467} → Ser	*Sph*I
3	ATCGGA**G**AATTCA**T**TTTAGCTAGAG	Thr^{427} → Asn	*Eco*RI
4	TTGG**GCATGC**GTCAA**TAA**ACATTCAAAG	Ser^{467} → Leu	*Sph*I
5	TTGG**GCATGC**GTCAA**TGT**ACATTCAAAG	Ser^{467} → Thr	*Sph*I
6	TTGG**GCATGC**GTCAA**TGC**ACATTCAAAG	Ser^{467} → Ala	*Sph*I
7	TTGG**GCATGC**GTCAA**ACA**ACATTCAAAG	Ser^{467} → Cys	*Sph*I

Table 2. Oligonucleotides for Site-Directed Mutagenesis. Restriction sites introduced are underlined and base changes are bolded. Three nucleotides coding for amino acid changes are double underlined.

4. Yeast Growth Curves.

Yeast (W303-1b and SN1015-2a) were inoculated into 50 ml YPD (2% Bacto-yeast extract, 1% peptone, 2% dextrose) or SC medium (0.67% Bacto-yeast nitrogen base w/o amino acids, 2% dextrose, 20 mg/l of uracil, adenine, L-tryptophan, L-histidine, L-arginine and L-methionine, 30 mg/l of tyrosine, leucine, isoleucine and lysine, 50 mg/l of phenylalanine, 100 mg/l of glutamic acid, and 200 mg/l threonine) (Sherman, 1991) and incubated at 30°C with constant agitation. Cells were grown to a starting OD_{640} of 0.1 which corresponded to t=0. Aliquots (1 ml) were then taken at one hour intervals for 8 consecutive hours and OD_{640} readings were recorded. Growth rates were measured in duplicate on two separate days.

5. Genomic Yeast DNA.

The procedure is described by Philippsen *et al.* (1991). Yeast cells from SN1015-2a were grown in 30 ml YPD at 30°C to an OD_{640} of 0.6. Cells were harvested at 3024 X*g* for 5 min at 4°C. The cells were resuspended in 10 ml dH_2O, pelleted at 3024 X*g* for 5 min, and then resuspended in 3 ml 0.9 M sorbitol / 0.1 M EDTA / 50 mM dithiothreitol (DTT), pH 7.5. To the suspension, 0.5 mg of Zymolase 20 000 (ICN Biomedicals, Ca.) dissolved in 200 µl 0.9 M sorbitol was added and incubated at 37°C with occasional shaking until the OD_{640} decreased by 80-90%. The resulting spheroplasts were centrifuged at 3024 X*g* for 5 min and resuspended in 3.0 ml 50 mM Tris·HCl / 50 mM EDTA, pH 8. Spheroplasts were incubated at 65°C for 30 min after the addition of 0.3 ml 10% SDS. Subsequently, 1.0 ml 5 M KOAc was added to the mixture with incubation on ice for 1

hour followed by a 30 min centrifugation at 23 708 X*g*. The supernatant was collected and DNA precipitated with 2 volumes of 99% EtOH. DNA was collected by centrifugation at 12 096 X*g* for 10 min. The pellet was washed with 80% EtOH and dried under vacuum. Nucleic acids were redissolved in 3.0 ml TE (10 mM Tris·HCl, 1 mM EDTA, pH 7.5) and then incubated with 150 µl of 1 mg/ml RNase at 37°C for 30 min. DNA was precipitated with an equal volume of isopropanol, and the resulting pellet was washed with 50% isopropanol, dried under vacuum and then redissolved in 0.5 ml TE. Yeast genomic DNA was stored at -20°C.

6. <u>Oligonucleotide Synthesis</u>

Oligonucleotides were synthesized in house using the Applied Biosystems DNA Synthesizer. DNA was eluted from the synthesis columns with 3 X 1 ml aliquots of ammonium hydroxide and incubated at 55°C overnight. The DNA was then lyophilized for 2 hours. The dried DNA pellet was resuspended in 500 µl dH_2O, lyophilized and resuspended in a minimal amount of dH_2O (50 -100 µl). Table 2 lists the oligonucleotides synthesized for site-directed mutagenesis along with the corresponding restriction sites that were introduced. Table 3 lists the oligonucleotides synthesized for PCR amplification of *trm*1.

#	5' Oligonucleotide 3'	Region of *TRM*1	
1	GCTCATCGCAAACTTAC	5'	-65 to -48
2	GATCCTTAGTTTCTTAC	3'	+1741 to +1758

Table 3. Oligonucleotides for the PCR Amplification of the *trm*1 Gene.

7. Phosphorylation of Mutagenic Oligonucleotides.

Each oligonucleotide (100 pmoles) was phosphorylated using 4 units of T4 polynucleotide kinase (Biocan) at 37°C for 1 hour. The reaction conditions were 50 mM Tris·HCl (pH 7.6), 10 mM $MgCl_2$, 5 mM DTT, 0.1 mM spermidine·HCl, 0.1 mM EDTA (pH 8.0) and 1 mM ATP (Sambrook *et al.*, 1989). The kinase was inactivated by heating to 70°C for 10 minutes.

8. Polymerase Chain Reaction.

To isolate the *trm*1 gene, the polymerase chain reaction (PCR) was used. Primers (Table 3) corresponding to the non-coding regions flanking the wild-type *TRM*1 open reading frame were chosen to amplify *trm*1 target sequences. The PCR reaction mixture consisted of 420 pmoles of each primer, 1 μg of genomic SN1015-2a DNA, 10 mM dNTPs, 1X Taq polymerase buffer and 1 μl Taq DNA polymerase (Biocan) in a final volume of 50 μl. Mineral oil (50 μl) was overlaid to prevent evaporation of sample at high temperature. The reaction was carried out in the Barnstead Thermolyne Temp-Tronic Series 669 Thermocycler with a hot start at 96°C for 5 min followed by 35 cycles of 96 °C/30 sec, 55°C/30 sec and 72°C/60 sec or longer. Each cycle at the 72°C step was

increased by 5 sec such that the final extension reaction time was 235 sec. PCR products were stored at -20°C.

9. Phenol Freeze Fracture.

Appropriate sized products (1.8 kbp) generated by PCR were isolated using the phenol freeze fracture technique (Bewsey *et al.*, 1991) from 1% agarose gels cast in TBE (0.045 M Tris-Borate, 0.001 M EDTA). In brief, an agarose block containing the DNA fragment of interest was vortexed vigorously with an equal amount of phenol and placed at -70°C for 5 min. The sample was then thawed at 37°C for 5 min and an equal volume of phenol was added. Another round of vortexing, freezing and thawing was performed. TE (100 µl) was added and the sample was vortexed and centrifuged at 14 000 X*g* for 10 min at 4°C. The aqueous phase was collected and extracted twice with phenol and once with ether. DNA was precipitated at -20°C with one tenth volume of 3 M sodium acetate (pH 5.2) and two volumes of 99% EtOH and recovered by centrifugation.

10. Cloning.

Cloning of the PCR-amplified DNA fragment into a PCR TA vector (pCRII) was accomplished using the TA Cloning Kit ™ (Invitrogen). Typical ligation reactions contained 50 ng pCRII vector, 100 ng PCR product (PCR1 or PCR2) and 4.0 Weiss units T4 DNA ligase (Biocan) in 10 µl 1X ligase buffer (Biocan) at 14-16°C for approximately 16 hours.

11. Bacterial Transformations and Transfections.

The standard transformation protocol described by Sambrook *et al.* (1989) involved adding approximately 50 ng of cloned DNA to 50 µl of competent cells and incubating the cells on ice for 30 min. The cells were heat shocked at 42°C for 60 sec and then immediately placed on ice for 2 min. The suspension was added to 450 µl SOC (2% Bacto-tryptone, 0.5% Bacto-yeast extract, 0.05% NaCl, 2.5 mM KCl (pH 7.0), 0.01 M $MgCl_2$, 20 mM glucose) and incubated at 37°C with shaking for 30 to 60 min. Cells were plated on LB agar containing 0.1 mg/ml ampicillin and incubated at 37°C. For mutagenesis experiments, transfection involved the addition of 5 µl of mutagenesis reaction to 100 µl competent JM105 cells with incubation on ice for 30 min. Cells were heated shocked for 2 min at 42°C and then 200 µl of an overnight JM105 culture was added. The resulting culture was added to 3 ml 0.6% B Broth top agar (1% tryptone, 0.3% yeast extract, 0.14 M NaCl, 0.6% agar) containing 0.3 mM IPTG (isopropyl-β-D-thio-galactopyranoside) and 0.3 mM X-Gal (5-bromo-4-chloro-3-indolyl-β-galactoside) and poured onto YT plates. Plaque formation occurred after incubation at 37°C for 12 hours.

12. Plasmid Preparation.

Transformants were inoculated into 5 ml LB (1.0% Bacto-tryptone, 0.5% Bacto-yeast extract and 1.5% NaCl) containing 0.1 mg/ml ampicillin and incubated at 37°C overnight with shaking. Plasmids were extracted using a modification of alkaline lysis PEG precipitation procedure of Birnboim (1983) as described by Applied Biosystems.

Plasmids were resuspended in 10 µl TE and stored at -20°C. Restriction enzyme digestion of the cloned products confirmed their identity.

13. Nested Deletions.

Deletions were produced using the Erase-a-Base™ kit (Promega) according to the instructions supplied by the manufacturer. The *trm*1 gene isolated as PCR1 was transferred from the pCRII vector (Invitrogen) to pBluescriptII KS+ (BSKS, Stratagene) as a 1.8 kbp *Eco*RI fragment generating pPCR1trm/BSK. Plasmids pPCR1trm/BSK and pPCR2trm/pCRII were used for sequencing the + and - strands, respectively.

Initially, 5-10 µg of pPCR1trm/BSK DNA were digested with *Xba*I which created a 5' overhang that was susceptible to Exonuclease III (Exo III) digestion. To generate Exo III resistant 3' ends which protect the primer binding sites (for sequencing), pPCR1trm/BSK was digested with *Sac*I. An alternative strategy to using 3' overhangs to block Exo III digestion was used with pPCR2trm/pCRII due to limiting restriction enzyme sites. The 3' recessed ends generated by *Xho*I digestion were filled-in with α-phosphorothioate dNTPs (Promega) using Klenow DNA polymerase making them resistant to Exo III digestion. To the *Xho*I digested DNA, α-phosphorothioate dNTPs to a final concentration of 40 µM, DTT to 1 mM and Klenow fragment to 50 u/ml were added and incubated at 37°C for 10 min. The Klenow enzyme was inactivated by heating the sample to 70°C for 10 min. The 5' overhang next to the insert was then generated by digestion of pPCR2trm/pCRII with *Xba*I.

The doubly cut plasmids (~5 µg) were phenol extracted, EtOH precipitated and

then dissolved in 60 µl Exo III 1X buffer. The DNA tube was warmed at 37°C and 500 units Exo III were added and mixed rapidly. Aliquots (2.5 µl) were removed at 30, 60, 90, 120, 150, 180, 210, and 240 sec for each strand, added to S1 nuclease mix (7.5 µl) and incubated at RT for 30 min. The reaction in each tube was stopped by adding 1 µl S1 stop buffer and heating to 70°C for 10 min. At this point, 2 µl aliquots from each time point were checked by agarose gel electrophoresis to determine the extent of the deletions. Reactions were transferred to 37°C and 1 µl Klenow mix (30 µl Klenow buffer and 3-5 units Klenow) was added to each sample. An incubation at 37°C for 3 min was followed by the addition of 1 µl dNTP mix (0.125 mM each dATP, dCTP, dGTP and dTTP), and another incubation at 37°C for 5 min. The samples were transferred to RT and 40 µl ligase mix (790 µl dH_2O, 100 µl ligase 10X buffer, 100 µl 50% $PEG_{7000\text{-}9000}$, 10 µl 100 mM DTT and 5 units T4 DNA ligase) was added and incubated at RT for 1 hour. Transformation of JM83 competent cells was carried out with 10 µl of the ligation products as described previously.

14. <u>Screening Deletion Clones.</u>

Rapid screening of deletion clones was accomplished by the cracking procedure as described in the Promega Erase-a-Base™ System technical manual. Individual colonies from each time point were patched onto LB agar plates containing 0.1 mg/ml ampicillin and incubated overnight at 37°C. Cells were scraped from the plates and resuspended in 50 µl of 10 mM EDTA by vortexing. To each sample, 50 µl 2X cracking buffer (2 ml 5 M NaOH, 0.5 ml 10% SDS, 10 g sucrose per 50 ml) was added, vortexed and incubated

at RT for 5 min. Subsequently, 1.5 µl 4 M KCl and 0.5 µl 0.4% bromophenol blue was added, and the sample was vortexed and incubated on ice for 5 min. Each sample was centrifuged at 14 000 X*g* in a microfuge for 3 min at 4°C. An aliquot (25 µl) of each sample was loaded onto a 0.8% TEA (0.04 M Tris-acetate, 1 mM EDTA) agarose gel and electrophoresed for 2 or 3 hours at 80 volts. Plasmids carrying inserts covering the entire length of each *trm*1 clone were selected from the gels, the plasmids isolated and the *trm*1 regions sequenced.

15. <u>Sequencing.</u>

DNA sequencing was carried out according to the procedure of USB Sequenase™ version 2.0 with minor modifications. DNA (3-5 µg) in a final volume of 12 µl was denatured by the addition of 4 µl 2 M NaOH and 4 µl 1 mM EDTA, followed by an incubation at RT for 10 min. DNA was precipitated with the addition of 10 µl 7.5 M NH_4OAc and 90 µl 99% EtOH, and stored at -70°C for 30 min. DNA was recovered by centrifugation, dried and resuspended in 7 µl of sterile dH_20. Annealing was accomplished with the addition of 2 µl Sequenase™ 5X reaction buffer and 0.5 pmoles of the appropriate primer. The mixture was heated to 65°C for 2 min and slow cooled to 35°C. The labelling reaction mix was prepared according to the manufacturer's instructions and added to 10 µl of the annealed template-primer. The final mixture was incubated at RT for 2 min and 3.5 µl aliquots were added to pre-warmed termination mixes (ddNTPs). Incubation was continued for 3 min at 37°C and the reaction stopped by the addition of 4 µl stop solution. Samples were boiled 2 min prior to loading onto a 6%

acrylamide sequencing gel (7 M urea, 5.7% acrylamide, 0.3% bis-acrylamide, 1X TBE). Sequencing gels (38 X 50 cm) were prerun for 15 min at each of the following voltages: 1000 V, 1500 V and 2000 V. Samples were electrophoresed at a constant voltage of 2000 V for times ranging from 5-16 hours. After electrophoresis, gels were dried under vacuum for 2 hours at 80°C and then exposed to X-ray film (Fuji).

16. Preparation of Single-Stranded DNA Template Containing Uracil.

The appropriate bacteriophage M13 recombinant (M13mp18 or M13mp19) containing the 3' region of *TRM*1 or *trm*1 gene was grown in the dut$^-$ ung$^-$ F' strain CJ236. Single-stranded DNA containing uracil was prepared as described by Sambrook *et al.* (1989) with minor modifications. Briefly, 30 ml YT (1.6% tryptone, 1 % Bacto-yeast extract, 0.09 M NaCl) containing 15 mg/ml chloramphenicol was inoculated with 150 µl CJ236 overnight culture and 150 µl of phage supernatant (from JM101 cells containing the appropriate phage), and incubated for 6 to 12 hours at 37°C with shaking. The culture (25 ml) was centrifuged at 3024 X*g* for 10 min at 4°C. To the supernatant, 0.15 volumes of 2.5 M NaCl / 20% w/v $PEG_{7000-9000}$ were added with incubation on ice for 20 min. The precipitated bacteriophage particles were recovered by centrifugation at 12 096 X*g* for 20 min. The pellet was dissolved in 25 µl TE and extracted twice with an equal volume of phenol, once with an equal volume of phenol:chloroform, and once with an equal volume of ether. The aqueous phase was collected and single-stranded DNA was precipitated with 0.1 volume of 3 M sodium acetate (pH 5.2) and 2 volumes of 99% ethanol at -70°C for 30 min, and the DNA was recovered by centrifugation.

17. Site-Directed Mutagenesis.

To introduce mutations into the *TRM*1 and *trm*1 genes, the single primer method (Kunkel, 1985; Kunkel *et al.*, 1987) was performed as described by Sambrook *et al.* (1989) with the following modifications. Single-stranded DNA containing uracil (1 μg) was annealed to 10 pmoles of the appropriate phosphorylated oligonucleotide (Table 2) in PE1 buffer (20 mM Tris·Cl (pH 7.5), 10 mM $MgCl_2$, 50 mM NaCl, 1 mM DTT) at 70°C for 5 min and slow cooled to 35°C. Bacteriophage T4 DNA ligase (5 Weiss units) and Sequenase or T4 polymerase (2.5 units), prepared in PE2 buffer (20 mM Tris·Cl (pH 7.5), 10 mM $MgCl_2$, 10 mM DTT, 1 mM ATP and 0.5 mM dNTPs) were added to the reaction mixture. The final reaction mixture was incubated 5 min on ice, 5 min at RT and 2 hours at 37°C. Transfection of *E. coli* JM105 cells was carried out as described previously using 5 μl of mutagenesis reaction. Replicative form of DNA was isolated as described above. The mutagenized portions of the *TRM*1 or *trm*1 genes were transferred to yeast shuttle vectors and the resulting plasmids were transformed into the yeast strain SN1015-2a or DBY745ΔTRM and assayed for m_2^2Gtase activity.

18. Yeast Transformations.

The yeast strains SN1015-2a and DBY745ΔTRM were transformed using the protocol of Schiestl and Gietz (1989). Briefly, 300 ml YPAD (YPD, 0.003% adenine) were inoculated with an overnight yeast culture and grown at 30°C to an OD_{640} of 0.6. The culture was centrifuged at 3836 X*g* at RT and cells were resuspended in 10 ml sterile dH_2O. The cell suspension was centrifuged at 5927 X*g* at RT and the pellet resuspended

in 1.5 ml TE / LiAc (10 mM Tris·HCl, 1 mM EDTA (pH 7.5), 100 mM LiAc). The resulting suspension was incubated at 30°C with constant agitation for 1 hour. Microfuge tubes were prepared containing plasmid DNA (3-5 μg), 200 μg salmon sperm carrier DNA, and TE / LiAc to a total volume of 60 μl. Yeast suspension (200 μl) was added to each tube and incubated at 30°C with agitation for 30 min. Subsequently, 1.2 ml of sterile 40% PEG_{4000} / TE / LiAc was added followed by another 30 min incubation at 30°C with agitation. The suspension was then heat shocked at 42°C for 15 min. Cells were pelleted in a microfuge for 5 sec and washed twice with 0.5 ml TE using a sterile toothpick to resuspend. Cell pellets were resuspended in a final volume of 0.3 ml TE, spread on selective SC medium lacking uracil (SC-Ura) and incubated at 30°C for 3-5 days.

19. <u>Plasmid Loss.</u>

Yeast transformants were grown in 5 ml YPD medium for 16 hours at 30°C with agitation. Dilutions (1/10, 1/100 or 1/1000) of the resulting culture were spread onto YPD plates and incubated at 30°C. Colonies were then replica-plated onto SC+Ura and SC-Ura plates and incubated at 30°C. Plates were scored for the number of colonies present on SC+Ura versus SC-Ura plates.

20. Crude Protein Extraction for m^2_2Gtase Activity Assays and Western Blots.

Yeast cell extracts were prepared by mechanical disruption of freshly grown cells as described by Li *et al.* (1989). Cells were grown aerobically in 30 ml YPD or SC-Ura media at 30°C with vigorous shaking to an OD_{640} of 1.0. Cells were harvested by centrifugation at 3024 X*g* at 4°C for 5 min. The pellet was resuspended in 0.5 ml NET-NP (150 mM NaCl, 5 mM EDTA, 50 mM Tris·HCl (pH 7.5), 0.5% NP-40), and transferred to a 1.5 ml microfuge tube. Cells were centrifuged 1 min at 14 000 X*g* and resuspended in 0.3 ml NET-NP / 1 mM PMSF. An equal amount of acid washed glass beads (425-600 microns, Sigma) was added and the cells were vortexed vigorously for 5 X 30 sec with cooling on ice between each interval. Upon centrifugation for 5 min, the supernatant was collected into pre-chilled tubes and total protein concentrations were determined following the procedure supplied with the BioRad protein assay kit. Crude protein extracts were kept on ice until ready for use.

21. Yeast tRNA Preparation for m^2_2Gtase Activity Assays.

The tRNA isolation procedure was adapted from Hopper *et al.* (1980). Yeast cells (W303-1b, SN1015-2a or DBY745ΔTRM) were grown in 100 ml YPD at 30°C to an OD_{640} of 1.0. The cells were pelleted at 3836 X*g* for 5 min, then resuspended in 3 ml TSE (0.01 M Tris·HCl (pH7.5), 0.01 M EDTA, 0.1 M NaCl) and 3 ml phenol. The mixture was incubated at 30°C for 1 hour with agitation followed by an incubation at 4°C for 2 hours. The phases were then separated by centrifugation and the aqueous phase was re-extracted once with phenol and once with chloroform. RNA was collected upon

addition of 2 volumes of 99% ethanol at -20°C.

22. Preparation of S-adenosyl-L-methyl-methionine.

For the standard m_2^2Gtase assay, 7.4 μM S-adenosyl-L-methyl-methionine (SAM) was used. A 1845 μM stock was prepared by diluting radiolabelled SAM (S-adenosyl-L-(methyl-^{3}H)-methionine, specific activity 15 Ci/mmol, NEN-Dupont) with unlabelled SAM (10 mg/ml stock prepared in 10 mM H_2SO_4:EtOH (9:1) Sigma) to a final ratio of 1:50. For assays used in the kinetic studies in which tRNA was varied and SAM was held constant at 148 μM, a concentration of SAM in the stock solution was raised to 6361 μM with the ratio of radioactive to unlabelled SAM changed to 1:200.

23. m_2^2Gtase Activity Assays.

The standard assay as described by Ellis *et al.* (1986) measured enzyme activity in a reaction mixture of 150 μl containing 100 mM Tris·Cl (pH 7.5), 0.1 mM EDTA, 10 mM $MgCl_2$, 20 mM NH_4Cl, 1 mM DTT, 7.4 μM S-adenosyl-L-(methyl-^{3}H) methionine, 8 μg m_2^2G-deficient yeast tRNA (SN1015-2a or DBY745ΔTRM) or wild-type yeast tRNA (W303-1b) and 100 μg of crude yeast protein. Reaction mixtures were incubated at 37°C for 30 min. Kinetic studies employed 10 μg protein with incubations for 20 min. A 130 μl aliquot of the reaction mixture was transferred to 870 μl ice-cold BSA (0.115 mg/ml) followed by the addition of 1 ml of 2 N HCl and an incubation on ice for 10 min. Precipitated tRNA was collected by filtration (Millipore filtration unit) through 1 N HCl pre-soaked GF/C filters (Whatman). Unincorporated free ^{3}H-SAM was eliminated with

five washes with 10 ml of 1 N HCl and two washes with 10 ml of 95 % ethanol. Filters were dried at 70°C for 10 min and placed in 4 ml scintillation cocktail (ICN). The amount of tritium incorporated into acid-precipitable material was determined by liquid scintillation counting (LKB Wallac-1218 Rackbeta). Each experiment was performed in duplicate and consisted of duplicate samples at each assay point. Kinetic studies consisted of 2-4 experiments.

24. <u>Western Blots.</u>

Crude yeast protein (100 μg) was separated on a mini 12% SDS-polyacrylamide gel at 100 volts for 2.5 hours using the Novex apparatus. The gel was soaked in transfer buffer (25 mM Tris / 192 mM glycine / 20% methanol) (Towbin *et al.*, 1979) for 10 min. Proteins were then transferred onto a nitrocellulose membrane (Amersham Hybond-C) at 50 volts for 1 hour using the Biorad 200/2.0 transblotter. When the transfer was complete, the membrane was rinsed with TBS-T (20 mM Tris·HCl (pH 7.5) / 0.5 M NaCl / 0.05% Tween-20) and dried at RT overnight.

For m_2^2Gtase detection, the membrane was initially blocked with 5% powdered milk prepared in TBS-T for 1 hour at RT and then briefly rinsed twice with 5 mls TBS-T, followed by one 15 min wash and two 5 min washes of 5 ml TBS-T at RT. The polyclonal rabbit anti-yeast m_2^2Gtase primary antibody (kindly provided by Dr. N. C. Martin, University of Louisville) was diluted 1:2500 in TBS-T and incubated with the membrane for 1 hour at RT. The primary antibody solution was removed and the membrane was rinsed twice with 5 ml TBS-T, followed by one 15 min wash and two

rinses with 5 ml TBS-T at RT. The alkaline phosphatase conjugated goat-anti-rabbit secondary antibody (Bio Rad) was diluted 1:500 in TBS-T and incubated with the membrane for 1 hour at RT. The secondary antibody was removed and the membrane was washed as described above. Detection was accomplished by incubating the membrane in colour development solution (10 ml 0.1 M Tris / 0.5 mM $MgCl_2$ with 100 µl AP reagent A and 100 µl AP reagent B (Bio-Rad)). The colour developing reaction was stopped with dH_2O.

Results

III. RESULTS

PART 1

Establishing the Phenotype of SN1015-2a

1. Growth Curves.

The growth rate of the yeast strain carrying the mutant *trm*1 allele (SN1015-2a) was compared to that of W303-1b which is wild-type for *TRM*1. Growth curves (Figure 8) indicate that under standard laboratory conditions, the rate of growth of SN1015-2a is indistinguishable from that of W303-1b in both rich (YPD) and minimal (SC) media.

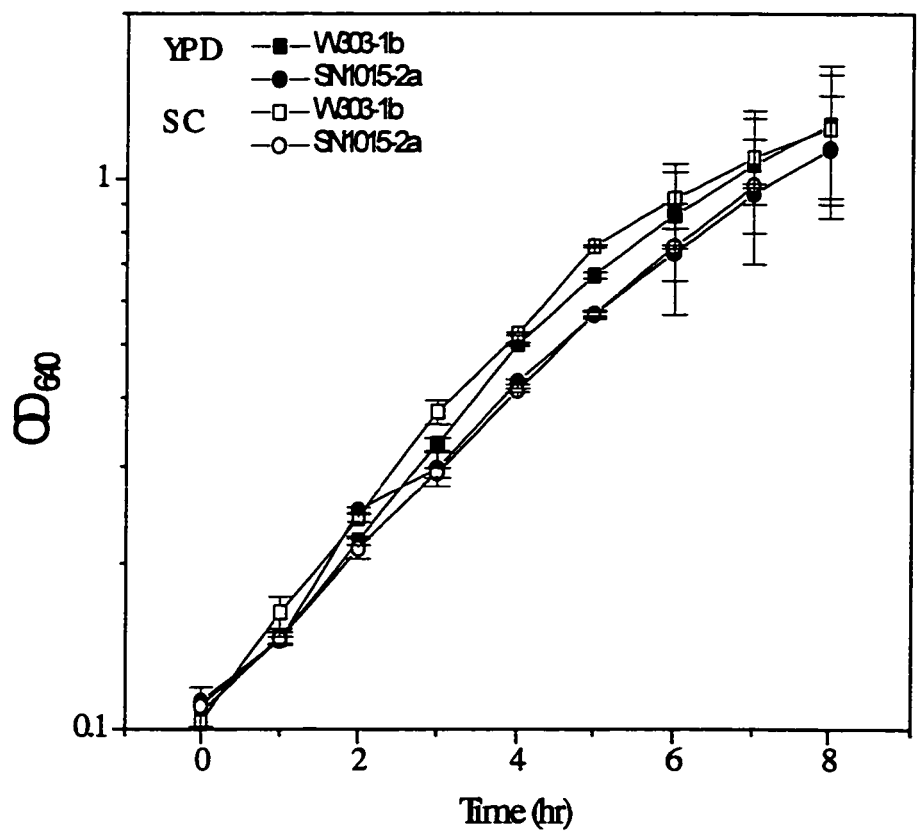

Figure 8. Yeast Growth Curves. Growth rates of W303-1b and SN1015-2a in YPD and SC media were measured as an increase in OD_{640} at one hour intervals. Data are mean (±SE mean) values of duplicate experiments and are plotted on a logarithmic scale.

2. m_2^2Gtase Activity Assays.

Measurement of m_2^2Gtase Activity.

The assay of tRNA methyltransferase (m_2^2Gtase) activity is based on the measurement of radioactivity incorporated as tritiated methyl groups into undermethylated tRNA after incubation with S-adenosyl-L-(methyl-^{3}H) methionine (Figure 5). Despite the fact that crude cell lysates were used as a source of enzyme in the assay, specific m_2^2Gtase activity was measured. This was accomplished by measuring the difference in the levels of tritium incorporated into two populations of tRNA: 1) substrate tRNAs devoid of $m_2^2G_{26}$ isolated from the yeast strain SN1015-2a, and 2) substrate tRNAs containing $m_2^2G_{26}$ isolated from the yeast strain W303-1b. The difference between the isotope incorporated into tRNAs from SN1015-2a and that incorporated into tRNAs from W303-1b is taken to reflect the incorporation at G_{26}. Specific incorporation of radiolabelled methyl groups at bases other than G_{26} is assumed to be the same in both cases. Figure 9 compares the levels of tritiated methyl groups incorporated into tRNAs isolated from strain SN1015-2a (total), strain W303-1b (nonspecific) and the difference between these two values (specific). Protein extracts were prepared from seven yeast strains and were examined for m_2^2Gtase activity. W303-1b displayed the highest level of specific m_2^2Gtase activity while, as expected, no activity was evident in the *S. cerevisiae* strain, SN1015-2a. Five other yeast species (*Kluyveromyces lactis, Candida glabrata, Saccharomyces exiguus, Schizosaccharomyces pombe* and *Sarcomycopses fibuligera)* also exhibited varying levels of m_2^2Gtase activity ranging from *K. lactis,* which displayed levels comparable to W303-1b, to *S. fibuligera* at approximately 20 % of this level. All subsequent figures will show

specific m_2^2Gtase activity measured in CPM or expressed in nmol of tritium incorporated per mg protein per min.

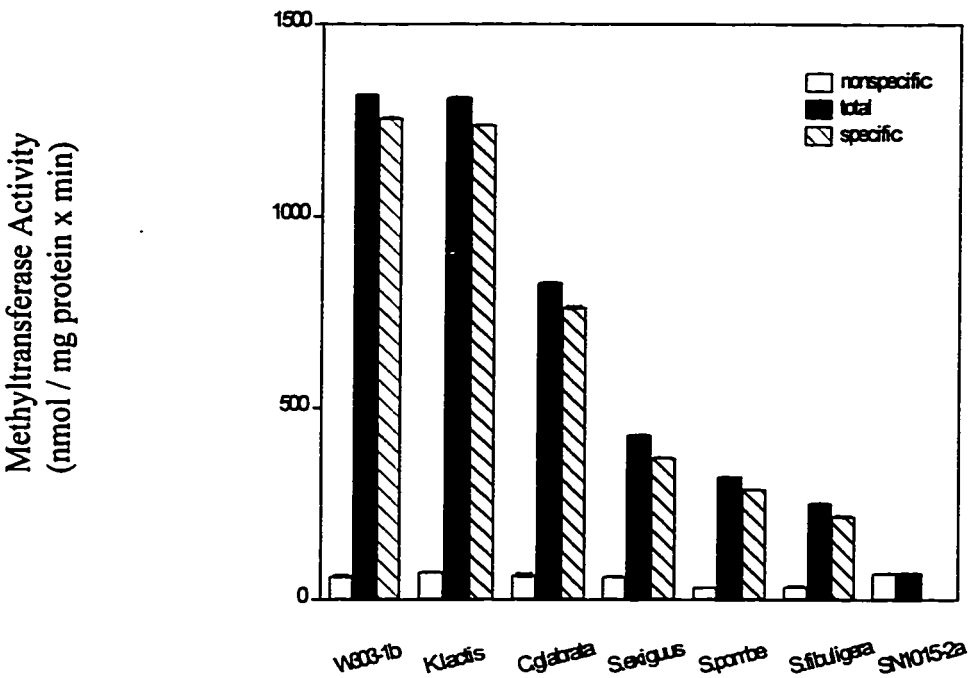

Figure 9. m_2^2Gtase Activity of Differently Related Yeasts. White bars represent nonspecific methylase activity, black bars represent total methylase activity and hatched bars represent specific m_2^2Gtase activity (see text for further explanation). Data are mean (±SE mean) values for duplicate experiments.

Determining That SN1015-2a Lacks Detectable m_2^2Gtase Activity.

To confirm that SN1015-2a lacks any detectable G_{26}-specific m_2^2Gtase activity, crude protein (100 μg and 1000 μg) was isolated from this strain and assayed for m_2^2Gtase activity at various incubation times under near saturating substrate concentrations: 20 μM tRNA and 148 μM SAM. Similarly, crude protein from W303-1b (10 μg and 100 μg) also was assayed in parallel. Figure 10 illustrates that under these assay conditions, there is no detectable m_2^2Gtase activity in SN1015-2a over the time period or protein levels assayed. In contrast, the levels of enzyme activity increase with increasing amounts of W303-1b protein.

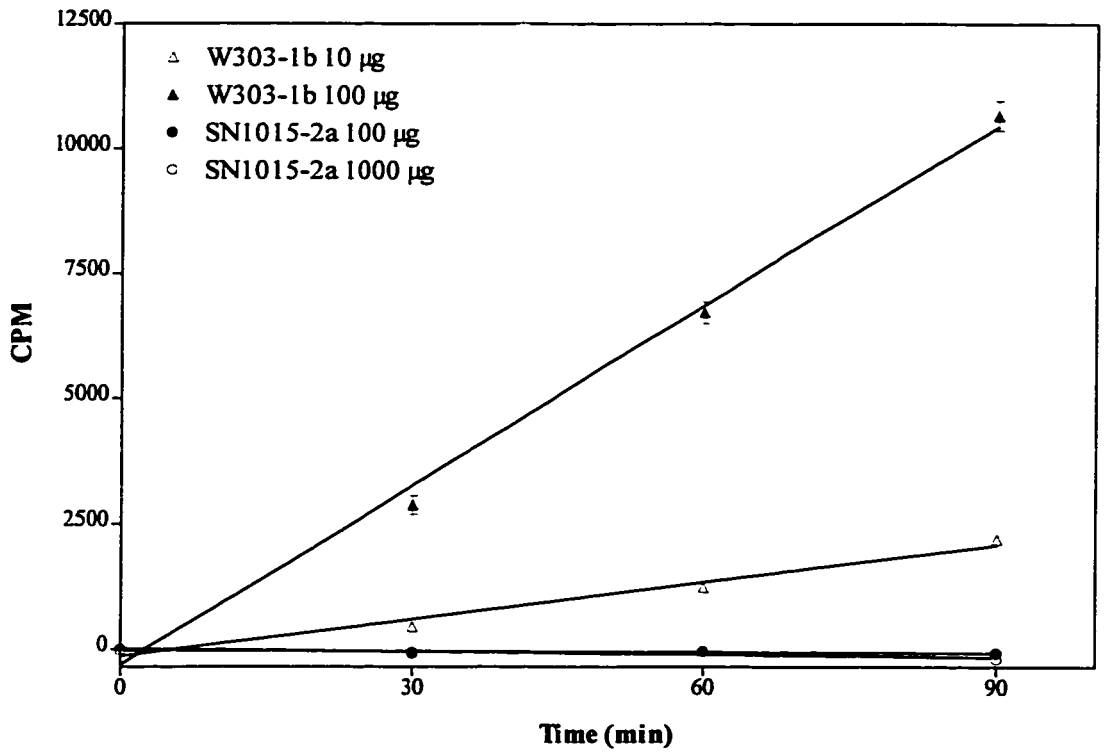

Figure 10. Time Course for m_2^2Gtase Specific Activity at Different Protein Concentrations. The level of incorporation of ^{3}H-methyl groups into m_2^2G-deficient tRNA was measured at 30 min intervals and expressed as CPM incorporated. Data are mean (±SE mean) values of 2 experiments (n=4).

3. Western Blot.

Western analysis was used to confirm that m_2^2Gtase is produced in the strain SN1015-2a which lacks m_2^2Gtase activity. A previously characterized anti-m_2^2Gtase antibody (Li *et al.*, 1989) was used as a specific probe for Western blotting to confirm the presence of m_2^2Gtase in various yeast strains (Figure 11). The crude protein extracts were prepared from the strain W303-1b, from the *trm*1 mutant strain SN1015-2a, from the strain DBY745, and from the strain DBY745ΔTRM which carries a disrupted allele of *TRM*1. The antipeptide antibody recognized a protein of 63 KDa in W303-1b, SN1015-2a and DBY745 protein samples (lanes 1, 2 and 3, Figure 11A) confirming the presence of m_2^2Gtase in strain SN1015-2a. This specific band for m_2^2Gtase was not observed in crude protein extracts of DBY745ΔTRM (lane 4). A second protein band of approximately 60 kDa was observed in all samples (lanes 1-4). Figure 11B demonstrates the same conditions without primary m_2^2Gtase antibody. The specific band for m_2^2Gtase at 63 KDa as well as the second band at 60 KDa were not observed.

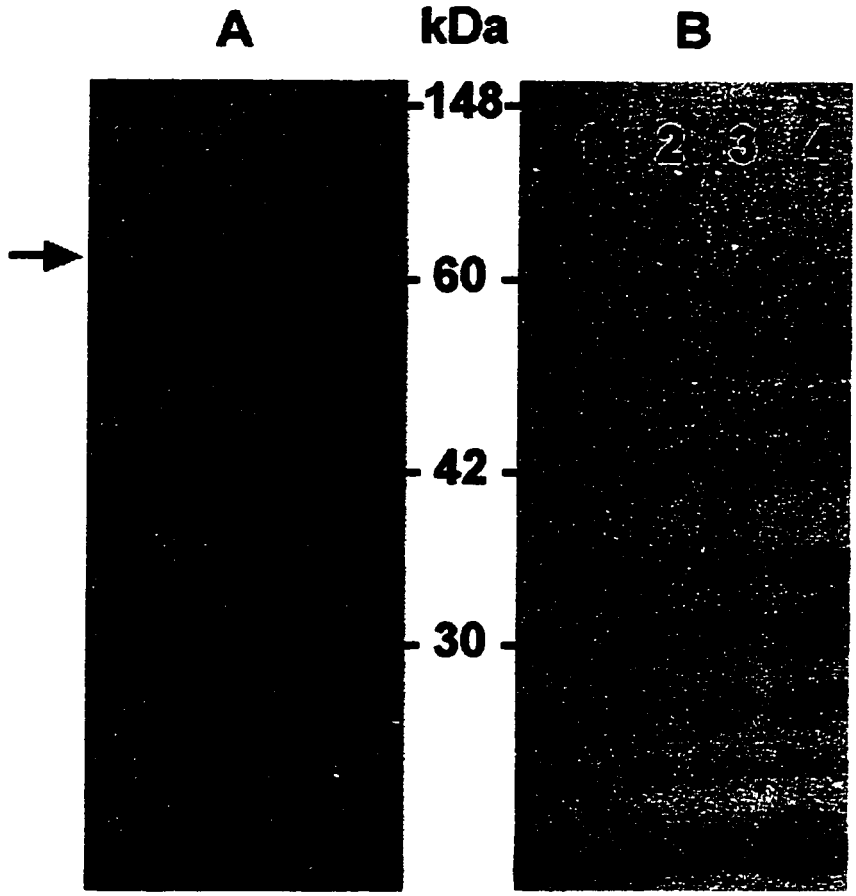

Figure 11. Western Analysis. Identification of the m_2^2Gtase protein with immunoblot using m_2^2Gtase antipeptide antibody (A). Immunoblot (B) represents non-specific bands due to secondary antibody conjugated with alkaline phosphatase. Lane 1 corresponds to protein isolated from W303-1b, lane 2 from SN1015-2a, lane 3 from DBY745 and lane 4 from DBY745ΔTRM. MW markers in kDa are indicated between blots A and B. The arrow marks m_2^2Gtase at 63 kDa.

PART 2

Cloning and Sequencing of the *trm*1 Gene

1. Cloning the *trm*1 Gene.

For PCR amplification of the coding region of *trm*1, oligonucleotide primers flanking the gene were designed (Table 1) based on the published wild-type *TRM*1 gene sequence (Ellis *et al.*, 1987). The mutant *trm*1 gene was isolated by PCR from SN1015-2a genomic DNA (template 1 and template 2) obtained from two independent yeast colonies. As a result, two separate appropriately sized 1.8 kbp PCR fragments (PCR1 and PCR2) were isolated from agarose gels (Figure 12) and cloned into the pBSKS and pCRII vectors, respectively, resulting in plasmids pPCR1trm/BSK and pPCR2trm/pCRII.

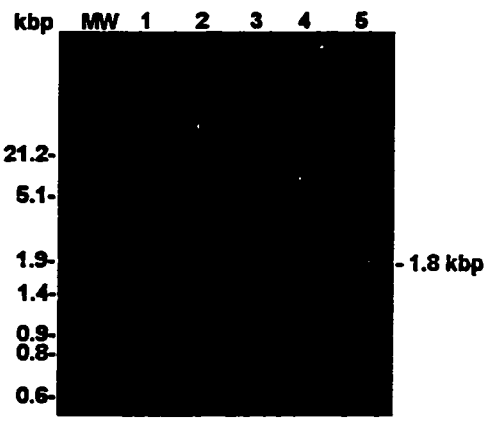

Figure 12. PCR Products. PCR products were separated on a 0.8 % agarose gel; MW markers = λ DNA digested with *Eco*RI and *Hin*dIII; lane 1 = SN1015-2a genomic DNA template without primers; lane 2 = template 1 + primer 1; lane 3 = template 1 + primer 2; lane 4 = template 1 + primer 1 + primer 2 (PCR1); lane 5 = template 2 + primer 1 + primer 2 (PCR2).

2. Nested Deletions.

Nested deletions were prepared from the + strand and the - strand of pPCR1trm/BSK and pPCR2trm/pCRII, respectively. A total of 80 clones (10 from each time point) was screened from each strand, and 10 were selected from the + strand and 9 from the - strand for sequencing. Figure 13 shows two agarose gels used to determine the size of the deletion clones employed for sequencing. Estimation of insert size was accomplished by electrophoresing the deletion clones alongside marker plasmids either containing or lacking the *trm*1 gene obtained by PCR. The sizes of the chosen deletion clones lie within the range defined by the markers.

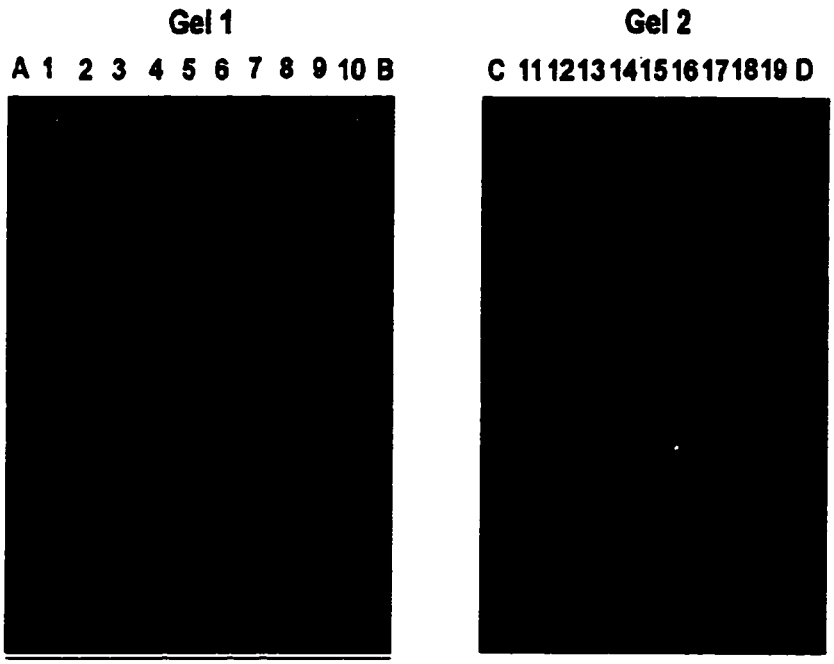

Figure 13. Sizing Gels. Deletion clones were electrophoresed at 70 volts on 0.8% TEA agarose gels. Gel 1 (left) was electrophoresed for 3 hours: lane A = pPCR1trm/BSK, lanes 1-10 = deletion clones 1-10 respectively of the + strand, lane B = BSKS vector. Gel 2 (right) was electrophoresed for 2 hours: lane C = pCRII vector, lanes 11-19 = deletion clones 11-19 respectively of the - strand, lane D = pPCR2trm/pCRII.

Figure 14 illustrates the strategy employed to sequence *trm*1. Each arrow represents the approximate length and location of a clone with respect to the *trm*1 gene. The clones overlap partially and, therefore, cover the entire length of the gene. A total of 10 deletion clones was employed to sequence the + strand and 9 clones for the - strand.

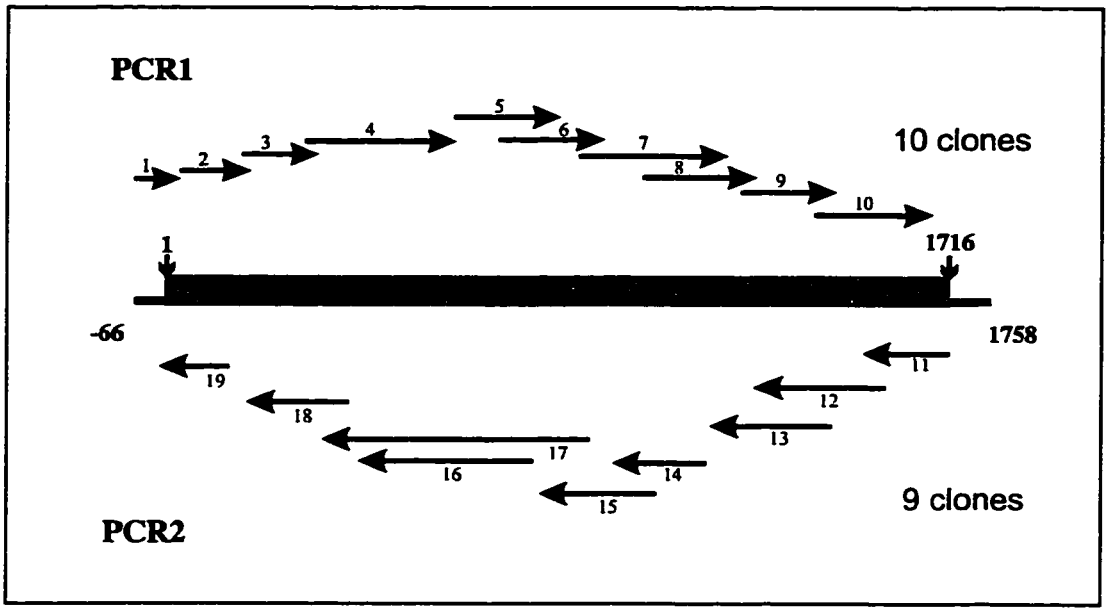

Figure 14. Sequencing Strategy Employed to Determine the Nucleotide Sequence of the *trm*1 Gene. Arrows depict the direction and extent of sequence generated from each deletion with respect to the *trm*1 gene (grey bar). Numbering of bases are as follows: 1 is the first base of the first ATG start codon, -66 represents the upstream sequence available, 1716 is the last base of the UGA stop codon and 1758 is the last downstream base available.

3. Sequencing the *trm*1 Gene.

Nucleotide sequences were determined according to the procedure described in the USB Sequenase™ kit based on the Sanger method (Sanger *et al.*, 1977). SN1015-2a *trm*1 DNA sequences (1838 bp) were obtained from two separate PCR products (PCR1 and PCR2) and compared to the published sequence of wildtype *TRM*1 (Ellis *et al.*, 1987) (Figure 15). The number and types of mutations found are summarized in Table 4. There are approximately 6 fold and 8 fold more transition-type base mutations than transversion-type mutations in the *trm*1 PCR1 and PCR2 products, respectively. From the amino acid sequence predicted from the nucleotide sequence, amino acid changes from the wild-type were identified in the two PCR products. These changes and their relative positions are illustrated in Figure 16. Sequence comparison to the wildtype *TRM*1 gene revealed 14 silent point mutations and 4 amino acid substitutions that are common to both PCR1 and PCR2: Gly^{3}→ Ser, Thr^{203}→Ser, Ser^{467}→Leu, and Gly^{517}→Arg. The changes in the side chains introduced by these mutations are depicted in Figure 17. As Gly^{3} is contained in the mitochondrial targeting signal of m_2^2Gtase, and is not present in the short form of the enzyme, it is not required for enzyme activity. Therefore, only the latter three substitutions were further examined to see what role they may play in inactivating m_2^2Gtase. Four other amino acid residue substitutions (Gln^{67}→Arg, Val^{177}→Ala, Val^{397}→Met and Asn^{427}→Thr) indicated in Figure 16 were found that were not shared between the two PCR products. Figure 18 is a semi-graphical representation of the protein secondary structure as predicted by the Garnier method (Garnier *et al.*, 1978) for m_2^2Gtase based on the *TRM*1 gene sequence. The four mutations common to PCR1 and PCR2 lie in the following predicted regions: Ser^{3} = helical conformation, Ser^{203} = coil conformation, Leu^{467} and Arg^{517} = turn conformation.

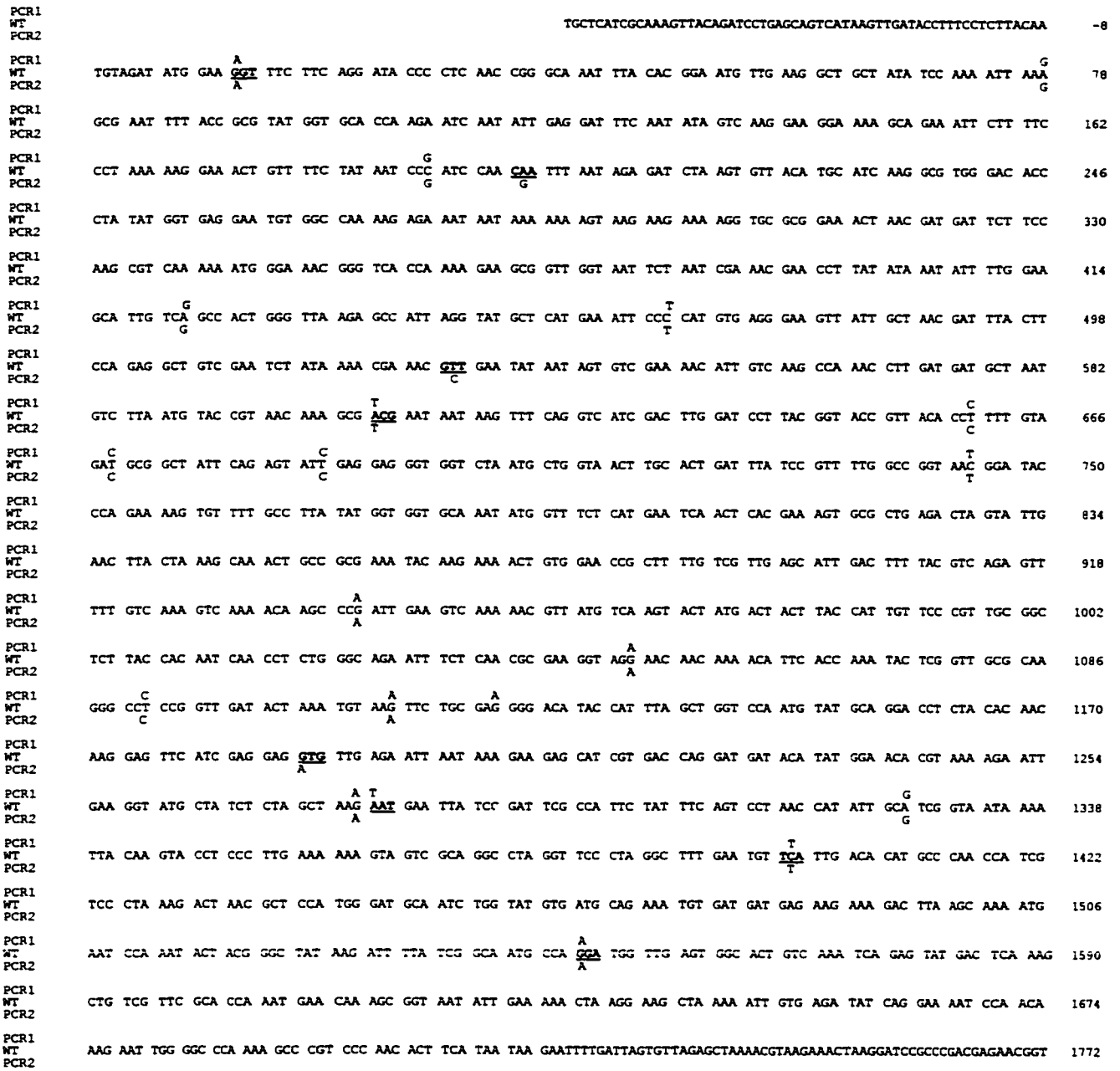

Figure 15. Sequence of the *trm*1 Gene. DNA sequence comparison of the *trm*1 PCR products from SN1015-2a with the *TRM*1 gene sequence of *S. cerevisiae* (Ellis *et al.*, 1987). Point mutations in PCR1 and PCR2 products are indicated above and below the wild-type sequence respectively, while missense mutations are underlined. Numbers to the right of the sequence correspond to the nucleotide position in *TRM*1. Nucleotide A of the first in frame ATG is taken as position 1.

*trm*1	Total # of Mutations	Transitions	Transversions	Silent Point Mutations	Amino Acid Substitutions
PCR1	20	17	3	15	5
PCR2	21	19	2	14	7

Table 4. Summary of Mutation Types Found in the PCR Products Generated from the *trm*1 Gene.

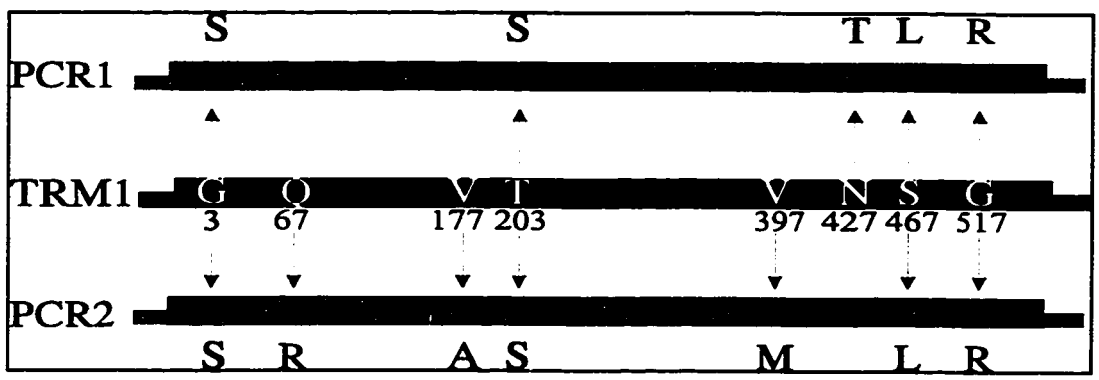

Figure 16. Amino Acid Substitutions. Comparison of amino acid sequences predicted from the nucleotide sequences of *TRM*1 (black bar) and mutant *trm*1 PCR products (grey bars). Arrows denote the amino acid substitution from wild-type to mutant. The relative position of mutations are indicated with an x. Numbers below the *TRM*1 sequence denote the amino acid position in m_2^2Gtase.

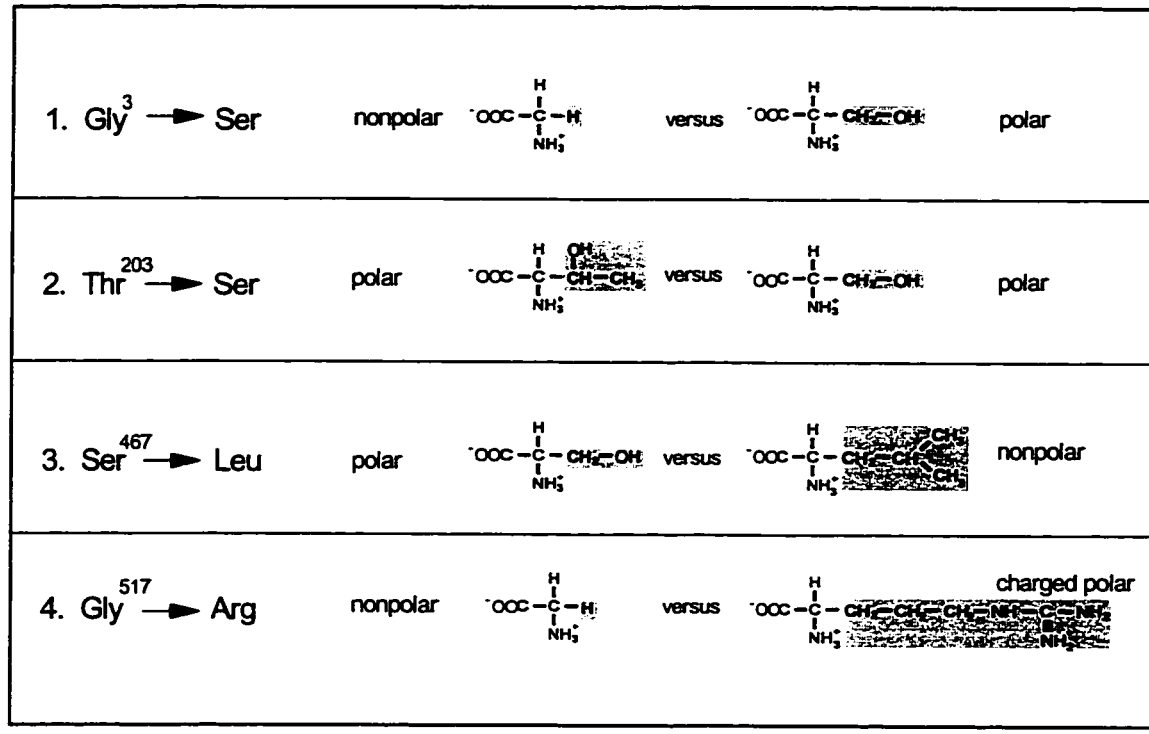

Figure 17. Four Shared Amino Acid Mutations Found in PCR1 and PCR2 Products. The amino acid residue structure is illustrated with its side chain outlined in grey.

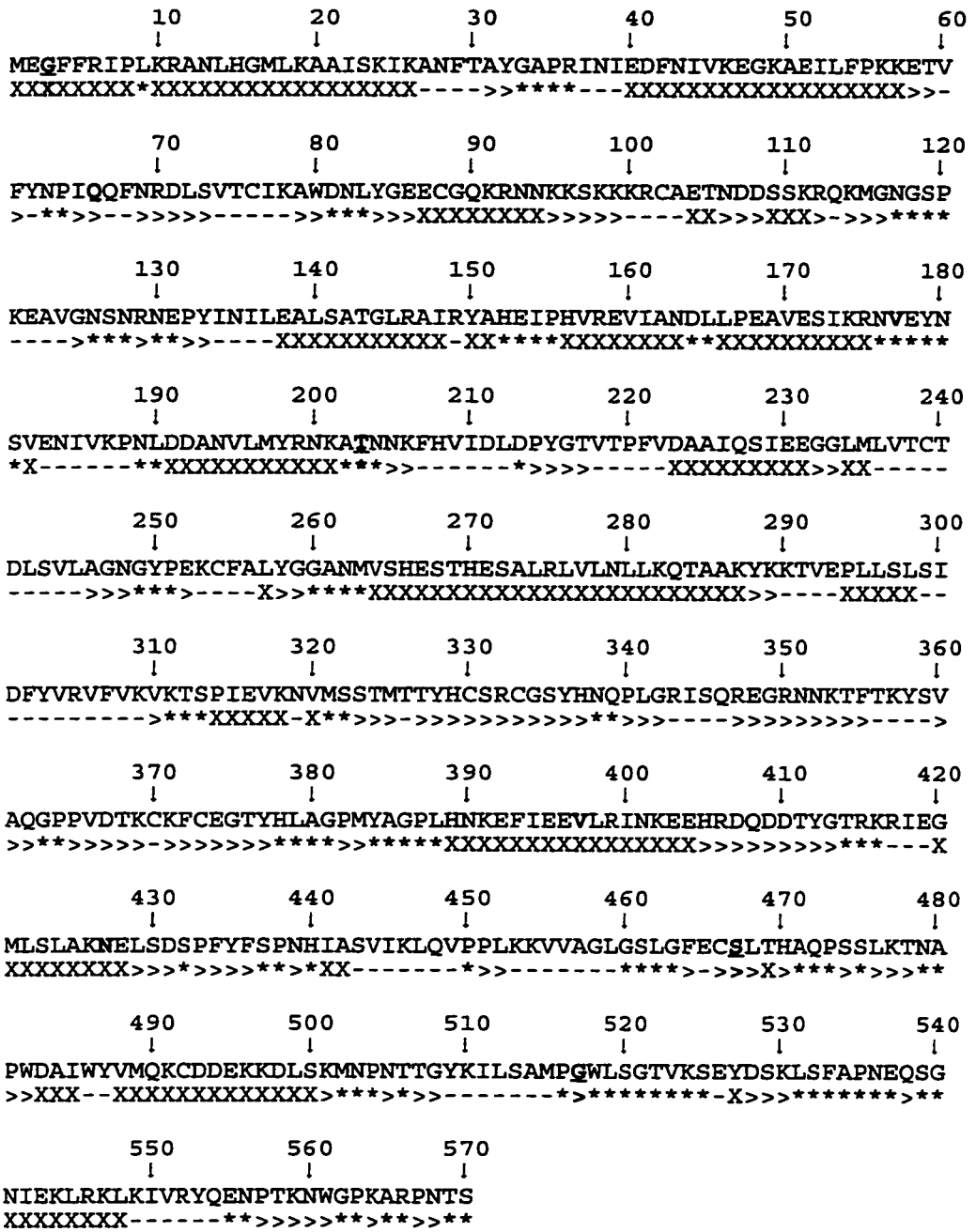

Figure 18. Protein Secondary Structure Prediction by the Method of Garnier (Garnier *et al.*, 1978). Analysis was conducted on 570 amino acid residues predicted from the complete *TRM1* gene sequence. Symbols used in the semi-graphical representation are: Helical conformation: X; Extended conformation: - ; Turn conformation: > ; and Coil conformation: *. Wild-type residues that are bolded and underlined represent the positions where the same amino acid substitution occurs in the protein sequences predicted from both PCR products. Positions containing amino acid substitutions that are not common to both products are bolded only.

PART 3

Identifying Residues Responsible for the Loss of m_2^2Gtase Activity

1. Sub-cloning I.

Replacement of 3 Amino Acid Residues at the 3' End of the *TRM*1 Gene.

It seemed likely that the mutation responsible for loss of activity would be either Ser^{467}→Leu or Gly^{516}→Arg, as the Thr^{203}→Ser substitution represents the most conservative change (Figure 19). Therefore, mutant *trm*1 alleles were created by replacing the 1114 bp wild-type *Bam*HI fragment (sites at position 636 and 1751) at the 3' end of the *TRM*1 gene from YCpPJMR4 with similar *Sau*3A fragments containing Leu^{467} and Arg^{516} from the PCR1 and PCR2 products. The resulting plasmids are pTRMPCR1-3' and pTRMPCR2-3' (Figure 7b) each of which carries three mutations: Thr^{427}, Leu^{467}, Arg^{517}, or Met^{397}, Leu^{467}, Arg^{517}, respectively (Figure 19). This subcloning allows for a more precise fine structure map of the possible amino acid substitutions responsible for inactivation to be carried out. These plasmids were used to transform the mutant yeast strain SN1015-2a which lacks functional m_2^2Gtase, and yeast colonies were selected for uracil prototrophy. To ensure that these plasmids had been taken up by SN1015-2a and that functional m_2^2Gtase activity was correlated with uracil prototrophy and not due to reversion at the *trm*1 locus, plasmid loss experiments were performed. Approximately 95% plasmid loss was observed after initial growth on rich YPD media followed by growth on minimal SC-ura media, thus confirming that the plasmids, pTRMPCR1-3' and pTRMPCR2-3', were responsible for m_2^2Gtase activity.

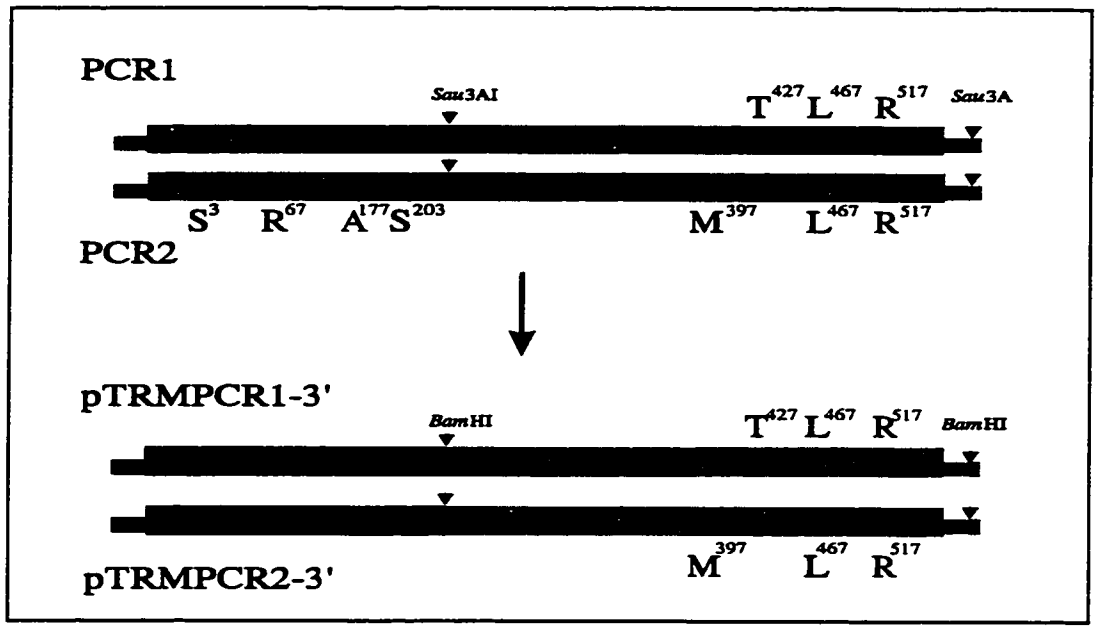

Figure 19. Plasmids pTRMPCR1-3' and pTRMPCR2-3'. Wild-type *TRM1* is represented by black bars and mutant *trm1* by grey bars. Replacement mutant residues are indicated with an x.

The m_2^2Gtase activity assay was performed using crude protein isolated from the SN1015-2a strain carrying the appropriate plasmid. This assay was performed in duplicate on separate days using different protein preparations. The negative control was YCp50 which lacks the *TRM1* gene and the positive control was pTRM-3' which contains the wild-type *TRM1* gene. The plasmid pTRM-3' underwent the same manipulations used to create the hybrid plasmids pTRMPCR1-3' and pTRMPCR2-3', except that after restriction digestion of YCpPJMR4 with *Bam*HI, the wild-type 1114 bp *Sau3*AI fragment containing the wild-type sequence was reintroduced. Results indicate that replacement of the 1114 bp *TRM1* *Bam*HI fragment with *Sau*3AI fragments carrying the 3 mutations Thr^{427}, Leu^{467} and Arg^{517} from PCR1, or Met^{397}, Leu^{467} and Arg^{517} from PCR2 was sufficient to eliminate activity from the wild-type enzyme (Figure 20).

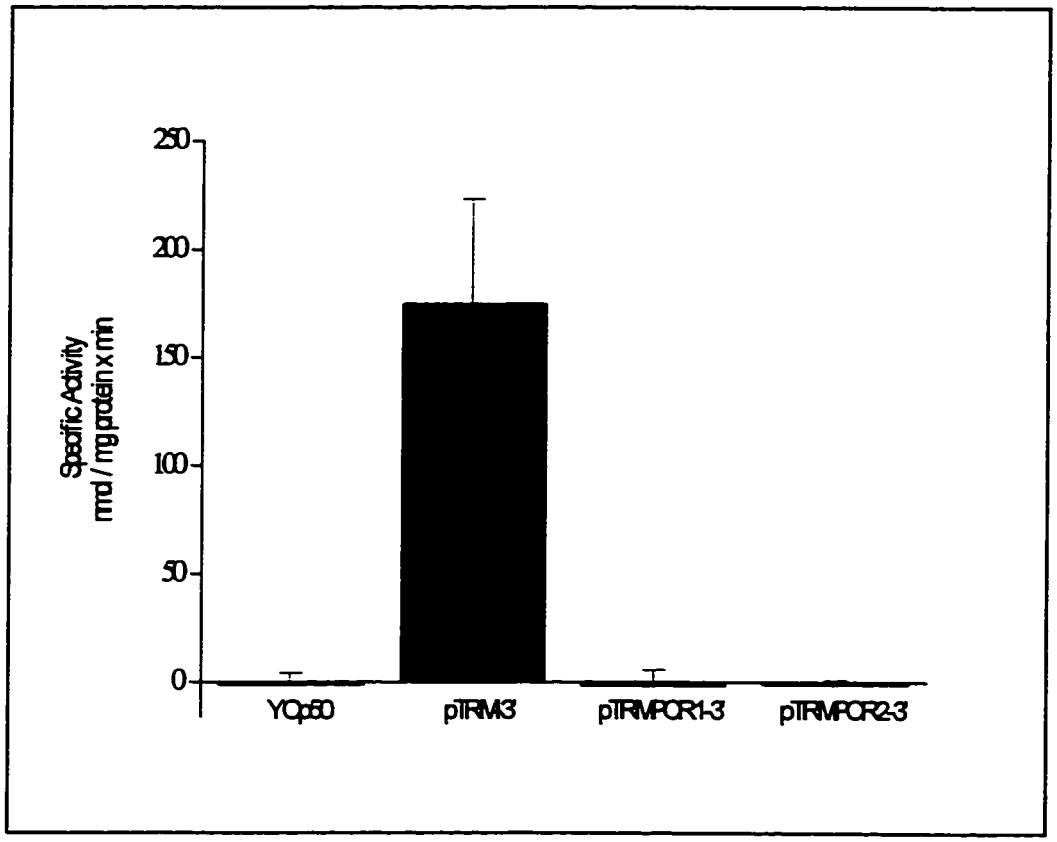

Figure 20. Effects of Replacement of 3 Residues at the 3' End of the *TRM*1 Gene on m_2^2Gtase Activity. The strain SN1015-2a was transformed with the following plasmids: YCp50 and pTRM-3' are negative and positive controls, respectively; pTRMPCR1-3' and pTRMPCR2-3' contain three amino acid substitutions found in PCR1 and PCR2, respectively, that are not present in the wild-type m_2^2Gtase. The vertical axis represents the mean (±SE mean) m_2^2Gtase specific activity expressed in nmol tritium/mg protein per min of duplicate experiments (n=4).

2. Subcloning II.

Replacement of Wildtype Residue Gly^{517} with Arg.

To further fine structure map the mutation responsible for loss of m_2^2Gtase activity, a mutant *trm*1 allele was created by replacing the 242 bp *Apa*I/*Nco*I fragment (spanning positions 1441 to 1683 in the wild-type gene (Ellis *et al.*, 1987)). This fragment contains Gly^{517} in the wild-type m_2^2Gtase while the corresponding fragment from PCR1 contains Arg^{517} and no additional amino acid changes. The resulting plasmid is pTRMPCR1-Arg (Figure 21). This plasmid was used to transform SN1015-2a and colonies were selected for uracil prototrophy.

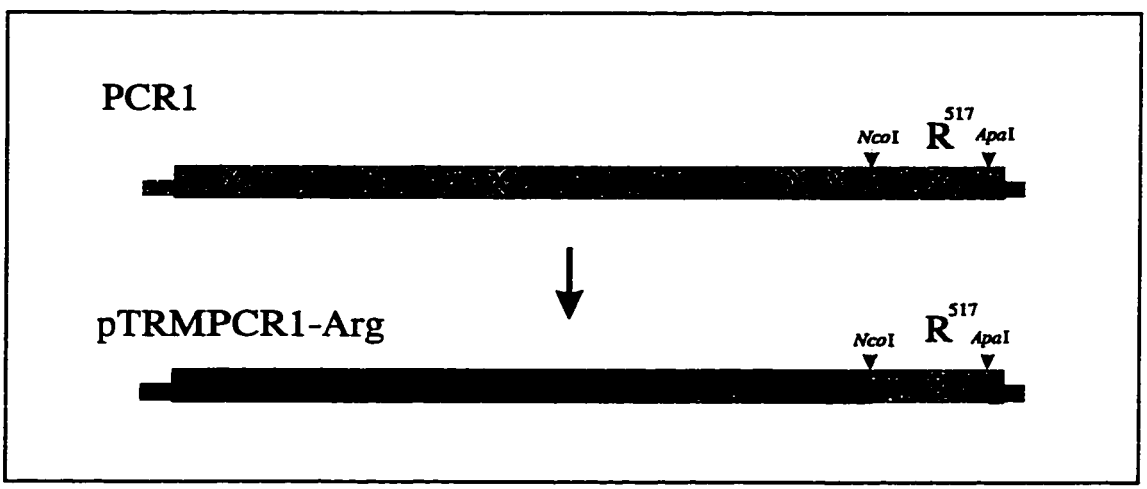

Figure 21. Plasmid pTRMPCR1-Arg. An *Apa*I and *Nco*I fragment (242 bp) from PCR1 containing the Arg^{517} mutation from *trm*1 (grey bar) was moved into the wild-type *TRM*1 gene (black bar). Positions of the *trm*1 mutations are indicated with an x.

The assays for m_2^2Gtase activity were performed using crude protein isolated from the transformed SN1015-2a yeast. Results indicate that replacement of Gly^{517} with an Arg residue does not affect wild-type m_2^2Gtase activity levels (Figure 22). SN1015-2a transformed with pTRMPCR1-Arg displayed similar enzyme activity to that of yeast transformed with the positive control pTRM-Gly. The plasmid pTRM-Gly carries the *TRM*1 allele that underwent the same manipulations as pTRMPCR1-Arg except that Gly^{517} was not replaced. The negative control plasmid was pTRMPCR1-3' which carries the 3 mutations Thr^{427}, Leu^{467} and Arg^{517} found at the 3' end of PCR1 and previously had been shown to lack m_2^2Gtase activity.

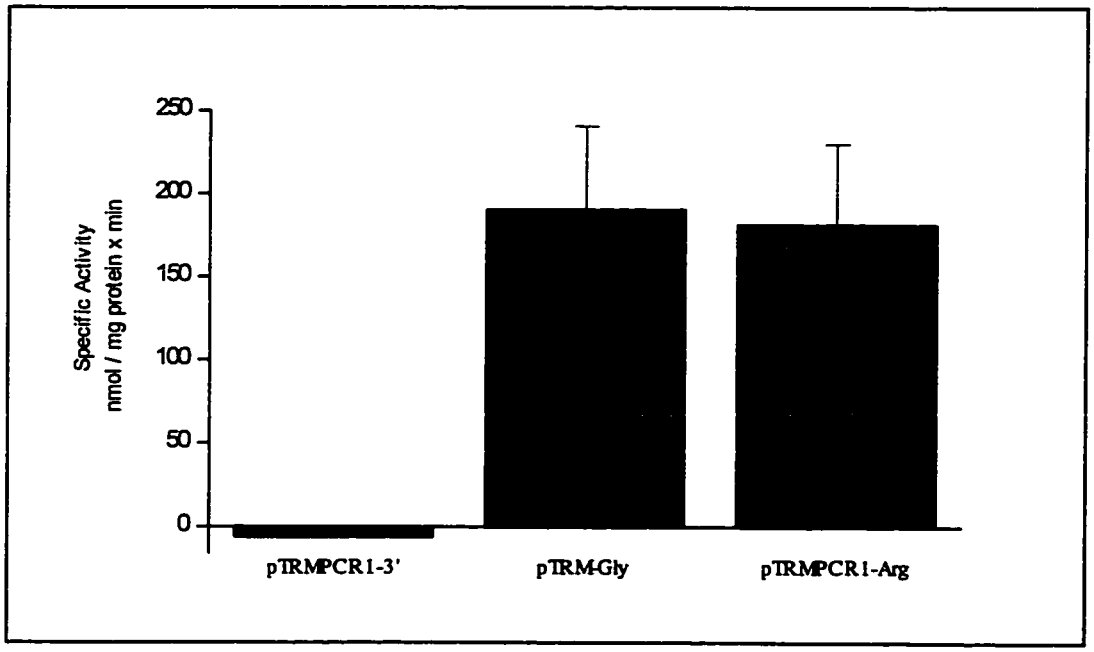

Figure 22. Effect of Replacement of Gly^{517} from the *TRM*1 Gene with Arg on m_2^2Gtase Activity. The vertical axis represents the mean (±SE mean) m_2^2Gtase specific activity expressed in nmol tritium/mg protein per min of duplicate experiments (n=4). SN1015-2a was transformed with the following plasmids: pTRMPCR1-3' and pTRM-Gly are the negative and positive controls, respectively; pTRMPCR1-Arg contains *TRM*1 with the Arg^{517} mutation.

3. **Site-directed mutagenesis.**

Identification of Residue Leu^{467} Responsible for Inactivation of m_2^2Gtase.

As described previously, a mutant *trm*1 allele, pTRMPCR1-3', was created by replacing the 1114 bp *Bam*HI fragment of the wild-type gene with a similar fragment carrying the desired mutations (Figure 19). Variants of this mutant m_2^2Gtase were produced using site-directed mutagenesis to systematically substitute residues in the mutant protein with those found in the functional protein (Figure 23). The resulting plasmids are: pTRMPCR1-Asn in which Thr^{427} was converted to the wild-type residue Asn, pTRMPCR1-Ser where Leu^{467} is changed to Ser, and pTRMPCR1-Gly where Arg^{517} is changed to Gly.

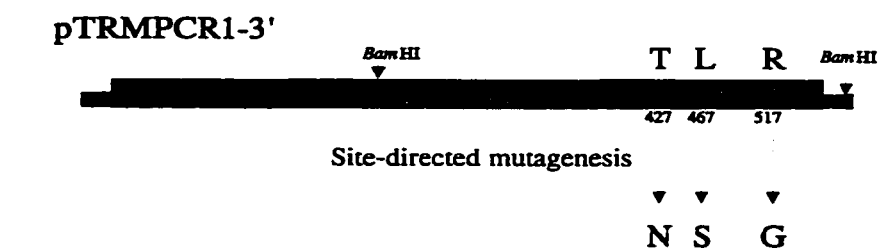

Figure 23. Site-Directed Mutagenesis. Three mutations found in PCR1 (grey bar) were changed systematically back to wild-type residues. A portion of the *TRM*1 gene is represented by the black bar.

The m_2^2Gtase activity assays were used to verify which amino acid residue substitutions in the mutant protein restore methyltransferase activity. SN1015-2a was transformed with plasmids pTRMPCR1-Asn, pTRMPCR1-Gly and pTRMPCR1-Ser, and colonies carrying the plasmid were selected for uracil prototrophy. Colonies transformed with these modified *TRM1* alleles were assayed for m_2^2Gtase activity. Figure 24 demonstrates that replacement of the mutant Leu^{467} residue by the wild-type Ser was sufficient to restore m_2^2Gtase activity in SN1015-2a, while converting Arg^{517}→Gly or Thr^{427}→Asn was not. The activity level was found to be higher than in the control condition pTRM-3' containing the wild-type *TRM1*. These results suggest that the Ser^{467}→Leu substitution is responsible for the inactivation of m_2^2Gtase.

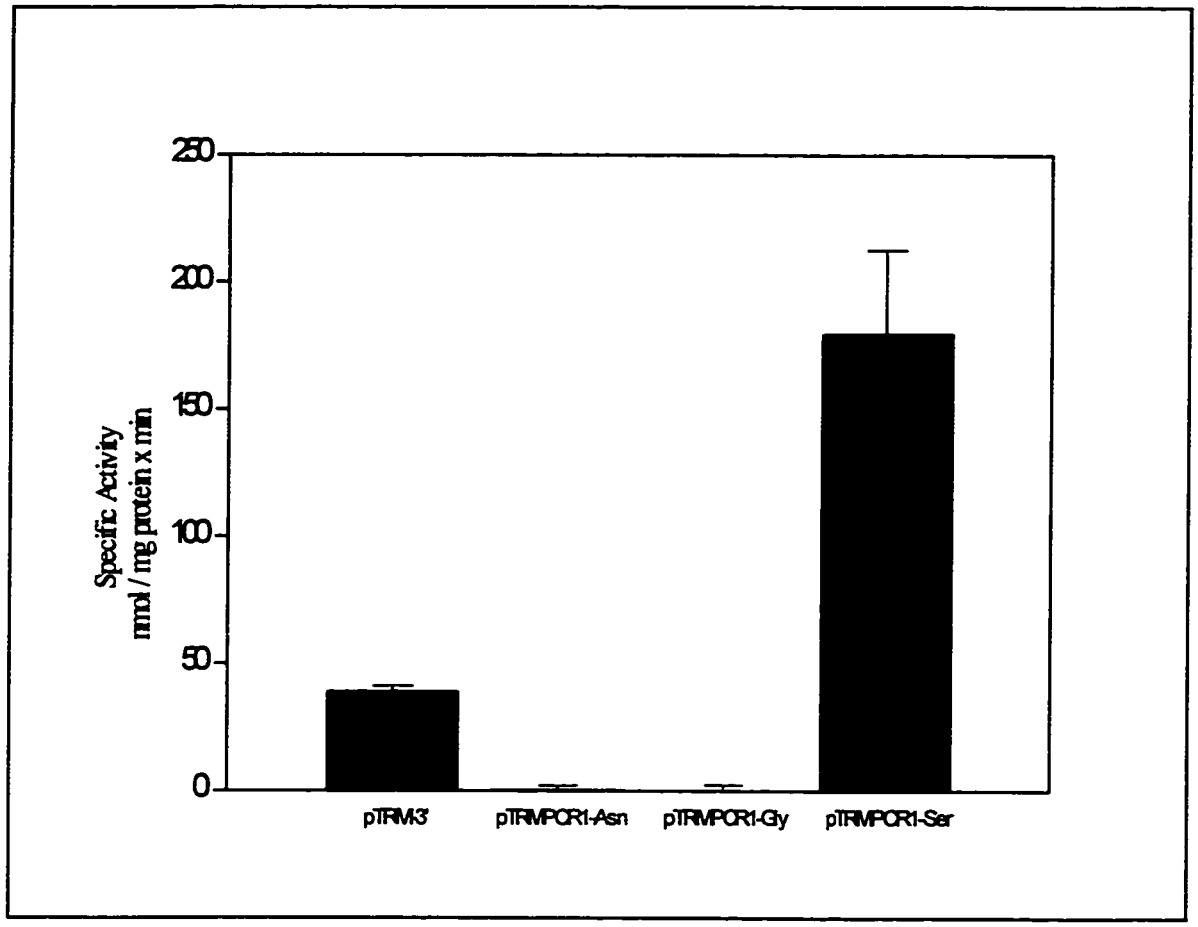

Figure 24. Effects on m_2^2Gtase Activity of the Replacement of Mutant Residues at the 3' End of the *trm*1 Gene with Wild-Type Residues. SN1015-2a was transformed with the following plasmids: pTRM-3' which carries the wild-type *TRM*1 gene is the positive control; pTRMPCR1-Asn has Thr^{426} changed to Asn; pTRMPCR1-Gly has Arg^{517} changed to Gly ; pTRMPCR1-Ser has Leu^{467} changed to Ser. The vertical axis represents the mean (±SE mean) m_2^2Gtase specific activity expressed in nmol tritium/mg protein per min of duplicate experiments (n=4).

PART 4

Defining the Role of Ser^{467}

1. Site-Directed Mutagenesis.

Variant m_2^2Gtase enzymes were created by modifying the *TRM*1 gene such that Ser^{467} was converted to four other amino acid residues (Figure 25). The resulting plasmids are: pTRMSer-Leu, pTRMSer-Ala, pTRMSer-Thr and pTRMSer-Cys.

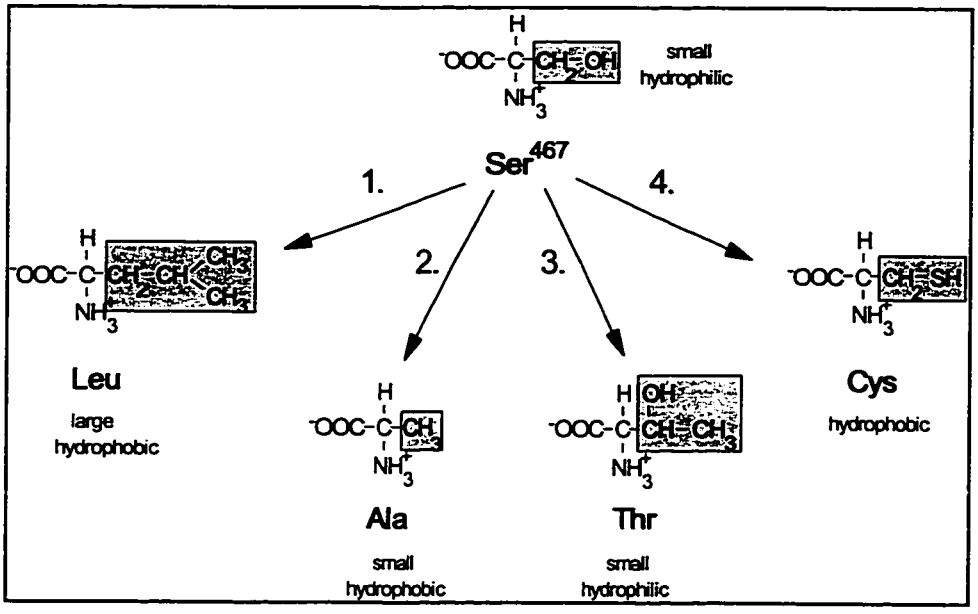

Figure 25. Changing Wild-Type *TRM*1 Ser^{467}. The structures of the amino acid residues are depicted with their side chains outlined in grey.

Plasmids pTRMSer-Leu, pTRMSer-Ala, pTRMSer-Thr and pTRMSer-Cys were employed to transform DBY745ΔTRM yeast. This yeast was employed because no m_2^2Gtase is synthesized due to the disruption of the *TRM1* gene with *LEU2*. This would allow for m_2^2Gtase assays to be conducted without contamination with native enzyme. Colonies were selected for uracil prototrophy and m_2^2Gtase activity assays were performed using protein isolated from transformed DBY745ΔTRM (Figure 26). Results indicate that replacement of Ser^{467} for Leu eliminates wild-type m_2^2Gtase activity resulting in levels that are comparable to the negative control plasmid, pTRMPCR1-3', which carries the three mutations Thr^{427}, Leu^{467} and Arg^{517} found at the 3' end of PCR1. However, substitution of Ser^{467} by Thr, Ala and Cys does not affect enzyme activity as all three variant proteins displayed similar levels of activity to that of DBY745ΔTRM transformed with wild-type *TRM1* (YCpPJMR4).

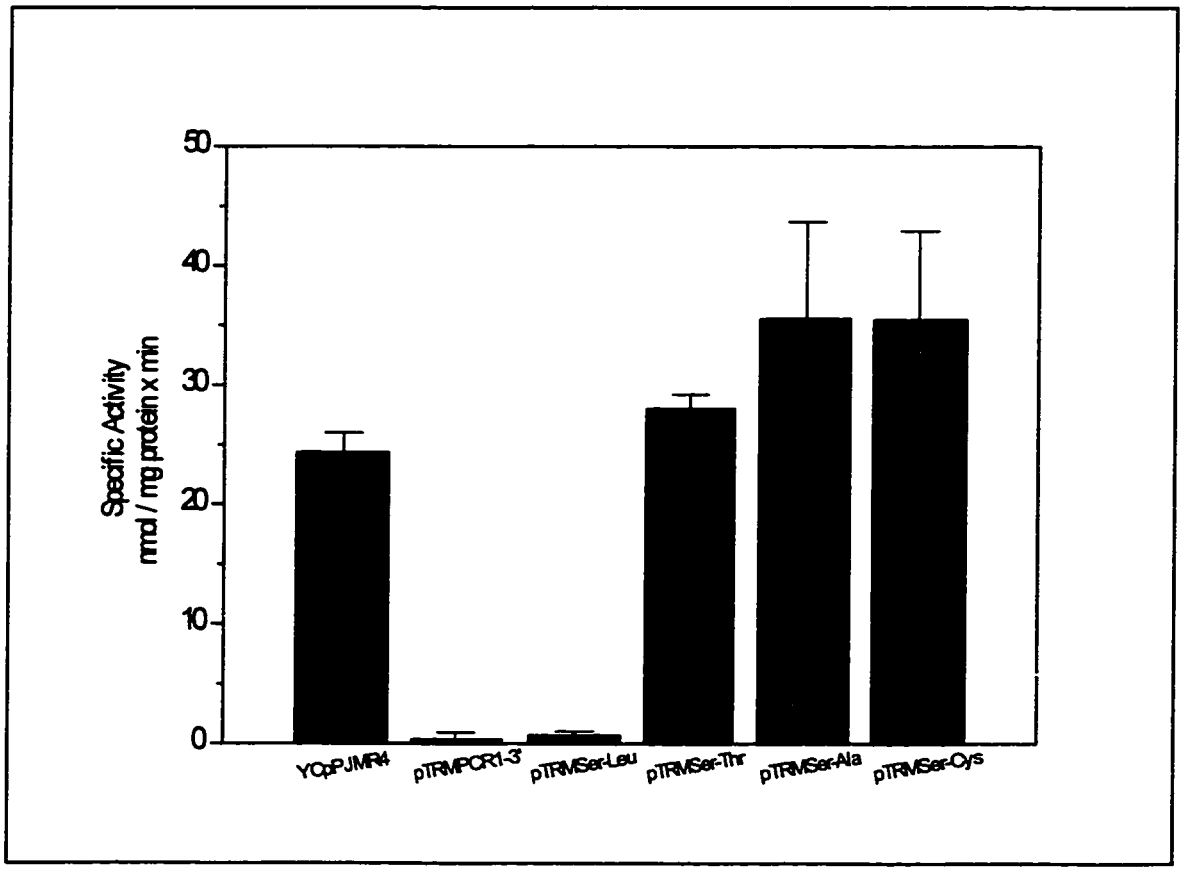

Figure 26. Effects on m_2^2Gtase Activity of Altering Wildtype Ser[467]. DBY745ΔTRM was transformed with the following plasmids and assayed for m_2^2Gtase activity: YCPJMR4 has wild-type *TRM*1 (positive control); pTRMPCR1-3' has 3 mutations, Thr[427], Leu[467] and Arg[517] from PCR1 (negative control); pTRMSer-Leu, pTRMSer-Thr, pTRMSer-Ala and pTRMSer-Cys have Ser[467] substituted by Leu, Thr, Ala and Cys, respectively. The vertical axis represents the mean ±SE m_2^2Gtase specific activity expressed in nmol/mg protein per min of duplicate experiments (n=4).

2. Secondary Structure Prediction.

The effects on the secondary structure of m_2^2Gtase of changing Ser^{467} to Leu, Ala, Thr, and Cys were examined using the Garnier method (Garnier *et al.*, 1978). This method predicted possible structural conformational changes due to each of the substitutions. Figure 27 shows the semi-graphical representations of the protein secondary structure obtained using the amino acid sequence predicted from the entire *TRM1* gene with the following substitutions at position 467; Leu, Ala, Thr and Cys. Only residues in the region of 460 to 480 of the *TRM1* sequence are shown.

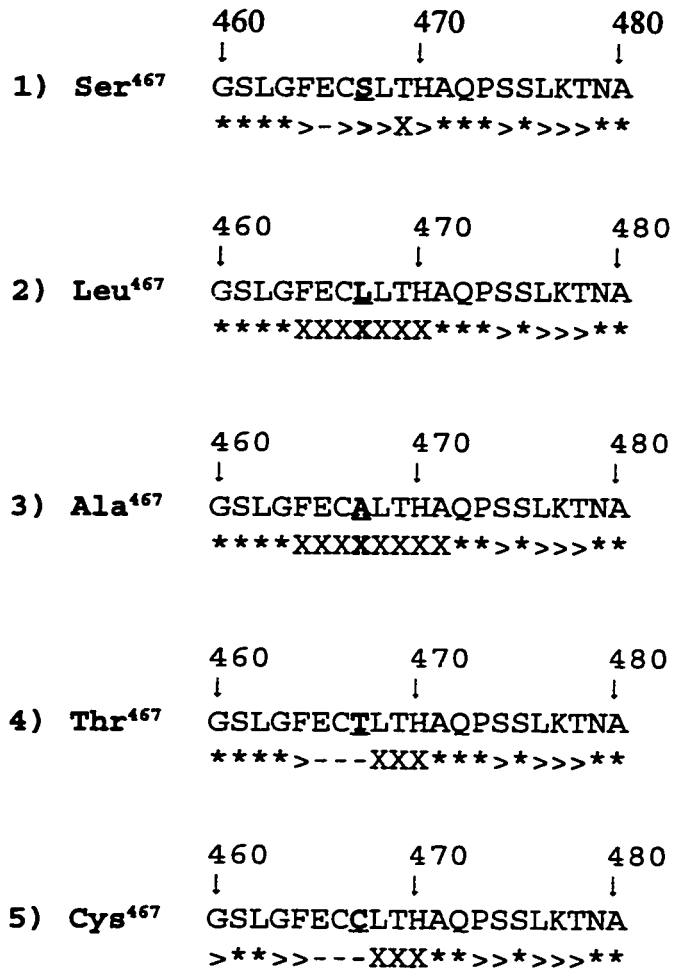

Figure 27. The Effects on Protein Secondary Structure of Converting Ser^{467} as Predicted by the Garnier Method (Garnier *et al.*, 1978). Analysis was conducted using 570 amino acid residues of the *TRM*1 sequence (1), and then with each of the four amino acid substitutions: (2) Ser^{467} to Leu, (3) Ser^{467} to Ala, (4) Ser^{467} to Thr, and (5) Ser^{467} to Cys. Only amino acids 460 to 480 are shown with the altered residues bolded and underlined. Symbols used in the semi-graphical representation are: Helical conformation: X; Extended conformation: - ; Turn conformation: > ; and Coil conformation: *.

3. Enzyme Kinetic Studies.

As a preliminary examination of how the Ser^{467}→Leu substitution could inactivate m_2^2Gtase, some kinetic characterization of the various mutants was carried out.

Establishing Incubation Times.

The incubation time to be employed in the kinetic studies was determined by monitoring m_2^2Gtase activity over time. Two different time course experiments were performed, each in duplicate. Aliquots of crude protein (10 μg) isolated from DBY745ΔTRM yeast transformed with wild-type *TRM*1 (YCpPJMR4) were assayed at 37°C under various substrate concentrations. In Time Course 1 (Figure 28A), the amount of tRNA was held constant at 2.0 μM, while three different SAM concentrations were tested (0.74, 7.4 and 74 μM). In Time Course 2 (Figure 28B), the amount of tRNA was varied (0.2, 2.0 and 20 μM) while the SAM concentration was held at 7.4 μM. The methylation reaction was monitored over time by assaying the incorporation of ^{3}H-methyl groups into $m_2^2G_{26}$-deficient tRNA at times t = 0, 10, 15, 20, 25, 30, 40 and 60 min. Figure 28 shows that the reactions were linear for at least one hour. The time point t=20 minutes, which lies in the linear range, was chosen as the incubation time for subsequent reactions in the kinetic analysis. The linear regression model was used to fit the data points to a straight line.

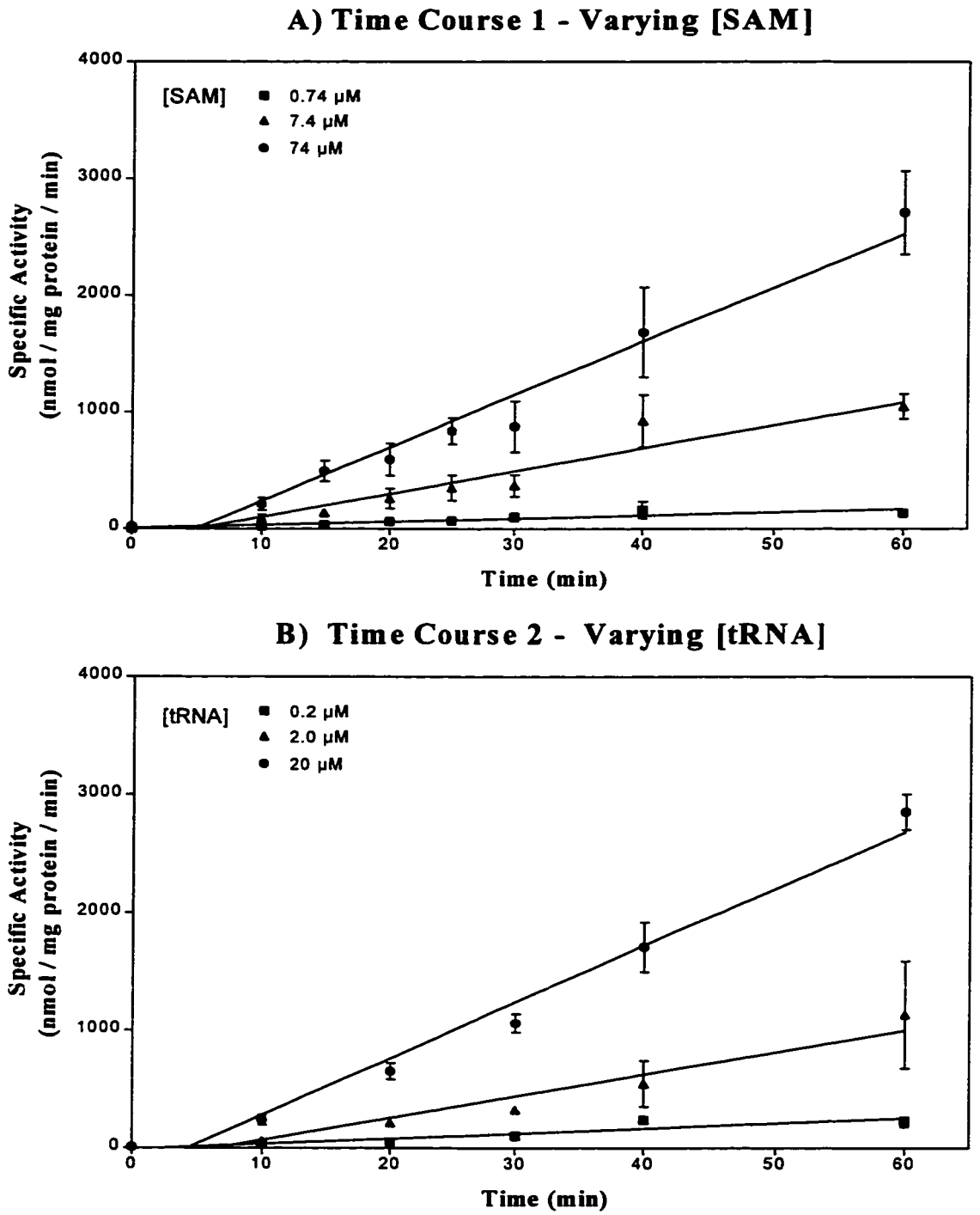

Figure 28. Time-Dependent Incorporation of Methyl Groups. A) Time Course 1 was obtained using three different SAM concentrations (0.74, 7.4 and 74 µM). B) Time Course 2 was obtained using three different tRNA concentrations (0.2, 2.0 and 20 µM). The vertical axis represents the mean (±SE mean) of m_2^2Gtase specific activity expressed in nmol tritium/mg protein per min of duplicate experiments (n=4). The horizontal axis represents time expressed in minutes.

Varying SAM Substrate.

The effects on the activity of various m_2^2Gtase mutants of altering SAM concentration were examined. DBY745ΔTRM yeast was transformed with either plasmid YCpPJMR4, pTRMSer-Thr, pTRMSer-Ala, or pTRMSer-Cys and was assayed for m_2^2Gtase activity. Crude protein (10 μg) was assayed at 37°C for 20 min at various SAM concentrations (0.74 to 148 μM) while the amount of tRNA was held constant at 2.0 μM. Figure 29 shows typical hyperbolic kinetics of m_2^2Gtase activity displayed by each mutant as a function of SAM concentration. The apparent K_M and apparent V_{max} values listed in Table 5 were calculated from nonlinear regression analyses. The apparent V_{max} of the three m_2^2Gtase variants was found to be in the same range as that of the wild-type protein (YCpPJMR4). The Ser^{467}-Thr mutant displayed an apparent K_M value similar to the value for wild-type m_2^2Gtase, while variants Ser^{467}-Ala and Ser^{467}-Cys displayed apparent K_M values that were approximately three-fold higher than the apparent K_M for the wild-type m_2^2Gtase.

Varying tRNA Substrate.

The effects on the activity of various m_2^2Gtase mutants of altering tRNA concentration are illustrated in Figure 30. DBY745ΔTRM yeast was transformed with either plasmid YCpPJMR4, pTRMSer-Thr, pTRMSer-Ala, or pTRMSer-Cys and was assayed for m_2^2Gtase activity. Crude protein (10 μg) was assayed at 37°C for 20 min with various amounts of tRNA (0.2 to 20 μM) while the concentration of SAM was held constant at 148 μM. Kinetic studies led to plots typical of tRNA substrate saturation for all mutants. Table 5 lists the apparent K_M and apparent V_{max} values obtained from these plots through nonlinear regression. All m_2^2Gtase proteins (wild-type *TRM*1 and variants) displayed similar apparent V_{max} and K_M values.

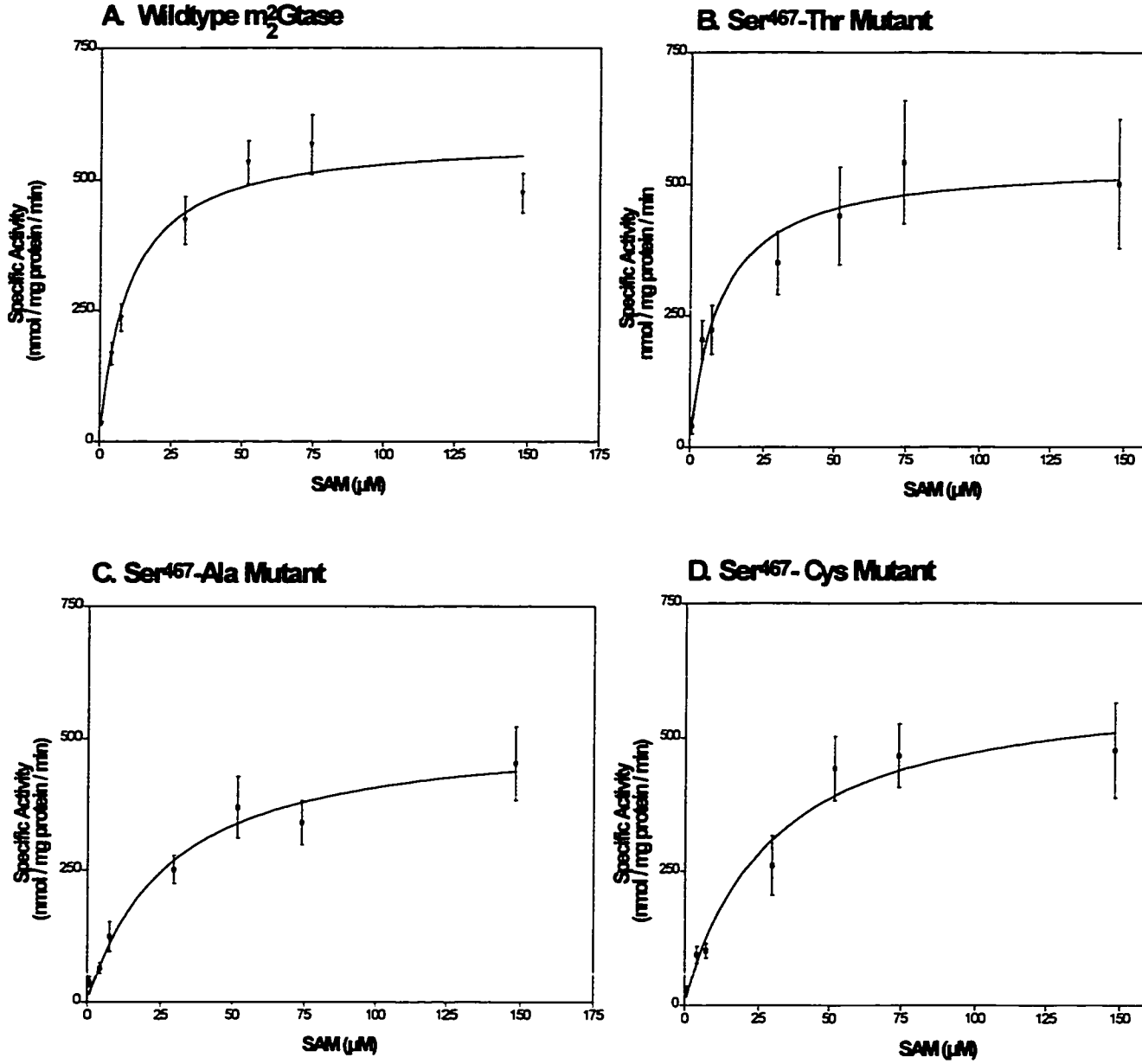

Figure 29. m_2^2Gtase Specific Activity as a Function of SAM Concentration. Graph A outlines the kinetics displayed by wild-type m_2^2Gtase. Graphs B, C and D represent the kinetics exhibited by m_2^2Gtase variants Ser^{467}-Thr, Ser^{467}-Ala and Ser^{467}-Cys, respectively. The vertical axis represents the mean (±SE mean) m_2^2Gtase specific activity expressed in nmol tritium/mg protein per min of triplicate or quadruplicate experiments (n=6 to n=10). The horizontal axis represents the concentration of SAM substrate.

	SAM		tRNA	
	apparent K_M (μM)	apparent V_{max} (nmol/mg protein/min)	apparent K_M (μM)	apparent V_{max} (nmol/mg protein/mi
YCpPJMR4	9.7 ± 2.8	580.3 ± 38.8	2.3 ± 0.9	711.1 ± 79.9
$S^{467}\rightarrow T$	9.8 ± 2.9	542.4 ± 37.8	4.5 ± 1.3	643.8 ± 67.8
$S^{467}\rightarrow A$	27.8 ± 7.2	519.7 ± 44.2	2.7 ± 1.1	611.3 ± 79.9
$S^{467}\rightarrow C$	28.9 ± 9.4	608.8 ± 65.9	3.0 ± 0.6	538.1 ± 32.4

Table 5. Summary of Apparent K_M and Apparent V_{max} Values of m_2^2Gtase and m_2^2Gtase Variants. The apparent K_M and apparent V_{max} values shown above were calculated from nonlinear regression analyses. The means and ±SE are a result of triplicate or quadruplicate experiments.

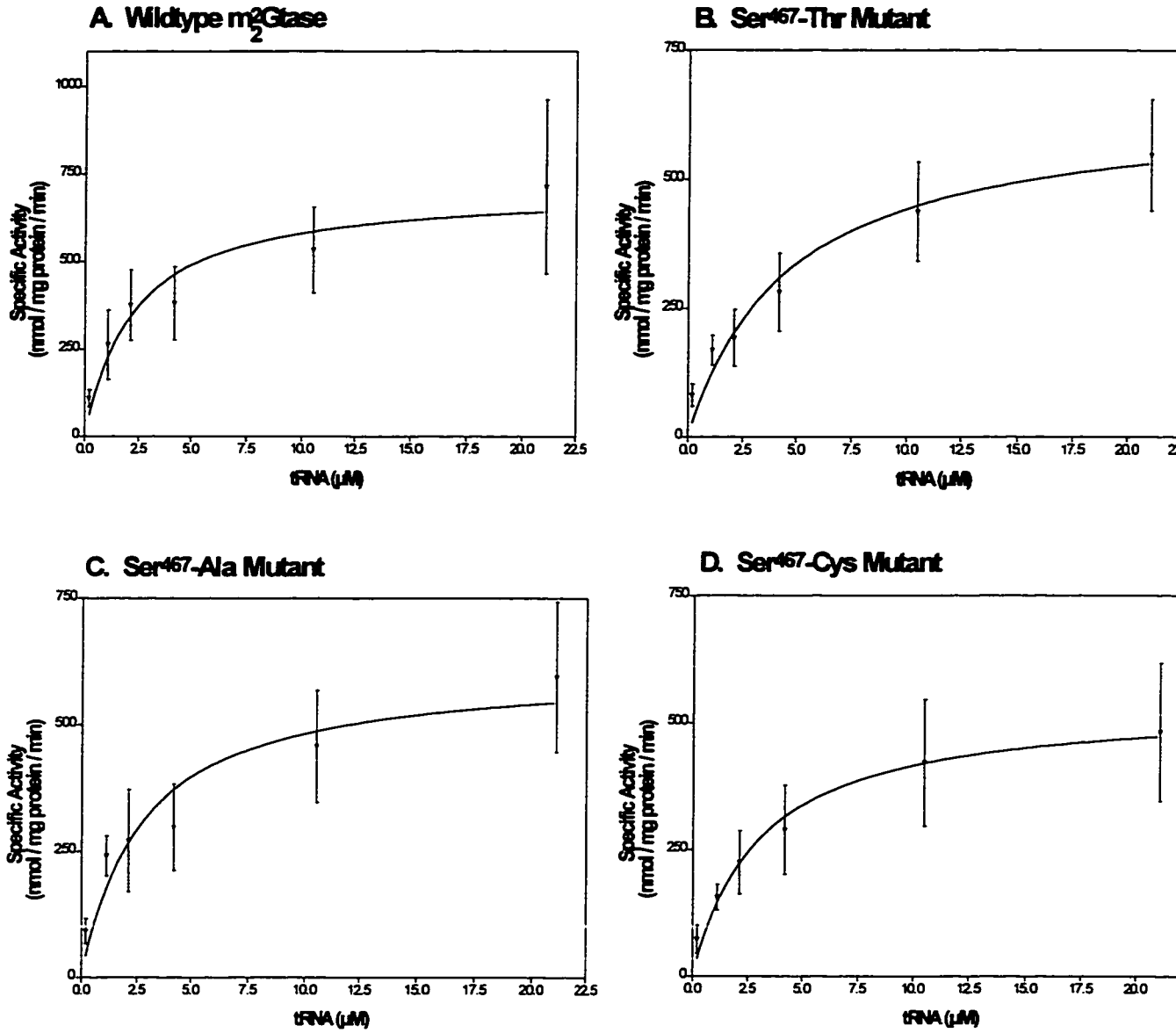

Figure 30. m_2^2Gtase Specific Activity as a Function of tRNA Concentration. Graph A outlines the kinetics displayed by wild-type m_2^2Gtase. Graphs B, C and D represent the kinetics exhibited by m_2^2Gtase variants Ser^{467}-Thr, Ser^{467}-Ala and Ser^{467}-Cys respectively. The vertical axis represents the mean (±SE mean) m_2^2Gtase specific activity expressed in nmol tritium/mg protein per min of triplicate or quadruplicate experiments (n=6 to n=10). The horizontal axis represents the amount of tRNA substrate.

4. The Presence of m_2^2Gtase in Other Organisms.

Protein Sequence Alignments.

All protein sequence analyses were conducted using the Swiss-Prot and GenBank databases. The predicted amino acid sequence for yeast m_2^2Gtase was used as the dataset to search for other proteins or predicted proteins. Ten proteins from a variety of organisms had sequences producing high-scoring segment pairs (data not shown). Only those having sequence alignments to the region in which Ser^{467} of yeast m_2^2Gtase is found are displayed in Figure 31. The predicted ZC376.5 protein of *Caenorhabditis elegans* displayed 60% positives (39/65 residues) in this region, while m_2^2Gtase from *Methanococcus jannaschii* displayed 55% positives (31/56 residues) in this region.

```
Yeast:          427  NELSDSPFYFSPNHIASVIKLQVPPLKKVVAGLGSLGFEC
                     NE  D   Y+  N +A+V+K+ VP  + V + + + GF+
C.elegans:      379  NEELDDVLYYEHNQMANVVKVSVPKSQSVRSAILNAGFKV

Yeast:          467  SLTHAQPSSLKTNAPWDAIWYVMQK  491
                     S +H  P ++KTNAP   +W + ++
C.elegans:      419  SGSHCNPRAIKTNAPMHLLWDIYRQ  444


Yeast:          436  FSPNHIASVIKLQVPPLKKVVAGLGSLGFECSLTHAQPSS
                     +  + I  ++K+ VPP++ ++  l  +GF   +TH  P
M.jannaschii:   314  YDTHQIGKMLKISVPPMQDIINKLKEMGFNAVVTHYNPKG

Yeast:          476  LKTNAPWDAIWYVMQKC  492
                     +KT+A    +   + +C
M.jannaschii:   354  IKTDATLKNVIEAIYQC  370
```

Figure 31. Protein sequence alignments. Consensus sequences are shown between the two sequence alignments. The Ser^{467} in yeast m_2^2Gtase and the corresponding residues from the other organisms are bolded and underlined. Numbers indicate position in the original sequence.

Secondary Structure Predictions.

The secondary structures of the predicted ZC376.5 protein from *C. elegans* and m_2^2Gtase from *M. jannaschii* were examined using the Garnier method (Garnier *et al.*, 1978). Only residues residing in the region in which Ser^{467} of yeast m_2^2Gtase is found are depicted in Figure 32. Shown are the semi-graphical representations of the protein secondary structure obtained from the Swiss-Prot database using the amino acid sequence predicted from the *TRM1* gene sequence as the data input.

1. ZC376.5 protein from *C. elegans:*

```
379
↓
NEELDDVLYYEHNQMANVVKVSVPKSQSVRSAILNAGFKVSGSHCNPRAIKTNAPMHLLW
XXXXXXXXXXXXXXXXXX-----*>**-------*X>>>>>>>**>>>>*>***>X-XX

  444
   ↓
DIYR
XX->
```

2. m_2^2Gtase from *M. jannaschii:*

```
314                                                          370
↓                                                             ↓
YDTHQIGKMLKISVPPMQDIINKLKEMGFNAVVTHYNPKGIKTDATLKNVIEAIYQC
>XXXXXXX----****XXXXXXXXXXXXXXX----->*>>>---XXXXXXXXXXX->
```

Figure 32. The Secondary Structure as Predicted by the Garnier Method (Garnier *et al.*, 1978). Analysis was conducted using 65 and 57 amino acid residues of the ZC376.5 protein of *C. elegans* and m_2^2Gtase from *M. jannaschii,* respectively. The residues that align with Ser^{467} of the yeast m_2^2Gtase are bolded and underlined. Symbols used in the semi-graphical representation are: Helical conformation: X; Extended conformation: - ; Turn conformation: > ; and Coil conformation: *.

Discussion

IV. DISCUSSION

The enzyme, N^2,N^2-dimethylguanosine-specific tRNA methyltransferase, belongs to the best known class of tRNA modifying enzymes, the tRNA methylases. Although there are many examples of tRNA methylases, little is known about their molecular mechanisms. The major goal of this study was to employ an *S. cerevisiae* SN1015-2a mutant, defective in m_2^2Gtase activity, in an attempt to gain some insights into the mode of action of tRNA methylases. PCR products generated from the mutant strain were cloned and sequenced and the sequence revealed a predicted amino acid sequence of the mutant m_2^2Gtase. The inactivating mutation in yeast m_2^2Gtase was identified and further characterized by mutagenesis and kinetic studies.

SN1015-2a Lacks Functional m_2^2Gtase.

As the aim of this study was to attempt to define which regions of m_2^2Gtase might be required for enzyme activity by analyzing a m_2^2Gtase-deficient mutant, it was initially necessary to demonstrate that strain SN1015-2a lacked m_2^2Gtase activity. Preliminary studies suggested that yeast carrying the *trm*1 mutation and lacking $m_2^2G_{26}$ are viable and have no obvious growth defect under standard laboratory growth conditions (Figure 8). However, this gross observation does not rule out subtle changes in its metabolism or regulation. Therefore, it was necessary to conduct enzyme assays on crude protein extracts to determine whether or not a yeast strain contained an active enzyme. Results from time course measurements of m_2^2Gtase activity in extracts from SN1015-2a further

substantiated findings that this mutant lacks any detectable enzyme activity, even under near saturating substrate conditions (Figure 10).

Lack of m_2^2Gtase activity may be due to a number of factors including a mutation that; 1) blocks transcription, 2) blocks translation, 3) results in the synthesis of a nonfunctional protein, or 4) results in the synthesis of an unstable protein that is readily degraded. Previous experiments (Li *et al.*, 1989) suggested that m_2^2Gtase is synthesized but is non-functional. Western analysis (Figure 11) confirmed this observation. When an antibody generated to the last 16 C-terminal amino acids of m_2^2Gtase was employed, a 63 kDa protein was detected in the yeast strains W303-1b and DBY745 (both wild-type for m_2^2Gtase) and in the strain SN1015-2a (which lacks m_2^2Gtase activity). In contrast, the strain DBY745ΔTRM, which has the *TRM1* gene deleted and should not produce any m_2^2Gtase, did not display the m_2^2Gtase band at 63 kDa. This confirms that there is positive hybridization with the m_2^2Gtase antibody. There is, however, a signal at approximately 60 kDa which is present in all samples (Figure 11). This is probably another yeast protein that cross reacts with the primary antibody. This band at 60 kDa is more pronounced in the DBY745ΔTRM protein extract and this may be due to the fact that the 63 KDa protein is not present to compete for the primary antibody. Although the presence of the second band in the area of the m_2^2Gtase signal makes it difficult to precisely determine the amount of m_2^2Gtase present, it appears that the intensity of the m_2^2Gtase band is similar in all three protein extracts containing m_2^2Gtase. Since the extracts were prepared from the same amount of cells at the same growth phase, this observation implies that under these conditions of cell harvesting and lysis, the wild-type and mutant m_2^2Gtase proteins have

approximately the same level of stability. This suggests that the apparent absence of enzyme activity is not due to a significant increase in the instability and degradation of the mutant m_2^2Gtase. Finally, from this immunoblot, it is apparent that the molecular weight of the wild-type and mutant proteins are similar and that the C-terminal antibody cross-reacts with the mutant enzyme. This observation supports the hypothesis that the lack of m_2^2Gtase activity is due to missense mutation(s) or a small in-frame deletion and not to a major deletion or frame shift.

The Cloning and Sequencing of the *trm*1 Gene.

The first step in identifying the mutation(s) responsible for loss of m_2^2Gtase activity involved isolating, cloning and sequencing the *trm*1 gene from SN1015-2a. The nucleotide sequences of two PCR products (PCR1 and PCR2) isolated from SN1015-2a genomic DNA were compared to the previously published wild-type *TRM*1 gene sequence (Ellis *et al.*, 1987) and to all *TRM*1 gene sequences in GenBank. Point mutations resulting in 14 silent mutations and 4 nonsense mutations were common to both products (Figure 15) and were dispersed throughout the gene. In both PCR1 and PCR2, the presumably X-ray induced point mutations found were highly diverse with the number of shared transitions (16) exceeding the number of shared transversions (2) by a ratio of 8:1 (Figure 15). The following classes of transitions and transversions were recovered: G↔A and T↔C transitions which accounted for 9/18 and 7/18 of the single base substitutions respectively, and C↔G and A↔T transversions each of which accounted for 1/18 substitutions. These findings agree well with studies identifying the spectrum of

X-ray induced point mutations in bacteria in which transitions, mainly G→A and T→C, occur more frequently than transversions (Takimoto *et al.*, 1991).

Subsequently, two separate clones of the *trm*1 gene obtained from two independent PCR amplification reactions revealed four shared amino acid substitutions: 1) Gly^{3}→Ser, 2) Thr^{203}→Ser, 3) Ser^{467}→Leu, and 4) Gly^{517}→Arg. These amino acid substitutions result from two G→A transitions, a C→T transition and an A→T transversion, and are distributed throughout the entire coding region of the gene from residue 3 to residue 517. Interestingly, it was observed that PCR1 differed from PCR2 at four additional positions (Figure 16). PCR1 had one substitution from the *TRM*1 gene sequence that was not found in PCR2, while PCR2 had 3 substitutions from the *TRM*1 gene sequence that were not shared with PCR1. As these four amino acid substitutions were not common to both of the cloned PCR products, they were considered as potential PCR-induced errors and were therefore deemed secondary in importance for this study. From Figure 15, PCR1 contains two nucleotide changes not found in PCR2, while PCR2 contains three nucleotide changes not found in PCR1. Assuming these changes result from errors incurred during PCR amplification, this suggests an error frequency of 1.1 errors per 1000 bp for PCR1 versus 1.7 errors per 1000 bp for PCR2. This error frequency for the PCR method employing *Taq* polymerase is not completely surprising as studies measuring the overall error frequency of PCR using *Taq* have reported rates ranging from 0.1/1000 to 0.6/1000 (Cariello *et al.* 1991; Chen and Viola, 1991). In our experimental conditions, no specific methods were used to limit PCR-induced base substitutions (Eckert and Kunkel, 1991), although, two different PCR products were

sequenced in the hopes of controlling for any PCR-induced changes.

Leu^{467} is Responsible for the Loss of m_2^2Gtase Activity.

Upon examination of the four amino acid substitutions common to both PCR products of *trm*1, it was concluded that the Gly^3→Ser mutation was not of importance as it is contained in the mitochondrial targeting signal (MTS) of m_2^2Gtase. Futhermore, the "short form" of the enzyme, which lacks the MTS and therefore lacks Gly^3, has been shown to be functional (Ellis *et al.*, 1987). The Thr^{203}→Ser substitution also did not seem the most likely candidate to inactivate the enzyme as it was a conservative change; both Ser and Thr are small hydroxylated residues. Upon initial analysis, the Ser^{467}→Leu and Gly^{517}→Arg substitutions appeared most interesting as they produced significant changes in their amino acid side chain. More specifically, the small and hydroxylated Ser residue is changed to the large, branched and nonpolar Leu, while the small nonpolar Gly residue is converted to Arg which is large, nonpolar and charged (Figure 17). Replacement of a fragment of the wild-type *TRM*1 gene with a *trm*1 fragment from PCR1 and PCR2 that contained these two mutations (Figure 19) supported our prediction as it resulted in the loss of m_2^2Gtase activity (Figure 20). This result indicated that mutations contained in the PCR1 or PCR2 *Sau*3AI fragments were sufficient to eliminate m_2^2Gtase activity. Although each PCR fragment contained a third mutation, both shared the Ser^{467}→Leu and Gly^{517}→Arg substitutions indicating that these mutations, and not the third, resulted in the loss of enzyme activity. To determine if both Leu^{467} and Arg^{517} were required for loss of enzyme activity, further sub-cloning and site-directed mutagenesis experiments were

carried out. When a fragment of the *TRM1* gene was replaced with its corresponding PCR1 fragment containing only the Gly^{517}→Arg substitution (Figure 21), enzyme activity was not lost (Figure 22) indicating that this substitution alone was not sufficient to inactivate the enzyme. In contrast, site-directed mutagenesis resulting in the conversion of Ser^{467}→Leu in the *TRM1* gene resulted in the complete elimination of m_2^2Gtase activity (Figure 26). These results indicate that the single amino acid change of Ser^{467}→Leu is sufficient to inactivate m_2^2Gtase.

These data were further supported by site-directed mutagenesis experiments in the fusion *TRM1*PCR1 gene (Figure 23) where conversion of Arg^{517}→Gly did not restore enzyme activity, while conversion of Leu ^{467}→Ser did (Figure 24). Taken together, these data suggest that Leu^{467} is the mutation responsible for loss of m_2^2Gtase activity and that the Ser^{467}→Leu amino acid substitution alone is sufficient to inactivate m_2^2Gtase.

These results were initially surprising as Gly^{517}→Arg was considered to be a more likely candidate for inactivating m_2^2Gtase due to the very dramatic change in the character of the side chain (Figure 17). However, despite their dissimilar structures, Gly and Arg share the property of being poor helix formers and substitution of one for the other does not produce a significant change in the predicted structure of m_2^2Gtase. The Garnier method for secondary structure prediction (Garnier *et al.*, 1978) suggests that this Gly^{517} to Arg change simply results in an additional turn in this region of the protein (data not shown).

A single change of an amino acid residue in a macromolecular protein can have a

profound effect on the activity of the enzyme. For example, a particular amino acid may be involved in the binding of substrates, such that its substitution may result in the alteration of a specific interaction between substrate and enzyme. Additionally, a specific amino acid residue may be required to catalyze a reaction. For example, the serine proteases, such as trypsin and chymotrypsin, possess a reactive serine residue that is required to form covalent adducts with some substrates and inhibitors (Creighton, 1993). In contrast, the change of a single residue may result in the alteration of the conformation of a protein. One recent study has demonstrated that a single point mutation leading to an amino acid substitution of Ala^{80}→Pro, can cause the loss of catalytic activity in human thiopurine S-methyltransferase (Krynetski *et al.*, 1995). As proline is known to cause distortions in protein structures, the authors suggest that this substitution may result in alterations in the three-dimensional structure of the protein. The reason for the loss of m_2^2Gtase activity resulting from the Ser^{467}→Leu substitution is unknown, but could be attributed to loss of an active site residue, changes in the folding patterns of the protein as seen for thiopurine S-methyltransferase, or the blocking of the active site. Ser is a polar residue that is commonly found at active sites due to its fairly reactive hydroxyl group. Its substitution by a nonpolar residue such as Leu may interfere with catalysis by elimination of the hydroxyl group required for substrate binding or catalysis. On the other hand, Leu is a bulky amino acid residue and may cause distortions in protein structure or block the active site preventing substrate from binding. It still remains to be seen how Leu results in the loss of m_2^2Gtase activity.

To try to elucidate what role Ser^{467} may have in m_2^2Gtase, site-directed mutagenesis

was carried out to convert Ser^{467} to the following residues: 1) threonine, 2) alanine, and 3) cysteine. Thr was chosen because it represents a very minor modification. Both Ser and Thr are small, hydroxylated residues and Thr differs from Ser only by an additional methyl group. Ala was selected because sterically, it is very similar to Ser, differing only by the absence of the hydroxyl group. Cys was chosen because spatially, it closely resembles Ser. It differs only in that the hydroxyl group is replaced by a thiol group. These changes seem rather subtle in terms of the size of the side chain, but they test the importance of the hydroxyl group of Ser^{467} on enzyme activity. If the variants methylate tRNA to different extents, this would indicate that they differ in their specificity, thus possibly implicating Ser^{467} as being an active site residue involved in catalysis or binding of substrates.

Ser^{467} is not Essential for m_2^2Gtase Activity.

The effects of converting wild-type Ser^{476} to Leu, Thr, Ala and Cys were examined using m_2^2Gtase activity assays (Figure 26). As described previously, a Leu substitution at position 467 of m_2^2Gtase causes inactivation of the enzyme. Furthermore, changing Ser^{467} to Thr did not alter m_2^2Gtase activity levels from those of the wild-type enzyme. This was not unexpected since this was a rather conservative change as the hydroxyl group was maintained at this position. However, the Ser^{476}→Ala and Ser^{476}→Cys substitutions also did not decrease m_2^2Gtase activity. These results imply that Ser^{467} is not essential for the catalytic function of m_2^2Gtase. Moreover, it is not the loss of the Ser hydroxyl group that accounts for the inactivation of the enzyme, but the introduction of

the large hydrophobic side chain of Leu at this position that is responsible for the loss of m_2^2Gtase activity.

Due to the fact that the enzyme with Leu^{467} displayed no detectable activity under any conditions asssayed (Figure 10), it was not possible to carry out any kinetic analyses with this enzyme. Therefore, to ascertain what possible effect a Ser to Leu substitution at position 467 could have on m_2^2Gtase activity, secondary structure predictions (Garnier *et al.*, 1978) were made (Figure 27). Ser^{467} lies in a turn region of m_2^2Gtase (Figure 27). The Garnier algorithm predicts that when this Ser in the wild-type protein is replaced by a Leu, the turn region is lost and a more helical structure is generated (Figure 27). Taken alone, this outcome might suggest that the Ser^{476}→Leu substitution results in an altered secondary structure that inactivates the enzyme. However, a similar increase in this helical region occurs when Ser^{467} is converted to Ala (Figure 27), but without the loss of enzyme activity (Figure 26). The Thr and Cys substitutions also resulted in the loss of the turn region (Figure 27), but again activity was essentially equal to wild-type levels (Figure 26). Only those amino acid residues in the vicinity of Ser^{467} are presented, as the substitutions described do not alter the secondary structure of the protein outside the regions illustrated in Figure 27. Unfortunately, in the absence of a crystal structure, little useful information can be generated from this approach.

It still remains to be determined how the Ser^{467}→Leu substitution contributes to the loss of m_2^2Gtase activity. There are two plausible explanations for how the large side chain at position 467 can inactivate the enzyme: 1) Leu, with its rather large side chain, is sufficient to alter the higher order structure of m_2^2Gtase, or 2) Leu somehow affects the

ability of substrate(s) to bind or interact with the catalytic sites. Providing that the change in higher order structure was large enough, the former hypothesis could be tested using the technique of circular dichroism (CD) which analyzes the secondary structure of proteins in solution. This method would allow for the detection of changes in common secondary structure motifs such as α-helix, β-pleated sheets and β-turns (Greenfield, 1996). If no change in higher order structure is observed, this would imply either that the change is too small to be detected by the CD method or that it is not a change in conformation that results in inactivation. Instead, perhaps the large side chain of Leu blocks access of one or both substrates to the active site. The latter hypothesis is more difficult to test. Ultimately, the crystal structure of m_2^2Gtase bound to its substrates would be an invaluable asset.

Ser^{467} is not Involved in Catalysis and Binding.

Further evidence consistent with the idea that Ser^{467} is not critical for m_2^2Gtase activity was provided by kinetic studies. The kinetic parameters, K_M and V_{max}, were determined for the m_2^2Gtase mutants containing Thr^{467}, Ala^{467} or Cys^{467}. It must be noted that because these V_{max} and K_M values were obtained with crude protein extracts, they do not represent accurately the interaction between substrates and enzyme and are considered apparent constants rather than true constants. Figures 29 and 30 show typical hyperbolic kinetics of m_2^2Gtase activity as a function of SAM or tRNA concentration. Results obtained from kinetic studies on these mutants indicate that the overall catalysis and binding are not affected. The apparent V_{max} values obtained from all mutants were not

significantly altered for either substrate. Values ranged from 519.7 to 608.8 nmol/mg protein/min for SAM and 538.1 to 711.1 nmol/mg protein/min for tRNA (Table 5). The apparent K_M values for SAM range from 9.7 μM to 28.9 μM (Table 5) which coincide with the order of magnitude of K_M values reported for mammalian tRNA methylases (1.5-3 μM) (Nau, 1976) and *E. coli* tRNA (guanosine-1) methyltransferase (15 μM) (Holmes *et al.*, 1992). The apparent K_M value obtained for the Ser^{467}→T mutant is virtually identical to that of the wild-type m_2^2Gtase, suggesting that addition of an extra methyl group does not alter the ability of substrate to enter the active site. The apparent K_M values obtained for the mutants Ser^{467}→Ala and Ser^{467}→Cys are 3 fold higher than those obtained for the wild-type protein. This suggests that these changes may have slightly weakened SAM binding. However, a change in K_M of this magnitude is probably not significant. The K_M for tRNA is less defined since it is difficult to assess with precision what proportion of a given tRNA preparation is actually a substrate for the enzyme (Nau, 1976). Nevertheless, the effects of tRNA concentration on m_2^2Gtase activity are reported in Figure 30. Results for the apparent K_M values range from 2.3 to 4.5 μM (Table 5) and indicate that tRNA binding is not affected in these mutants. These apparent K_M values compare with 3.25 μM reported for tRNA for *E. coli* tRNA (guanosine-1) methyltransferase (Holmes *et al.*, 1992). As mentioned here, these experiments generate apparent K_M and V_{max} values. Purer m_2^2Gtase preparations are required for more detailed kinetic studies on the molecular mechanism of the interaction of this enzyme with tRNA and SAM. Regardless, these kinetic data have provided evidence that Ser^{467} is not involved directly in catalysis and binding.

m_2^2Gtase Protein Sequence Alignments.

Protein sequence alignments were employed to explore the existence of possible sequence similarities between yeast m_2^2Gtase and other proteins. When the yeast m_2^2Gtase amino acid sequence was used to search the protein sequence databases, it was found that ten proteins from a variety of organisms had sequences producing high-scoring segment pairs. However, only two organisms displayed consensus sequences in the region containing Ser^{467}: 1) a nucleotide sequence from chromosome III of *Caenorhabditis elegans* revealed 60% sequence similarity to residues 427 to 491 of the m_2^2Gtase sequence with Ser^{467} conserved, and 2) the m_2^2Gtase from the methanogenic archaeon, *Methanococcus jannaschii,* displayed 55% positives when compared to residues 436 to 492 of the yeast m_2^2Gtase. However, in this case Ser^{467} was not conserved as a valine residue was found in its place. Secondary structure predictions (Garnier *et al.*, 1978) on these regions depicted in Figure 32 revealed that in *C. elegans*, the conserved Ser^{419} residue lies in a strong turn region as does Ser^{476} in yeast m_2^2Gtase (Figure 27). In contrast, the corresponding Val^{345} residue in the m_2^2Gtase from *M. jannaschii* lies in an extended region. The lack of sequence similarity of m_2^2Gtase with any other methyltransferases is surprising given the large number of SAM and tRNA binding enzymes that exist and the large amount of sequence available in databases. For example, the m_2^2Gtase sequence was compared to a motif found in the segment from *E. coli* UbiG (amino acid residues 59 to 77) (Wu *et al.*, 1992). The methyltransferases that share this motif include rRNA adenine-N6 methyltransferases, protein-β-aspartate methyltransferases, protein-γ-glutamate *O*-methyltransferases and some DNA methyltransferases. Yeast m_2^2Gtase is not included in this list. This lack of sequence

similarity may be accounted for by the evolutionary variations of a protein as proteins may have essentially the same biological function yet different amino acid sequences.

The Presence of m_2^2Gtase in *S. cerevisiae* and Other Related Yeast.

In spite of the apparent lack of any detectable phenotype associated with a loss of m_2^2Gtase activity, it is interesting that a similar activity is present in a wide variety of yeast species including those closely related to *S. cerevisiae*, such as *C. glabrata* and *K. lactis* as well as the more distantly related fission yeast *S. pombe* (Figure 9). Varying levels of m_2^2Gtase activity were displayed, with *C. glabrata* and *K. lactis* exhibiting levels similar to that of the *S. cerevisiae* strain W303-1b. These three yeasts are closely related by many criteria including small subunit ribosomal RNA sequences (Van de Peer *et al.*, 1992). In contrast, the more distantly related yeasts *S. exiguus*, *S. fibuligera* and *S. pombe* all demonstrated relatively low m_2^2Gtase activities. It is possible that the the low m_2^2Gtase activity levels seen in these yeasts reflect: 1) higher levels of proteases in the yeasts such that the enzyme is degraded during protein preparation, 2) lower natural levels of this enzyme in these yeasts, or 3) less specificity of the enzyme for the *S. cerevisiae* tRNAs used as substrate in a heterologous system. Although not much is known about the methylation patterns at G_{26} in tRNAs in these species, it is interesting to see that they do have some detectable level of methylation on G_{26}. This again raises questions of the importance of $m_2^2G_{26}$ in tRNA.

The tRNA Methylation Reaction Catayized by m_2^2Gtase may be a Two-Step Process.

The time courses generated for tRNA and SAM binding (Figure 28) are also of interest due to the observation of an apparent lag time seen in the tRNA and SAM time courses. This lag may suggest that either tRNA or SAM dissociates between successive methylations which could be evidence for a two-step mechanism for the formation of $m_2^2G_{26}$. This would be consistent with a study which explored the mono- and di-methylating activity of tRNA (guanine)-methyltransferase from *Tetrahymena* (Reinhart *et al.*, 1986) in which a significant lag was observed in time course experiments. Furthermore, this study determined that the quantities of m^2G versus m_2^2G were not constant over time as the monomethylated product predominated at early times and the dimethylated one accumulated only at later time periods. This study was however conducted in a heterologous system employing *E. coli* tRNA. Edqvist *et al.* (1992 and 1994) have demonstrated that there exists a difference in methylation patterns depending on which system is used. They provided evidence for a one-step reaction by employing a homologous system using partially purified yeast m_2^2Gtase and yeast tRNA. Edqvist *et al.*(1994) showed that the dimethylation reaction was so efficient that no m^2G_{26} intermediate was detectable. Based on this, they proposed that the enzymatic formation of $m_2^2G_{26}$ involved a single tRNA-enzyme association event without the release of the intermediate monomethylated product. Edqvist *et al.* (1995) suggest that the presence of monomethylated G_{26} may result only when the tRNA dissociates from the enzyme after the first methylation if the molecule does not bind tightly enough to the enzyme. They further propose that this may explain the accumulation of the monomethylated form as

seen by Reinhardt *et al.* (1986) in a heterologous system utilizing *E. coli* tRNA and *Tetrahymena* enzyme. A possible explanation for the difference in the results presented here (Figure 28) and those of Edqvist *et al.* (1994) may lie in the experimental approaches employed. While both studies employed a homologous *in vitro* system, Edqvist *et al.* (1994) utilized *in vitro* transcripts of yeast tRNA which resulted in a single population of tRNA and crude protein extracts which were obtained from yeast which overexpressed the *TRM*1 gene. In contrast, studies presented here employed a mixed population of yeast tRNA and crude protein yeast extracts containing natural levels of m_2^2Gtase. Although it is not clear how these factors may influence the methylation pattern of tRNA at position G_{26}, the two-step formation of m_2^2G cannot be dismissed. More detailed studies, which would involve detecting the presence of the modified bases m^2G and m_2^2G by 2-dimensional thin layer chromatography and measuring their levels over time, would be beneficial in answering this question.

Conclusions.

Through gene cloning and DNA sequencing procedures, the *trm*1 gene from SN1015-2a was isolated and characterized. Sub-cloning and site-directed mutagenesis led to the identification of a single base mutation resulting in the Ser^{467}→Leu substitution as being responsible for the loss of m_2^2Gtase activity. Converting Ser^{467} to other residues such as Thr, Ala and Cys had no effect on the catalysis and binding of the substrates indicating that Ser^{467} is not essential for the function of m_2^2Gtase. In contrast, the Ser^{467}→Leu substitution was sufficient to inactivate the enzyme. The reason for this loss

of activity remains unclear. Leu^{467} may alter the conformation of the enzyme and inactivate it, or it may somehow block substrate binding. To address these questions, future work may involve overexpression of the *trm1* gene and its variants, and purification of these m_2^2Gtases such that circular dichroism or X-ray crystallography may be employed to follow changes in higher order structure.

References

V. REFERENCES

Bewsey, K.E., Johnson, M.E., and Huff, J.P. (1991). Rapid isolation and purification of DNA from agarose gels: The phenol-freeze-fracture method. Biotechniques *10*, 724-725.

Birnboim, H.C. (1983). A rapid alkaline extraction method for the isolation of plasmid DNA. Methods Enzymol. *100*, 234-255.

Bjork, G.R. and Isaksson, L.A. (1970). Isolation of mutants of *Escherichia coli* lacking 5-methyluracil in transfer ribonucleic acid or 1-methylguanine in ribosomal RNA. J. Mol. Biol. *51*, 83-100.

Bjork, G.R., Ericson, J.U., Gustafsson, C.E., Hagervall, T.G., Jonsson, Y.H., and Wikstrom, P.M. (1987). Transfer RNA modification. Annu. Rev. Biochem. *56*, 263-287.

Bjork, G.R. (1995). Biosynthesis and function of modified nucleosides. In tRNA: Structure, Biosynthesis, and Function. D. Soll and U. RajBhandary, eds., Washington, D.C. American Society for Microbiology, pp. 165-205.

Borek, E., Ryan, A., and Rockenbach, J. (1955). Nucleic acid metabolism in relation to the lysogenic phenomenon. J. Bacteriol. *69*, 460-467.

Boyle, J., Robillard, G.T., and Kim, S.H. (1980). Sequential folding of transfer RNA: A nuclear magnetic resonance study of successively longer tRNA fragments with a common 5' end. J. Mol. Biol. *139*, 601-625.

Caiello, N.F., Swenberg, J.A., and Skopek, T.R. (1991). Fidelity of *Thermococcus litoralis* DNA polymerase (Vent) in PCR determined by denaturing gradient gel electrophoresis. NucleicAcids Res. *19*, 4193-4198.

Chen, J., and Viola, M.V. (1991). A method to detect ras point mutations in small subpopulations of cells. Anal. Biochem. *195*, 51-56.

Chen, M.C., Giege, R., Lord, R.C., and Rich, A. (1975). Raman spectra and structure of yeast phenylalanine transfer RNA in crystalline state and in solution. Biochemistry *14*, 4385-91.

Cheng, X., Kumar, S., Posfai, J., Pflugrath, J.W., and Roberts, R.J. (1993). Crystal structure of the *HhaI* DNA methyltransferase complexed with S-adenosyl-L-methionine. Cell *74*, 299-307.

Creighton, T.E. (1993). Enzyme Catalysis. In Proteins: Structures and Molecular Properties. New York. W.H. Freeman and Company, pp. 385-430.

Eckert, K.A., and Kunkel, T.A. (1991). DNA polymerase fidelity and the polymerase chain reaction. PCR Methods and Applications *1*, 17-24.

Edqvist, J., Grosjean, H., and Straby, K.B. (1992). Identity elements for N^2-dimethylation of guanosine-26 in yeast tRNAs. Nucleic Acids Res. *20*, 6575-6581.

Edqvist, J., Blomqvist, K., and Straby, K.B. (1994). Structural elements in yeast tRNAs required for homologous modification of guanosine into dimethylguanosine-26 by the yeast Trm1 tRNA-modifying enzyme. Biochemistry *33*, 9546-9551.

Edqvist, J., Straby, K.B., and Grosjean, H. (1995). Enzymatic formation of N^2,N^2-dimethylguanosine in eukaryotic tRNA: importance of the tRNA architecture. Biochimie *77*, 54-61.

Ellis, S.R., Morales, M.J., Li, J.M., Hopper, A.K., and Martin, N.C. (1986). Isolation and characterization of the *TRM*1 locus, a gene essential for the N^2,N^2-dimethylguanosine modification of both mitochondrial and cytoplasmic tRNA in *Saccharomyces cerevisiae*. J. Biol. Chem. *261*, 9703-9709.

Ellis, S.R., Hopper, A.K., and Martin, N.C. (1987). Amino-terminal extension generated from an upstream AUG codon is not required for mitochondrial import of yeast N^2,N^2-dimethylguanosine-specific tRNA methyltransferase. Proc. Natl. Acad. Sci. USA *84*, 5172-5176.

Ellis, S.R., Hopper, A.K., and Martin, N.C. (1989). Amino-terminal extension generated from an upstream AUG codon increases the efficiency of mitochondrial import of yeast N^2,N^2- dimethylguanosine-specific tRNA methyltransferases. Mol. Cell. Biol. *9*, 1611-1620.

Fleissner, E. and Borek, E. (1962). A new enzyme of RNA synthesis: RNA methylase. Proc. Natl. Acad. Sci. USA *48*, 1199-1203.

Garnier, J., Osguthorpe, D.J., and Robson, B. (1978). Analysis of the accuracy and implications of simple methods for predicting the secondary structure of globular proteins. J. Mol. Biol. *120*, 97-120.

Greenfield, N.J. (1996). Methods to estimate the conformation of proteins and polypeptides from circular dichroism data. Anal. Biochem. *235*, 1-10.

Grosjean, H., Bjork, G.R., and Maden, B.E.H. (1995). Nucleotide modification and base conversion of RNA: Summary and outlook. Biochimie 3-6.

Gu, X.R. and Santi, D.V. (1991). The T-arm of tRNA is a substrate for tRNA (m^5U54)-methyltransferase. Biochemistry *30*, 2999-3002.

Gu, X.R. and Santi, D.V. (1992). Covalent adducts between tRNA (m^5U54)-methyltransferase and RNA substrates. Biochemistry *31*, 10295-10302.

Hall, R.H. and Dunn, D.B. (1975). Natural occurrence of the modified nucleosides. In Handbook of Biochemistry and Molecular Biology. G.D. Fasman, ed., Cleveland, CRC Press, pp. 216-250.

Hamahata, A., Takata, Y., Gomi, T., and Fujioka, M. (1996). Probing the S-adenosylmethionine-binding site of rat guanidinoacetate methyltransferase. Effect of site-directed mutagenesis of residues that are conserved across mammalian non-nucleic acid methyltransferases. Biochem. J. *317*, 141-145.

Holbrook, S.R., Sussman, J.L., Warrant, W., and Kim, S.H. (1978). Crystal structure of yeast phenylalanine transfer RNA - II. Structural features and functional implications. Mol. Biol. *123*, 631-660.

Holley, R., Apgar, J., Everett, G.A., Madison, J.T., Marquisee, M., Merrill, S.H., Penswick, J.R., and Zamir, A. (1965). Structure of a ribonucleic acid. Science *147*, 1462-1465.

Holmes, W.M., Andraos-Selim, C., Roberts, I., and Wahab, S.Z. (1992). Structural requirements for tRNA methylation. Action of *Escherichia coli* tRNA (guanosine-1) methyltransferase on tRNA (1Leu) structural variants. J. Biol. Chem. *267*, 13440-13445.

Hopper, A.K. (1978). A yeast mutant which accumulates precursor tRNAs. Cell *14*, 211-219.

Hopper, A.K., Schultz, L.D., and Shapiro, R.A. (1980). Processing of intervening sequences: a new yeast mutant which fails to excise intervening sequences from precursor tRNAs. Cell *19*, 741-751.

Hopper, A.K., Furukawa, A.H., Pham, H.D., and Martin, N.C. (1982). Defects in modification of cytoplasmic and mitochondrial transfer RNAs are caused by single nuclear mutations. Cell *28*, 543-550.

Hotchkiss, R.D. (1948). The quantitative separation of purines, pyrimidines, and nucleosides by paper chromatography. J. Biol. Chem. *175*, 315-332.

Kagan, R.M. and Clarke, S. (1994). Widespread occurrence of three sequence motifs in diverse S- adenosylmethionine-dependent methyltransferases suggests a common structure for these enzymes. Arch. Biochem. Biophys. *310*, 417-427.

Kealey, J.T., Gu, X.R., and Santi, D.V. (1994). Enzymatic mechanism of tRNA (m^5U54)methyltransferase. Biochimie *76*, 1133-1142.

Kowalak, J.A., Dalluge, J.J., McCloskey, J.A., and Stetter, K.O. (1994). The role of posttranscriptional modification in stabilization of transfer RNA from Hyperthermophiles. Biochemistry *33*, 7869-7876.

Krynetski, E.Y., Schuetz, J.D., Galpin, A.J., Pui, C.H., Relling, M.V., and Evans, W.E. (1995). A single point mutation leading to loss of catalytic activity in human thiopurine S-methyltransferase. Proc. Natl. Acad. Sci. USA *92*, 949-953.

Kumar, S., Cheng, X., Pflugrath, J.W., and Roberts, R.J. (1992). Purification, crystallization, and preliminary X-ray diffraction analysis of an M.*Hha*I-AdoMet complex. Biochemistry *31*, 8648-8653.

Kunkel, T.A. (1985). Rapid and efficient site-specific mutagenesis without phenotypic selection. Proc. Natl. Acad. Sci. USA *82*, 488-492.

Kunkel, T.A., Roberts, J.D., and Zakour, R.A. (1987). Rapid and efficient site-specific mutagenesis without phenotypic selection. Methods Enzymol. *154*, 367-382.

Labahn, J., Granzin, J., Schluckebier, G., Robinson, D.P., Jack, W.E., Schildkraut, I., and Saenger, W. (1994). Three-dimensional structure of the adenine-specific DNA methyltransferase M.*Taq* I in complex with the cofactor S-adenosylmethionine. Proc. Natl. Acad. Sci. USA *91*, 10957-10961.

Li, J.M., Hopper, A.K., and Martin, N.C. (1989). N^2,N^2-dimethylguanosine-specific tRNA methyltransferase contains both nuclear and mitochondrial targeting signals in *Saccharomyces cerevisiae*. J. Cell Biol. *109*, 1411-1419.

Littauer, U.Z. and Inouye, H. (1973). Regulation of tRNA. Annu. Rev. Biochem. *42*, 439-70.

Marinus, M.G., Morris, N.R., Soll, D., and Kwong, T.C. (1975). Isolation and partial characterization of three *Escherichia coli* mutants with altered transfer ribonucleic acid methylases. J. Bacteriology *122*, 257-265.

Moras, D., Comarmond, M.B., Fischer, J., Weiss, R., Thiery, J.C., Ebel, J.P., and Giege, R. (1980). Crystal structure of yeast $tRNA^{Asp}$. Nature *288*, 669-674.

Nau, F. (1976). The methylation of tRNA. Biochimie *58*, 629-645.

Persson, B.C. (1993). Modification of tRNA as a regulatory device. Molecular Microbiology *8*, 1011-1016.

Philippsen, P., Stotz, A., and Scherf, C. (1991). DNA of *Saccharomyces cerevisiae*. Methods Enzymol. *194*, 169-182.

Phillips, J.H. and Kjellin-Straby, K. (1967). Studies on microbial ribonucleic acid. IV. Two mutants of *Saccharomyces cerevisiae* lacking N^2-dimethylguanine in soluble ribonucleic acid. J. Mol. Biol. *26*, 509-518.

Reinhart, M.P., Lewis, J.M., and Leboy, P.S. (1986). A single tRNA (guanine)-methyltransferase from *Tetrahymena* with both mono- and di-methylating activity. Nucleic Acids Res. *14*, 1131-1148.

Robertus, J.D., Ladner, J.E., Finch, J.T., Rhodes, D., Brown, R.S., Clark, B.F., and Klug, A. (1974). Structure of yeast phenylalanine tRNA at 3Å resolution. Nature *250*, 546-551.

Rose, A.M., Joyce, P.B.M., Hopper, A.K., and Martin, N.C. (1992). Separate information required for nuclear and subnuclear localization: additional complexity in localizing an enzyme shared by mitochondria and nuclei. Mol. Cell. Biol. *12*, 5652-5658.

Salvatore, F. (1977). The Biochemistry of adenosylmethionine, New York: Columbia University Press, pp.187-230.

Sambrook, J., Fritsch, E.F., and Maniatis, T. (1989). Molecular cloning: A laboratory manual, Cold Spring Harbor: Cold Spring Harbor Press.

Sanger, F., Nicklen, S., and Coulson, A.R. (1977). DNA sequencing with chain-terminating inhibitors. Proc. Natl. Acad. Sci. USA *74*, 5463-5467.

Saridakis, V.C. (1995). Purification of tRNA $m^2_2G_{26}$-methyltransferase from *Lupinus albus*. (M.Sc. Thesis, Concordia University)

Schiestl, R.H. and Gietz, R.D. (1989). High efficiency transformation of intact yeast cells using single stranded nucleic acids as a carrier. Curr. Genet. *16*, 339-346.

Schmidt, O., Mao, J., Ogen, R., Beckmann, J., Sakano, H., Abelson, J., and Soll, D. (1980). Dimeric tRNA precursors in yeast. Nature *287*, 750-752.

Sherman, F. (1991). Getting started with yeast. Methods Enzymol. *194*, 3-21.

Smith, J.D. and Dunn, D.B. (1959). The occurrences of methylated guanines in ribonucleic acids from several sources. Biochem. J. *72*, 294-301.

Smolar, N. and Svensson, I. (1974). tRNA methylating activity of yeast mitochondria. Nucleic Acids Res. *1*, 707-718.

Steinberg, S. and Cedergren, R. (1995). A correlation between N^2-dimethylguanosine presence and alternate tRNA conformers. RNA *1*, 886-891.

Stewart, T.S., Roberts, R.J., and Strominger, J. (1971). Novel species of tRNA. Nature *230*, 36-38.

Stryer, L. (1988). Biochemistry, New York: W.H. Freeman and Company, pp. 740-741.

Sussman, J.L., Holbrook, S.R., Warrant, W., Church, G.M., and Kim, S.H. (1978). Crystal structure of yeast phenylalanine transfer RNA - I. Crystallographic refinement. Mol. Biol. *123*, 607-630.

Takata, Y., Konishi, K., Gomi, T., and Fujioka, M. (1994). Rat guanidinoacetate methyltransferase. Effect of site-directed alteration of an aspartic acid residue that is conserved across most mammalian S-adenosylmethionine-dependent methyltransferases. J. Biol. Chem. *269*, 5537-5542.

Takimoto, K., Uchino, K., Ishizaki, K., and Ikenaga, M. (1991). Specificity of mutational DNA sequence changes induced by X-rays in the cloned *Escherichia coli crp* gene. Mutation Research *254*, 199-206.

Towbin, H., Staehelin, T., and Gordon, J. (1979). Electrophoretic transfer of proteins from polyacrylamide gels to nitrocellulose sheets: procedure and some applications. Proc. Natl. Acad. Sci. USA *76*, 4350-4354.

Van de Peer,Y., Hendriks, L., Goris, A., Neefs, J.M., Vancanneyt, M., Kersters, K., Berny, J.F., Hennebert, G.L., and De Wachter, R. (1992). Evolution of basidiomycetous yeasts as deduced from small ribosomal subunit RNA sequences. System. Appl. Microbiol. *15*, 250-258.

Wu, G., Williams, H.D., Zamanian, M., Gibson, F., and Poole, R.K. (1992). Isolation and characterization of Escherichia coli mutants affected in aerobic respiration: the cloning and nucleotide sequence of *ubiG*. Identification of an S-adenosylmethionine-binding motif in protein, RNA, and small-molecule methyltransferases. J. Gen. Microbiol. *138*, 2101-2112.

APPLIED IMAGE, Inc
1653 East Main Street
Rochester, NY 14609 USA
Phone: 716/482-0300
Fax: 716/288-5989